Published in final edited form as:
Chem Res Toxicol. 2012 October 15; 25(10): 2007–2035. doi:10.1021/tx3002548.

Quantitation of DNA adducts by stable isotope dilution mass spectrometry

Natalia Tretyakova[†,*], **Melissa Goggin**[†,‡], and **Gregory Janis**[‡]

[†]Department of Medicinal Chemistry and Masonic Cancer Center, University of Minnesota, Minneapolis, MN 55455

[‡]MEDTOX Scientific, St. Paul, MN 55112

Abstract

Exposure to endogenous and exogenous chemicals can lead to the formation of structurally modified DNA bases (DNA adducts). If not repaired, these nucleobase lesions can cause polymerase errors during DNA replication, leading to heritable mutations potentially contributing to the development of cancer. Due to their critical role in cancer initiation, DNA adducts represent mechanism-based biomarkers of carcinogen exposure, and their quantitation is particularly useful for cancer risk assessment. DNA adducts are also valuable in mechanistic studies linking tumorigenic effects of environmental and industrial carcinogens to specific electrophilic species generated from their metabolism. While multiple experimental methodologies have been developed for DNA adduct analysis in biological samples – including immunoassay, HPLC, and ^{32}P-postlabeling – isotope dilution high performance liquid chromatography-electrospray ionization-tandem mass spectrometry (HPLC-ESI-MS/MS) generally has superior selectivity, sensitivity, accuracy, and reproducibility. As typical DNA adducts concentrations in biological samples are between 0.01 – 10 adducts per 10^8 normal nucleotides, ultrasensitive HPLC-ESI-MS/MS methodologies are required for their analysis. Recent developments in analytical separations and biological mass spectrometry – especially nanoflow HPLC, nanospray ionization MS, chip-MS, and high resolution MS – have pushed the limits of analytical HPLC-ESI-MS/MS methodologies for DNA adducts, allowing researchers to accurately measure their concentrations in biological samples from patients treated with DNA alkylating drugs and in populations exposed to carcinogens from urban air, drinking water, cooked food, alcohol, and cigarette smoke.

1. Introduction

Deoxyribonucleic acid (DNA) is referred to as “the molecule of life” due to its central role in the storage and transmission of genetic information. In all living organisms, genetic information is encoded in the nucleobase sequence comprising the polynucleotide chain of DNA. During DNA replication, DNA polymerases employ the Watson-Crick base pairing rules (where G specifically pairs with C, and A with T) to generate an accurate and complete copy of the original cellular genome in its entirety. Encoded genetic information is retrieved as needed during gene expression, when specific regions of the genome are transcribed into RNA, and the RNA transcripts are then translated into the amino acid sequence of the proteins.

Cancer is a group of diseases which are all characterized by uncontrolled growth and the proliferation of abnormal cells. These mutated, genetically dysfunctional cells escape

[*]Corresponding author: 760E MCRB, Masonic Cancer Center, University of Minnesota, 806 Mayo, 420 Delaware St. S.E., Minneapolis, MN 55455, USA, Tel. (612) 626-3432; Fax: (612) 626-5135; trety001@umn.edu.

normal growth control signals, bypass programmed cell death, evade immunological surveillance, and invade into surrounding tissues.[1] In order to gain such unusual phenotypes, cancer cells must accumulate mutations in critical genes controlling genomic stability, cell differentiation, signal transduction, the cell cycle, cellular senescence, and apoptosis. While genetic changes can occur spontaneously due to the presence of rare tautomers of nucleobases and inherent DNA polymerase errors, the probability of genetic damage is greatly increased by DNA adducts resulting from cellular exposure to exogenous or endogenous electrophiles (Scheme 1).

Many carcinogens require metabolic activation to electrophilic intermediates (e.g. epoxides, carbonium ions, quinone methides, α, β-unsaturated carbonyls, diazonium ions, and nitrenium ions) before they are capable of reacting with DNA to form covalent adducts.[2] These bioactivation reactions are catalyzed by xenobiotic metabolizing enzymes such as cytochrome P450 monooxygenases, sulfotransferases, N-acetyltransferases, and monoamino oxidases.[3] An inherent broad substrate specificity allows xenobiotic metabolizing enzymes to metabolize a wide variety of exogenous and endogenous substrates. While such metabolic reactions facilitate the excretion of foreign compounds by increasing their polarity and water solubility, metabolic biotransformations can also generate electrophilic intermediates capable of modifying nucleophilic sites in DNA.

Genotoxic chemicals and their metabolites can chemically damage DNA through the processes of alkylation, arylation, arylamination, oxidation, deamination, and cross-linking.[4–6] DNA contains many nucleophilic sites targeted by reactive electrophiles, including the N-7, the O-6, the C-8 and the N-2 of guanine; the N-1, N-3, and the N-7 of adenine; the O-2 and the O-4 of thymine; and the O-2 and the N-4 of cytosine (Scheme 2).[2] Therefore, exposure to exogenous and endogenous electrophiles generates a diverse array of covalently modified bases.

Carcinogen binding to DNA nucleobases alters their molecular shape and hydrogen bonding characteristics, potentially compromising the ability of the modified base to form specific Watson-Crick base pairs. As a result, the presence of the structurally modified DNA bases (DNA lesions) increases the probability of polymerase errors during DNA synthesis (Scheme 1). For example, O^6-alkylated guanines preferentially pair with thymine instead of the normal guanine partner, cytosine. In the second round of replication, cytosine with pair with guanine (Scheme 3).[7,8] The resulting DNA strands will contain A-T base pairs in the location where the original G-C coding existed (G → A transition mutation). Alternatively, bulky and helix distorting DNA lesions such as DNA-DNA cross-links can block DNA polymerases, interfering with cell replication.[6]

All living cells have protective systems designed to detect and repair damaged DNA; they possess many genes coding for proteins responsible for DNA damage response and adduct removal. In most cases, DNA repair takes place before replication, restoring the native DNA structure, and thereby preventing mutagenesis.[2,9–16] These proteins are essential for cell survival, and their deficiencies can sensitize cells and organisms to chemical and environmental carcinogens. In addition, both bacterial and mammalian cells contain specialized lesion bypass polymerases capable of replicating past damaged nucleobases.[17,18] This damage bypass mechanism resolves a potential replicative crisis and allows for cell survival in the presence of DNA-damaging agents. However, lesion bypass polymerases have relatively low fidelity and can lead to mutations due to error-prone bypass synthesis.[17,19,20]

Because of their central role in chemical carcinogenesis, DNA adducts can be considered mechanism-based biomarkers of exposure. They serve as useful indicators of a biologically

relevant dose of a carcinogen; the presence of DNA adducts directly reflects the formation of reactive intermediates available for binding to cellular biomolecules.[21–23] The tissue concentrations of a specific DNA adduct can be used for hazard identification and risk assessment from exposure to carcinogens. Data from experimental animals have established dose-response relationships between exposure levels and DNA adduct formation.[21,24] Although such findings can be difficult to extrapolate between species due to significant differences in metabolic pathways, animal studies are invaluable for characterizing adduct structures, examining the roles of DNA repair pathways in adduct removal, and demonstrating the biological relevance of each group of structurally distinct lesions.[25,26] In human studies, DNA adducts can be used to identify individuals and populations at risk for developing cancer and also for setting human exposure limits for occupational and environmental chemicals.[21,22,27,28]

Typically, concentrations of DNA adducts in animal and human tissues are quite low, in the range of 0.01 – 10 adducts per 10^8 normal nucleotides.[26–31] Therefore, analytical methods used for quantification of carcinogen-DNA adducts must be ultra-sensitive, accurate, and specific, making it possible to quantify low abundance DNA lesions in the presence of a large molar excess of normal nucleosides.[22] ^{32}P-postlabeling involves thin layer chromatography or HPLC separation of radiolabeled nucleotides. While highly sensitive, this methodology but does not provide structural information for the damaged bases and may not provide accurate adduct levels because of potential inefficiency of labeling by polynucleotide kinase, RNA contamination, and incomplete resolution of nucleotide mixtures. Immunoassay exhibits a good specificity for analyte of interest, providing relative quantification. Mass spectrometry using stable isotope labeled internal standards (isotope dilution HPLC-ESI-MS-MS or IDMS) is considered a golden standard for DNA adduct analysis because it provides structural information and due to its high specificity, sensitivity, and accurate quantification.[22,30,31]

Several comprehensive reviews have been published over the years that discuss the use of isotope dilution mass spectrometry in DNA adduct analysis.[27,30–33] The present review is focused on the recent developments in isotope dilution HPLC-ESI-MS/MS and provides some up-to-date examples of mass spectrometry-based detection of DNA adducts in biological samples.

1.1 Sources of DNA for DNA adduct analyses

The specific steps involved in DNA adduct analysis are illustrated in Scheme 4. Organ tissues, blood, oral buccal cells, saliva, and urine are all utilized as biological sources of DNA for analyzing adducts. Typically DNA amounts between 1 and 200 μg are required for quantitative analysis, depending on the abundance of the lesion and the sensitivity of the analytical method. Studies conducted in laboratory animals typically use DNA isolated from liver, lungs kidney, thymus, and brain tissues.[24,34,35] However, these tissues are not typically available for human biomonitoring studies. Blood, saliva, urinary epithelial cells, and oral buccal swab samples are easier to obtain from human subjects and may be the only feasible sources of DNA for epidemiological studies.[36,37] Alternatively, DNA adducts can be measured as free nucleobases and nucleosides in urine, where they are excreted following spontaneous hydrolysis and/or active DNA repair.[38,39] Although human urine is a complex and variable matrix containing high concentrations of salts and other polar compounds, several laboratories have been successful at analyzing urinary nucleosides in humans by HPLC-ESI-MS/MS.[40–44] However, it should be noted that urinary adducts may not accurately represent the extent of cellular DNA damage due to the potential to form base adducts from free nucleosides and nucleotides and the fact that they represent the damage that has been repaired.

1.2 DNA hydrolysis

Because mass spectrometry (MS) analysis of small molecules generally has a better sensitivity, accuracy, and precision as compared to MS methods for large molecules, DNA is routinely hydrolyzed prior to analysis to release adducted nucleotides, nucleosides, or nucleobases. Some DNA adducts, including *N7*-alkylguanines and *N3*-alkyladenines, are thermally labile and can be readily and selectively released from a DNA backbone as free bases upon heating (thermal hydrolysis).[2,22,45–47] To analyze hydrolytically stable adducts, DNA must be enzymatically digested in the presence of nucleases and phosphatases to release deoxynucleosides. (Care should be taken when digesting chemically modified DNA as many adducts are capable of blocking nuclease enzymes, leading to incomplete enzymatic hydrolysis).[48] Alternatively, DNA heating in the presence of acid (mild acid hydrolysis) releases all purines as free nucleobases, including any adenine and guanine adducts present in DNA.[2,49] Unlike thermal hydrolysis that selectively releases adducted nucleobases, enzymatic and acid hydrolysis both generate complex mixtures containing a large excess of unmodified monomers, and the adducts of interest may require additional cleanup steps prior to MS analysis (see Section 1.3).

Some DNA lesions can be generated as artifacts during enzymatic digestion and other sample processing steps. If present, such problems are revealed by analyzing blank DNA spiked with defined amounts of the analyte and its internal standard (analytical method validation, see Section 2.5). The best known example is 8-oxoguanine (8-oxo-dG), which is readily produced from dG in an aerobic environment.[50–52] Boysen et al. employed a combination of antioxidants, metal chelators, and free radical trapping agents to reduce the artifactial formation of 8-oxo-dG during DNA isolation and sample processing.[53] Dedon et al. have recently reported quantitative methods for deaminated bases as biomarkers of nitrogen oxide-mediated deamination and lipid peroxidation.[54–56] These authors employed dC and dA deaminase inhibitors to avoid adventitious formation of 2′-deoxyuridine (dU) and 2′-deoxyinosine (dI), respectively, during DNA isolation and processing.[54–56]

1.3 Sample preparation

DNA hydrolysates containing adducts of interest typically require extensive cleanup to remove the bulk of unmodified nucleosides, proteins, inorganic salts, and other sample components which can interfere with MS analysis.[22,28] Some examples of sample enrichment methods used in DNA adduct analyses include ultrafiltration, liquid/liquid extraction, solid phase extraction, immunoaffinity purification, and off-line HPLC.

The partially depurinated DNA remaining after thermal or acid hydrolysis of DNA can be removed by ultrafiltration. This methodology is also useful for removing proteins following enzymatic hydrolysis of DNA. Disposable ultrafiltration units can be used to achieve a fast and efficient filtration. In our experience, centrifugation devices with a low molecular weight cutoff (e.g. 3,000 Da) produce cleaner samples, improving detection sensitivity.

Some DNA adducts can be enriched by liquid/liquid extraction using organic solvents, while polar components of the biologic matrix remain in the aqueous phase.[57] This method is effective and economical, but is limited to hydrophobic lesions such as those of polycyclic aromatic hydrocarbons and aromatic amines.

Solid phase extraction (SPE) has a broader applicability than liquid/liquid extraction since it is can be used to purify a variety of DNA adducts with varying hydrophobicity. In SPE, samples are loaded on a small disposable column packed with chromatographic stationary phase under conditions that facilitate analyte binding. Following washing steps to remove contaminants, the analyte of interest is eluted with an appropriate solvent. A large variety of SPE cartridges are available commercially, including cation exchange, anion exchange, and

mixed mode packing, which can be used to isolate specific DNA lesions from complex mixtures.[45,58–60] Immunoaffinity purification is based on a similar principle, with the exception that the sample enrichment is achieved via analyte binding to a monoclonal or polyclonal antibody attached to a solid support.[61]

Off-line HPLC can be effectively used to remove the bulk of impurities and to enrich the analyte to prior to MS analysis. HPLC fractions containing the compound of interest are collected, concentrated under vacuum, and injected onto another HPLC column for HPLC-MS analysis. The use of retention time markers during offline HPLC cleanup is important to control for any retention time variations due to potential temperature changes or influences from the sample matrix. Our laboratory has successfully employed off-line HPLC cleanup to enrich oxidative DNA lesions, 2,2-diamino-4-(2-deoxy-β-D-*erythro*-pentofuranosyl)amino]5(2H)-oxazolone (oxazolone)[62] and guanine-guanine adducts of 1,2,3,4-diepoxybutane (*bis*-N7G-BD) present in DNA hydrolysates prior to their quantitative analysis by nanoHPLC-nanospray MS/MS.[34,63] We found that offline HPLC purification prior to HPLC-MS/MS provided a better sensitivity that our previous methodology employing SPE cleanup.[45]

2. Instrumentation for HPLC-ESI$^+$-MS/MS analysis of DNA adducts

2.1 Liquid chromatography

Efficient separation of DNA adducts from normal nucleosides/nucleobases and other components of a biological sample is essential for their sensitive detection by mass spectrometry. Although mass spectrometers are capable of detecting ions of a specified *m/z* value in the presence of other components, MS signal suppression is a common problem in DNA adduct analysis, especially in cases when the analytes are present at exceedingly low concentrations (e.g. 1 adduct per 10^{10} normal nucleosides). This problem can be ameliorated by coupling the mass spectrometer to an HPLC system for an online separation of the analyte from other components of the biological sample. A variety of HPLC stationary phases with differing selectivity are available, including reverse phase, hydrophilic interaction chromatography (HILIC), ion exchange, and mixed-mode HPLC packing. In our experience, Synergi Hydro RP columns provide excellent separation of normal and structurally modified nucleosides/nucleobases, while unusually polar DNA lesions such as 2,2-diamino-4-(2-deoxy-β-D-*erythro*-pentofuranosyl)amino]5(2H)-oxazolone (oxazolone) can be efficiently analyzed using Thermo Hypersil-Keystone Hypercarb HPLC packing.[62] Other groups have successfully employed HILIC phase for analyses of DNA adducts that are poorly retained on reverse phase HPLC columns.[41,64–66] While the latter technique affords an excellent peak shape and sensitivity when analyzing pure nucleoside standards, the technique requires that the analytes possess good solubility in non-polar organic solvents; due to the high polarity of modified DNA bases, their solubility in such solvents is often limited.

2.2 Electrospray ionization

Direct coupling of HPLC to a mass spectrometer became possible with the invention of the electrospray ionization (ESI) ion source.[67] For the first time, structurally modified nucleosides or nucleotides dissolved in water could be directly analyzed without derivatization, allowing for sensitive detection and quantitation of DNA lesions in complex biological samples. [68] During the process of ESI, the effluent from an HPLC column (or sample dissolved in an aqueous solvent) is continuously sprayed through a stainless narrow bore capillary maintained under a high voltage relative to the ion sampling orifice (3–4 kV). This leads to the formation of a mist of fine, highly charged droplets (Figure 1).[69] Heat and/or drying gas is then used to strip the solvent off the droplets, generating either protonated or

deprotonated analyte ions in the gas phase. The ions are then transported into mass analyzer where electromagnetic fields are used to determine their *m/z* values. Since the ESI process occurs under atmospheric pressure, while the mass analyzers require high vacuum conditions (10^{-5} – 10^{-8} torr), a differentially-pumped vacuum system is used to remove the solvent and other gases and produce the vacuum required for MS analysis.

The process of generating ion via ESI is a competitive and saturable process; the presence of a high concentration of ions from the sample matrix can interfere with ionization of the analyte of interest. Utilizing HPLC directly interfaced to the ESI MS (HPLC-ESI-MS) enables the analyte to be temporally separated from the other components of the biological sample. As described below, some modern HPLC systems incorporate additional online analyte enrichment steps prior to HPLC-ESI-MS analysis (column switching), reducing the need for sample cleanup and improving analytical efficiency.[70–75] In some cases, column switching allows for direct injection of unpurified biological samples (such as urine) onto HPLC-MS system.[42]

Depending on voltage polarity, ESI generates either protonated or deprotonated molecules of the analyte. The best sensitivity is achieved for compounds possessing readily ionized acidic or basic functionalities. Since DNA nuclebases are readily protonated at pH ≤ 5, structurally modified nucleobases and nucleosides are typically analyzed in the positive ion mode.[27] In some cases, negative ion formation is preferred, such as for 8-nitroguanine which contains a strongly electron withdrawing nitro group.[76] Nucleotide monophosphates are commonly ionized in the negative ion mode since they are negatively charged under neutral pH conditions.[77] Other common ionization methods such as matrix assisted laser desorption (MALDI)[78] are not discussed in the present review since they not typically used in the context of isotope dilution HPLC-MS/MS.

2.3 Mass analyzers

Mass analyzers of fundamentally different designs are available commercially, including quadrupole mass filters, ion traps, the orbitrap, and time of flight (TOF) mass spectrometers.[79] These analyzers vary in their resolution power, dynamic range, duty cycle, and MS/MS capabilities, and they differ in their cost and the ease of use (Table 1).[69] In this section, the main types of mass analyzers and their advantages and disadvantages in quantifying DNA adducts will be described. We will also discuss MS scanning methods that can be used to enhance the selectivity and sensitivity of DNA adduct detection in complex biological samples.

2.3.1 Quadrupole mass analyzers—A quadrupole mass analyzer (Q) contains four precisely engineered, parallel rods arranged symmetrically in a square array array (Figure 2). Opposite pairs of electrodes are electrically connected. A quadrupole field is created by applying a positive direct current (dc) at a potential U with a superimposing radiofrequency (rf) potential V cosωt to the first electrode pair.[69] The alternating pair of electrodes receives the dc potential of – U and an rf potential of V cosωt, which is out of phase by 180°. Ions are injected in the direction of the quadrupole rods and move through the analyzer in a sinusoidal manner. At a given value of U and V, only ions of specified mass to charge ratio (*m/z*) have stable trajectories and are able to move through the quadrupole mass filter and reach the detector, while all the other ions are lost (Figure 2).[28] To obtain a mass spectrum, the quadrupole field is changed by simultaneously scanning U and V, but keeping their ratio constant, allowing ions of each *m/z* to be passed sequentially through the quadrupole and subsequently detected. In targeted analysis, the duty cycle and the sensitivity of the quadrupole mass analyzer can be improved by scanning within a narrow *m/z* range (selected ion monitoring, SIM).

Quantitative analysis of DNA adducts is routinely performed on triple quadrupole mass analyzers ($Q_1q_2Q_3$), which contain two quadrupole mass filters (Q_1 and Q_3) separated by a quadrupole collision cell/ion guide (q_2) (Figure 3). Analyte ions (precursor ions) are selected in the first mass analyzer (Q_1) and then are accelerated into the second quadrupole (q_2) utilized as a collision cell. The collision cell is filled with helium, nitrogen or argon gas at a pressure of 0.05 – 0.5 Pa and is operated in an RF only mode, creating an electrical field transmitting ions of all mass-to-charge ratios along the axis of the quadrupole rods. Upon entering the second quadrupole, analyte ions are accelerated to a high kinetic energy resulting in collisions with neutral gas; these collisions break molecular bonds creating mass fragments, a process known as collision induced dissociation (CID). Mass fragments are accelerated out of the collision cell to enter the third quadrupole (Q3), which is scanned through a defined mass range to determine the *m/z* ratios of the product ions. Like the first quadrupole, the third quadrupole can be set to a narrow *m/z* range. Maximum sensitivity and selectivity is achieved by allowing both the first and last quadrupoles to pass coordinated pairs of precursor and fragment ions at any given point in time, a technique referred to as selected reaction monitoring (SRM, see Section 2.4).

Due to their relatively low cost, compact size, efficient ion transmission, excellent sensitivity, and the ease of operation, triple quadrupole mass analyzers are commonly used for DNA adduct analysis. They can provide some structural information about novel lesions by characteristic MS/MS fragmentation patterns and allow for sensitive detection of nucleobase adducts in biological samples. A variety of tandem mass spectrometry experiments beyond targeted SRM analysis can be conducted using triple quadrupoles (see below Section 2.4), providing useful information. However, the quadrupoles have relatively low resolving power (~ 1,000) and lower mass accuracy as compared to time-of-flight and Orbitrap mass analyzers discussed below.

2.3.2 Ion trap mass analyzers—Traditional (3D) ion traps are composed of three cylindrical electrodes: a central ring electrode and two concave endcap electrodes each containing a single orifice for either ion entrance or ejection. A three-dimensional electrical field is created within the space enclosed by the electrodes by applying superimposed rf (V) and dc (U) fields to the ring electrode. This field traps ions of a broad *m/z* range within the dimensions of the ion trap. Trapped ions oscillate within the field in a sinusoidal manner, with frequencies dependent on their specific *m/z* values. Inert gas (He) added at ~10^{-3} Torr helps stabilize the ions, minimizing undesired side reactions and preventing ion loss. To obtain a mass spectrum, the values of V or U are systematically changed to destabilize the trajectories of ions at specific *m/z* value, leading to their ejection out of the trap and into the detector. By systematically varying the V and U field, different *m/z* can be sequentially ejected and detected.[80]

In a manner conceptually similar to CID conducted with triple quadrupole mass spectrometers, 3D ion traps can be used to fragment ions captured within the field of the electrodes. However, unlike triple quadrupoles, 3D ion trap mass spectrometers can perform sequential fragmentation reactions from a single precursor, generating up to approximately 10 cycles of fragments of fragments. This ability to perform multistage tandem mass spectrometry experiments (MS^n) is an important advantage of ion trap analyzers over triple quadrupoles, as additional structural information can be elucidated. For example, the major MS/MS fragmentation pattern of most nucleosides is the neutral loss of the sugar, providing little structural information; in contrast, MS^3 experiments can reveal structural details for the modified base allowing for its identification.[81] Although the applicability of ion traps in trace quantitative analysis has been traditionally limited due to their relatively low duty cycle and non-linear response,[79] the Turesky group has reported successful use of ion traps operated in the MS^3 mode for sensitive quantitative analyses of DNA adducts induced by

heterocyclic amines.[36,82–84] Improved sensitivity, specificity, and S/N ratios were achieved by monitoring specific MS^3 transitions.

Recently, the use of a hybrid QqQtrap instrument has been reported for quantitation of DNA adducts.[36] These instruments combine the initial mass selective quadrupole (Q1) and the collision cell (q2) of a triple quadrupole system, but the third quadruple is replaced with a linear ion trap. The QqQtrap can be configured to perform SRM experiments or can be operated in enhanced product ion (EPI) mode, in which precursor ions pass through Q_1 to q_2 where they are fragmented by CID. Fragment ions are then trapped within the linear ion trap region and sequentially ejected, producing a full mass spectrum of the CID fragments without significant loss of sensitivity.[79] Hybrid QqQtrap instruments are also capable of performing two sequential fragmentation reactions (one CID fragmentation and a subsequent fragmentation in the linear ion trap). Although this MS^3 technique is not frequently used for quantitation, the technique is capable of dramatically reducing the background noise.

2.3.3 Time of flight mass analyzers—Time-of-flight (TOF) mass analyzers separate ions according to the length of time they take to migrate through a field-free flight tube. Ions leaving the ion source are accelerated to the same kinetic energy (25–50 kV) and then enter a 1–2 m long drift tube, in which they travel towards the ion detector. Ions are separated according to their velocities; ions of higher *m/z* traveling slower than the ions of lower mass. The flight time is thus inversely proportional to ion velocity, and the *m/z* of each ion can be calculated from its flight time. TOF analyzers have a broader mass range as compared to quadrupoles and ion traps and can achieve the resolving power of 10,000 or better.[79] Additionally, whereas quadrupole mass analyzers can only transmit and detect ions of a single *m/z* at any given moment, TOF analyzers simultaneously collect and measure all ions within the mass range of the mass spectrometer.

The sensitivity of TOF mass analyzers is typically ~ 10-fold lower than that of triple quadrupoles, mostly due to their inability to conduct tandem mass spectrometry experiments.[85] However, QqTOF hybrid mass analyzers coupling a mass selective quadrupole and a collision cell to a TOF analyzer can be effectively used for quantitation.[85] The QqTOF design is similar to QqQ, with the exception that the third quadrupole is replaced by a TOF mass analyzer (Figure 4). The QqTOF can be operated in SIM/SRM scanning mode similar to that of a triple quadripole, but afford an improved mass resolution for the fragment ions, allowing to increased selectivity and improved signal to noise ratios.[85,86]

2.3.4 Orbitrap mass analyzer—The Orbitrap is a type of ion trap that uses FTMS principles to achieve excellent resolution and mass accuracy.[87] Ions are injected into the Orbitrap as a discrete bunch of specific kinetic energy and are trapped between the central “spindle” electrode and the outer “barrel” electrode by application of a static electrostatic field (Figure 5). During mass analysis, ions of all *m/z* values follow a circular orbit around the z axis. The frequency of their oscillation (ω) is dependent on their *m/z* value: $\omega = [(z/m) \times k]^{1/2}$, where z is the ion charge, m is the ion mass, and k is dependent on the field strength. Ion oscillations are detected using image current and are transformed into mass spectra using Fourier transformation (FT). A great advantage of Orbitrap is its high resolving power (150,000), excellent mass accuracy (2–5 ppm), and extended *m/z* range (6,000).[69]

Until recently, the application of Orbitrap mass analyzers has been limited to proteomics applications, probably due to its high cost and limited availability. However, several groups including ours have reported the successful use of Orbitrap methodology for quantitation of small molecules,[88,89] and its high mass resolution capability have been used to improve the

sensitivity of DNA adduct detection in human samples (see Section 4.3 below).[60] Excellent sensitivity and greatly improved signal to noise ratios have been reported for complex samples containing trace amounts of DNA adducts in the presence of a large excess of normal nucleosides.

2.4 MS/MS scanning methods

As mentioned above, various MS/MS scanning modes can be used to increase the selectivity of analyte detection in the presence of other components of a biological mixture. Such experiments require two or more mass analyzers coupled in series, such as triple quadrupoles (QqQ), quadrupole-time-of-flight (Q-TOF), the LTQ-Orbitrap, or triple quadrupole-linear ion trap (QqQtrap). Available enhanced MS/MS scanning modes are: precursor ion scanning, product ion scanning, selected reaction monitoring (SRM, also known as MRM), constant neutral loss (CNL), and enhanced product ion scanning (EPI) (Scheme 5).

The product ion scan mode described above (Section 2.3.1, Scheme 5A) allows the detection of fragments originating from molecular ions of a specified *m/z*; this mode provides useful information for structural characterization of novel DNA lesions. In the precursor scan mode, the first quadrupole scans within the specified mass range, while the third quadrupole is set to a specific *m/z* value, allowing only the detection of analytes which give rise to a specific fragment (Scheme 5B). This mode is most useful when looking for unknown compounds which share a common structural feature, e.g. in global studies of DNA modifications (adductomics, see Section 4.6 below). For example, the majority of guanine adducts produce a common mass fragment corresponding to protonated guanine, and will be detected in precursor scan mode if Q3 is set to the mass of the protonated guanine fragment, *m/z* 152.1.

The best sensitivity is generally achieved in the selected reaction monitoring (SRM) mode, which is sometimes referred to as multiple reaction monitoring (MRM). In this case, ions within a user-specified narrow *m/z* range are selected in the Q1 and are accelerated into a collision cell, where their fragmentation is induced, and the resulting fragments enter into Q3 where only those of a user-specified narrow *m/z* value range pass through Q3 to be measured by the ion detector (Scheme 5C). Since the *m/z* values of both the precursor and the product ion are fixed, this leads to an increased duty cycle of the mass analyzer and greatly improves detection sensitivity (100-fold as compared to full scan methods). The SRM mode also offers superior specificity for trace analyses since only the molecules of correct molecular weight which produce the specific fragments under CID are detected.

Constant neutral loss (CNL) scanning mode (Scheme 5D) makes it possible to detect multiple molecules that fragment by releasing the same neutral fragments during MS/MS analysis. In the CNL mode, Q_1 scans all ions within a specified *m/z* range. These are fragmented in q_2. Both Q1 and Q3 are set to scan through a mass range, but the two quadrupoles are scanning with a constant mass offset. Thus, only ions with the exact user-specified difference between Q_1 and Q_3 are transmitted to the mass detector. This method is useful when looking for unknown analytes of similar structures that all lose a similar fragment (e.g., a neutral loss of deoxyribose (116 Da) from 2′-deoxynucleosides).[90]

2.5 Isotope dilution HPLC-ESI-MS/MS

Isotope dilution HPLC-ESI MS/MS (IDMS) analysis involves the use of a stable isotope labeled analogue of the analyte (e.g. ^{15}N, ^{13}C, or D) as an internal standard for quantitation. Increased reproducibility and accuracy are achieved with this approach, especially in cases when a stable isotope-labeled internal standard is introduced early in the analysis. As

discussed above, DNA adducts present in biological samples must be subjected to several processing/enrichment steps prior to MS analysis to remove the bulk of the sample matrix. Even with the most efficient enrichment methods, a fraction of the analyte is lost during processing, and recovery may vary significantly from sample to sample. Because an isotopically labeled internal standard is structurally identical to the analyte (except for the presence of the heavy isotopes in its structure), isotope dilution accounts for any sample losses during sample processing. Furthermore, since the stable isotope labeled internal standard has a similar molecular weight and identical ionization properties as the analyte, it takes into account any matrix effects and ion suppression that may occur during HPLC-ESI-MS/MS analysis. Finally, the isotopically labeled internal standard added in excess can act as a carrier to improve analyte recovery and to enhance detection sensitivity. Quantitative analysis is achieved by comparing HPLC-ESI-MS/MS peak areas in the ion channels corresponding to the analyte and the corresponding signals of the internal standard. High isotopic purity of the internal standard (> 99%) is essential, since any contamination with the unlabeled compound will lead to an exaggerated analyte response.

To ensure accurate and reproducible quantitation of the analyte of interest in the biological sample, quantitative HPLC-MS/MS methods must be validated prior to use on actual study samples. The validation process consists of fortifying blank sample matrix with fixed amounts of the internal standard and increasing amounts of the analyte. The spiked DNA samples are then processed and analyzed using the HPLC-MS/MS method being validated. The results are expressed as a plot of measured analyte concentrations versus the amounts that were spiked into the matrix (Figure 6). Spiking experiments can also be used to determine the limit of detection (LOD) (S/N ≥ 3) and the limit of quantitation (LOQ) (S/N ≥ 10) of a new method. Method accuracy and precision (intraday and interday) can be calculated by repeated analyses of spiked samples.

Some recent applications of isotope dilution HPLC-ESI-MS/MS methodologies for *in vivo* quantitation of DNA adducts are presented below. A wide range of DNA adducts have been analyzed, including those induced by aromatic amines, nitrosamines, epoxides, and polycyclic aromatic hydrocarbons present in the air, food, drink, cigarette smoke, and occupational settings. Additional examples are summarized in Table 2, listing the major method characteristics, e.g. the source of DNA, sample purification strategy, and the LOD values. Table 2 is not intended as a complete list, but rather is a representative sampling illustrating the power of IDMS in DNA adduct detection.

3 Recent examples of HPLC-ESI-MS/MS analyses of DNA adducts

3.1 Natural products/drugs

Mass spectrometry has been used to analyze a variety of nucleobase adducts induced by DNA-alkylating drugs and natural products (Chart 1). Quantitative analysis of drug-induced DNA adducts can be used to correlate the molecular dose of the drug with the therapeutic effects, in order to evaluate patient's response to chemotherapy, to examine the origins of resistance and toxicity, and to determine the impact of other co-administered drugs on DNA adduct levels. For example, Van den Driessche and coworkers have developed an isotope dilution HPLC-ESIMS/MS method for quantifying *N7*-2′-deoxyguanosine adducts of melphalan (mel-dGuo) (Chart 1).[91] Melphalan is a chemotherapeutic nitrogen mustard agent used in the treatment of multiple myelomas, ovarian carcinoma, and other malignancies. Wistar rats were given 10 mg/kg melphalan by IV. The rats were euthanized either 10 or 25 h after dosing, and DNA was isolated from liver, kidney, and bone marrow tissues of the treated animals. DNA samples were spiked with 10 pg of [$^{15}N_5$]-meldGuo as an internal standard (IS) and were then enzymatically hydrolyzed. DNA hydrolysates were analyzed by capillary HPLC-ESI-MS/MS using a triple quadrupole mass spectrometer operated in the

SRM mode[67] monitoring the transitions *m/z* 536 → 240 and *m/z* 541 → 425 corresponding to the neutral loss of deoxyribose from protonated molecules of the analyte and [$^{15}N_5$] internal standard, respectively. At 24 hours following a single exposure of melphalan, the concentrations of mel-dGuo were 1 adduct/4.7 × 10^6 nucleosides in the bone marrow, 1 adduct/10^7 nucleosides in the kidney, and 1 adduct/2.7 × 10^8 nucleosides in the liver.[91]

Our laboratory has developed a quantitative method for *N,N-bis*[2-(*N7*-guaninyl) ethyl] amine DNA-DNA cross-links (G-NOR-G, Chart 1) induced by another nitrogen mustard drug, cyclophosphamide (CPA).[92] CPA is commonly used in the treatment of lymphoma, leukemia, and solid tumors.[93,94] The drug requires metabolic activation to phosphoramide mustard, which sequentially alkylates the N7 positions of two guanine bases to form 1,3-interstrand DNA-DNA crosslinks (G-NOR-G). These cross-links are strongly cytotoxic and are thought to be responsible for the biological activity of CPA. DNA was extracted from peripheral blood lymphoblasts of cancer patients receiving 50–60 mg/kg CPA intravenously. Extracted DNA samples (5–20 μg) were spiked with an internal standard of [$^{15}N_{10}$]-G-NOR-G and subjected to neutral thermal hydrolysis, releasing G-NOR-G nucleobase adducts from the DNA backbone. Following solid phase extraction, G-NOR-G conjugates were quantified by capillary HPLC-ESI-MS/MS in the selected reaction monitoring mode. The highest numbers of G-NOR-G adducts (up to 18 adducts per 10^6 normal nucleotides) were observed 4–8 h following CPA administration; adduct levels gradually decreased over time, probably due to their spontaneous depurination, active repair, and white blood cell turnover. [92] Interestingly, CPA-DNA adduct concentrations were elevated in patients with Fanconi Anemia as compared to non-Fanconi Anemia cancer patients; this is consistent with compromised interstrand DNA cross-link repair in Fanconi Anemia.[95]

Cisplatin is another useful chemotherapeutic agent widely used in the treatment of ovarian, testicular, and bladder cancer. The major DNA adducts induced by cisplatin treatment are 1,2 guanine-guanine intrastrand cross-links between the N7 positions of neighboring guanines [CP-d(GpG)] (Chart 1). Several methodologies have been employed for assessing cisplatin-DNA damage, including immunohistochemical assays, 32P postlabeling, ICP-MS, and tandem mass spectrometry.[96,97] Baskerville-Abraham et al. have developed a highly sensitive and specific isotope dilution UPLC-MS/MS assay for quantifying 1,2 guanine-guanine intrastrand cisplatin adducts [CP-d(GpG)].98 DNA was digested enzymatically and spiked with $^{15}N_{10}$-CP-d(GpG) internal standard. DNA extracts were enriched by offline HPLC with an Oligo-RP column prior to UPLC-MS/MS analysis using Waters Aquity HSS T3 UPLC column. This method required 25 μg of DNA per injection and produced a limit of quantification of 3 fmol or 3.7 adducts/10^8 nts. CP-d(GpG) were detected in the kidney, liver, and colon DNA from laboratory mice dosed with 7 mg/kg cisplatin.[98]

While the previous examples have discussed DNA adduct formation resulting from exogenously administered DNA-reactive drugs, naturally occurring estrogen hormones are known to induced DNA adducts potentially contributing to the development of breast cancer.[99] Estrogens are metabolized to electrophilic quinone methides which can react with DNA to form potentially promutagenic adducts. For example, the estrogen metabolite estradiol-3,4-quinone (E2-3,4-Q) produces spontaneously depurinating 4-hydroxyestradiol-N7-guanine (4-OHE_2-N7-guanine) adducts (Chart 1). Bransfield et al. employed an isotope dilution mass spectrometry based technique to quantify endogenous 4-OHE_2-N7G adducts in human urine.[38] Urine samples were purified by three sequential SPE clean-up steps using MCX columns and Bond Elut C18 cartridges. The authors found 4-OHE_2-N7G concentrations in the urine of premenopausal women at levels between 70–300 ng/mL.[38]

A variety of naturally occurring environmental toxins are known to produce DNA adducts. Aristolochic acid (AA) is a plant toxin that causes nephrotoxicity and urothelial cancer.

Exposure to AA occurs upon consuming contaminated grain and *Aristolochia* and *Asarum* plants which are commonly used in Chinese herbal medicine. Lin and collaborators employed ultra-performance liquid chromatography-tandem mass spectrometry (UPLC-MS/MS) to quantify 7-(deoxyadenosin-N^6-yl)aristolactam I (dA-AAI) adducts (Chart 1) in exfoliated urothelial cells of rats dosed with aristolochic acid.[100] Exfoliated cells were collected from urine samples, and cellular DNA was isolated and subjected to enzymatic digestion and solid-phase extraction. dA-AAI adducts were quantified in selected reaction monitoring mode, however, isotopically labeled internal standard was not available. The method possessed a detection limit of 1 ng/mL, which allowed for sensitive detection of dA-AAI in exfoliated urothelial cells from treated animals. Daily oral dosing of AAI for one-month (10 mg/kg/day) resulted in 2.1 ± 0.3 dA-AAI adducts per 10^9 normal adenines.

3.2 Aromatic amine adducts

Aromatic amines such 4-aminobiphenyl, 2-amino-3-methylimidazo[4,5-*f*]quinolone (IQ), and 2-amino-1-methyl-6-phenylimidazo[4,5-b]pyridine (PhIP) are known human carcinogens present in tobacco smoke, cooked meat, and hair dyes. 4-aminobiphenyl (4-ABP) is activated via N-oxidation to *N*-hydroxy-aminobiphenyl, which is capable of binding to DNA to form N-(deoxyguanosine-8-yl)-4-ABP adducts (C8-dG-4-ABP, Chart 2).[101] Human exposure to 4-ABP from tobacco smoke is suspected to contribute to the initiation of pancreatic cancer. A method for quantifying 4-ABP-DNA adducts in human pancreatic tissues has been developed by Ricicki and coworkers.[101] Pancreatic tissue from 12 donors, 6 male and 6 female, was used in this study. Isolated DNA was fortified with a deuterated internal standard (C8-dG-4-ABP-d_9) and purified by solid phase extraction on Isolute C18 cartridges. Samples were analyzed by LC-μESI-MS/MS using a Finnigan TSQ Quantum AM triple quadrupole mass spectrometer operated in positive ion mode. Quantitation was performed by SRM monitoring of the transitions *m/z* 435 → 319 (analyte) and *m/z* 444 → 328 (IS) using a calibration curve constructed with synthetic standards. dG-C8-ABP were quantified in six out of twelve samples, and no correlation was identified between adduct levels and donor age, gender, or smoking status. In fact, a male nonsmoker had the highest adduct levels at 60/10^8 nucleotides.[101]

2-amino-3-methylimidazo[4,5-*f*]quinoline (IQ) is a heterocyclic aromatic amine found in cigarette smoke as well as in cooked meat and fish. IQ is carcinogenic in laboratory animals, suggesting that it could contribute to human cancer development. Therefore, accurate and sensitive methods are needed to monitor for DNA adducts of IQ in samples from exposed laboratory animals and humans. The major DNA adduct formed upon exposure to IQ is C8-dG-IQ (Chart 2). Soglia and colleagues have developed an HPLC-μESI-MS/MS method quantifying C8-dG-IQ in hepatic DNA of rats exposed to 0.05 to 10 mg/kg of IQ.[102] Isolated DNA (300 μg) was fortified with an internal standard of C8-dG-IQ- d_3 and enzymatically digested to deoxynucleosides. The analyte was then enriched by solid phase extraction prior to LC-μESI-MS analysis using a TSQ700 triple quadrupole mass spectrometer operated in the ESI^+ SRM mode. The limit of quantitation of this method was determined as 6 fmol/300 μg DNA. In exposed rats, C8-dG-IQ was detected at levels of 3.5 adducts/10^8 nucleotides following a 0.05 mg/kg dose of IQ, and at 39 adducts/10^8 nucleotides following a 10 mg/kg dose of IQ. These findings are comparable to those obtained in ^{32}P-postlabelling experiments.[103] However, mass spectrometry-based detection results in a more specific and accurate quantitation of IQ-DNA adducts.

More recently, the same group has reported an HPLC-ESI-MS/MS method to detect DNA adducts of another heterocyclic aromatic amine also present in tobacco smoke, 2-amino-3,8-dimethylimidazo-[4,5f]quinoxaline (MeIQx).[104] Like IQ, MeIQx forms adducts at the C8 and the N^2 positions of guanine, producing C8-dG-MeIQx and N^2-dG-MeIQx, respectively (Chart 2). Male rats were treated with 0.05, 0.5, or 10 mg of MeIQx per kg of body weight

and sacrificed 24 h post dosing. DNA was isolated from excised livers. Isotopically labeled internal standards, C8-dG-MeIQ-d_3 and N^2-dG-MeIQ-d_3, were added to DNA samples (250 μg). Following enzymatic digestion, MeIQx-DNA adducts were isolated by solid phase extraction prior to HPLC-ESI-MS/MS analysis using a Finnigan TSQ 7000 triple quadrupole mass spectrometer operated in the SRM mode. The limit of detection of the assay was 0.5 – 1 adduct/10^8 bases. No adducts were detected at the lowest dose. Exposure to 0.5, or 10 mg IQ/kg body weight resulted in 0.45 and 3.06 adducts/10^7 bases, respectively.[104]

Bessette et al.[36] employed a liquid chromatography-electrospray ionization/multistage tandem mass spectrometry methodology (HPLC-ESI/MS/MS^n) for detecting dG-C8 adducts of 2-amino-1-methyl-6-phenylimidazo[4,5-b]pyridine (PhIP), MeIQx, and 4-ABP in saliva samples from 37 human volunteers. Their experiments employed MS^3 consecutive reaction monitoring with a linear quadrupole ion trap (LIT) mass spectrometer (MS). DNA adducts of PhIP (dG-C8-PhIP) were found most frequently: these adducts were detected in saliva samples of 13 of 29 smokers and 2 of 8 never-smoking volunteers. Adduct levels ranged from between 1 and 9 adducts per 10^8 normal nucleotides in both smoking and non-smoking groups. The authors[36] concluded that human saliva is a promising biological fluid for monitoring DNA adducts from tobacco and dietary carcinogens when analyzed using MS^3 IT MS techniques. The same methodology was recently applied to DNA isolated from human breast tissue.[84] However, only 1 of 70 breast biopsy samples contained measurable PhIP-DNA adducts (3 adducts per 10^9 nucleotides),[84] suggesting that PhIP and 4-ABP are not major DNA-damaging agents in mammary tissue.

3.3 Nitrosamine adducts

Nitrosamines can be present as contaminants in a number of consumer products including food (cured meats, bacon), beverages (beer), tobacco products, rubber products, and cosmetics. N-nitrosodiethanolamine (NDELA) and N-nitrosodimethylamine (NDMA) are classified as category 1B carcinogens. NDELA is metabolically activated forming two electrophilic species: 2-hydroxyethyldiazonium ion and glyoxal,[105] which react with DNA to form O^6-2-hydroxyethyl-2′-deoxyguanosine (OHEdG) and glyoxaldeoxyguanosine (gdG), respectively (Chart 3). In a study conducted by Dennehy and Loeppky,[105] male rats were given a single injection of either 0.2, 0.4, or 0.8 mmol NDELA/kg body weight. 4 hours post dose, the animals were sacrificed, and their livers removed for DNA extraction. Samples containing 400 μg DNA were enzymatically hydrolyzed, spiked with the corresponding internal standards (OHEdG-d_4 and ^{13}C, $^{15}N_2$-gdG), and filtered prior to HPLC-ESI^+-MS/MS analysis in SRM mode. No adducts were observed in animals treated with 0 or 0.2 mmol/kg of NDELA, and detectable but unquantifiable adduct levels were observed in the 0.4 mmol/kg dosing group. Treatment with 0.8 mmol/kg NDELA resulted in 4.4–11 gdG adducts/10^6 nucleotides, while OHEdG concentrations were 0.35 – 0.87 adducts/10^6 nucleotides.[105] These values are comparable to those previously detected by ^{32}P-post-labeling.[106]

The tobacco-specific nitrosamine, 4-(methylnitrosamino)-1-(3-pyridyl)-1-butanone (NNK), is a potent lung carcinogen in rodents and is hypothesized to play a central role in smoking-induced lung cancer.[5] NNK requires metabolic activation to 4-hydroxy-1-(3-pyridyl)-1-butanone (HPB), which reacts with DNA to form multiple pyridyloxobutyl (POB) adducts (Chart 3). Similar pathways act upon the NNK metabolite NNAL to produce pyridylhydroxybutyl (PHB)-DNA adducts (Chart 3). Isotope dilution HPLC-ESI-MS/MS methods have been developed to quantify four pyridyloxobutylated adducts of NNK in animals treated with NNK – O^6-[4-(3-pyridyl)-4-oxobut-1-yl]-2′-deoxyguanosine (O^6-POB-dGuo), 7-[4-(3-pyridyl)-4-oxobut-1-yl]guanine (7-POB-Gua), O^2-[4-(3-pyridyl)-4-oxobut-1-yl]cytosine (O^2- POB-Cyt), O^2-[4-(3-pyridyl)-4-oxobut-1-yl]thymidine (O^2-POB-dThd)

(Chart 3).[107] Liver and lung DNA extracted from rats exposed to saline, 5.2 mg/kg NNK, or 20.4 mg/kg NNK for 4 days was subjected to enzymatic hydrolysis. POB-DNA adducts were isolated by SPE on Strata-X cartridges prior to HPLC-ESI-MS/MS analysis. The LOD for adducts spiked into in 1 mg of DNA were 3 fmol for 7-POB-Gua, 1 fmol for O^6-POB-dGuo, 100 amol for O^2-POB-dThd, and 2 fmol for O^2-POB-Cyt. 7-POB-Gua and O^2-POB-dThd were most abundant adducts, followed by O^2-POB-Cyt and O^6-POB-dGuo.[107] All NNK adducts were more abundant in the liver than the lung, with the exception of O^6-POB-dGuo, which was more abundant in the lung. The same adducts were observed in rats chronically exposed to NNK, (*R*)-NNAL, and (*S*)-NNAL, however, NNAL exposure resulted in greater adduct levels in the lung as compared to the liver.[108] No significant differences in adduct levels were observed between NNK and (*S*)-NNAL treated rats; however, (*R*)-NNAL exposed rats had much lower amounts of adduct. A similar methodology was employed to quantify PHB adducts in animals following exposure to NNAL[109] and to compare POB and PHB adduct levels in mitochondrial DNA and nuclear DNA of NNK exposed rats.[110]

3.4 Exocyclic DNA adducts

Exocyclic etheno-dG, etheno-dC, and etheno-dA DNA adducts (Chart 4) can be created endogenously as a result of lipid peroxidation or can form upon exposure to industrial chemicals such as vinyl chloride.[111] Etheno DNA adducts are promutagenic and may be involved in the initiation of cancer.[13] Loureiro and colleagues have developed an HPLC-ESI-MS/MS method to quantify endogenous 1,N^2- etheno-dG adducts.[112] DNA was isolated from the livers of untreated female Wistar rats. DNA was spiked with [$^{15}N_5$]-1,N^2εdGuo as an internal standard, and enzymatically digested prior to HPLC-ESI-MS/MS analysis. A Quattro II mass spectrometer was operated in the ESI^+ SRM mode. This method allowed for detection of basal levels of 1,N^2-εdGuo adducts in untreated rat liver DNA at levels of 5.22 adducts/10^7 nucleotides. Commercial calf thymus DNA contained 1.7 adducts/10^7 nucleotides.[112]

Exocyclic 1,N^6-etheno-dA adducts (εdA, Chart 4) can form endogenously or upon exposure to vinyl carbamate epoxide, the reactive metabolite of urethane. Ham and collaborators developed a method to quantify εdA in tissues of laboratory mice treated with urethane.[61] Their method employed an immunoaffinity chromatography step prior to isotope dilution HPLC-ESI-MS/MS. The LOQ of the method was 2.5 fmol, and 2 adducts/10^8 normal dA were detected in untreated ctDNA. The method was used to compare εdA levels in alkyladenine DNA glycosylase (*Aag*) deficient animals and wild type animals. The half-life of εdA in lung DNA of *Aag* null animals was 185 h, while it was only 28 h in wild-type animals, suggesting that εdA is repaired by *Aag*.[61]

Zhang et al. employed an isotope dilution capHPLC ESI-MS/MS method to quantify 1,N^2-propanodeoxyguanosine adducts of acrolein in human leukocyte DNA; the authors measured (6R/S)-3-(2′-deoxyribos-1′-yl)-5,6,7,8-tetrahydro-6-hydroxypyrimido[1,2-a]purine-10(3H)one (R-OH-Acro-dGuo) and (8R/S)-3-(2′-deoxyribos-1′-yl)-5,6,7,8-tetrahydro-8-hydroxypyrimido[1,2-a]purine-10(3H)one (Acro-dGuo) (Chart 4).[113] The potential for the artifactual formation of OH-Acro-dG was minimized by employing a Ficoll-Hypaque double density gradient to isolate leukocytes from blood and by adding glutathione to buffers to scavenge any acrolein present in H_2O. No significant difference between the total AcrdGuo levels was detected in smokers (7.4 ± 3.4 adducts/10^9 nucleotides) versus nonsmokers (9.8 ± 5.5 adducts/10^9 nucleotides), suggesting that glutathione conjugation efficiently removes acrolein from the body of cigarette smokers, thereby preventing the formation of OH-Acro-dG adducts.[113]

3.5 Ethanol/acetaldehyde/formaldehyde adducts

Alcohol consumption is a risk factor for cancers of the upper aerodigestive tract, the breast, colon, and the liver. This has been attributed to the formation of acetaldehyde, reactive oxygen species (ROS), and 1-hydroxyethyl radicals following ethanol metabolism. Specifically, hydroxyethyl radicals have been shown to form C8-(1-hydroxyethyl)guanine adducts (C8(1- HE)-gua, Chart 5). Nakao and colleagues have developed an isotope dilution HPLC-ESI-MS/MS method to quantify C8(1-HE)gua in rats exposed to ethanol.[114] Male Sprauge-Dawley rats were treated via intergastric intubations of either water or ethanol (5g/kg); 3 or 12 hours later, the animals were sacrificed, and livers were removed for RNA and DNA extraction. Nucleic acids were hydrolyzed with 1N HCl to release purines, fortified with ^{13}C, $^{15}N_2$-C8-(1-HE)gua as an internal standard, and purified by offline HPLC. HPLC fractions containing C8(1-HE)gua were concentrated and analyzed by HPLC-ESI$^+$MS/MS using a Micromass QuattroII triple quadrupole mass spectrometer operated in the SRM mode. Quantitation was performed using a calibration curve constructed using synthetic standards. Although C8(1-HE)gua adducts were detected in RNA and DNA of treated rats, similar adduct levels were observed in untreated rats.[114]

Wang and colleagues have developed an HPLC-ESI-MS/MS method for quantitation of acetaldehyde-induced adducts in human liver DNA.[115] Acetaldehyde can form N^2-ethylidene-dGuo adducts at the N^2 position of guanine in DNA (Chart 5). This adduct is unstable on the nucleoside level, but can be stabilized by reduction to the stable N^2-ethyl-dGuo by treatment with a reducing agent such as $NaBH_3CN$. Synthetic standards of N^2-ethyl-dGuo and [$^{15}N_5$]-N^2-ethyl-dGuo were prepared for quantitation. DNA was homogenized in a buffer containing $NaBH_3CN$ to minimize artifact formation and to stabilize the adduct to its reduced form, enzymatically digested, and analyzed by LC-ESI-MS/MS. This method has recently been applied to investigate effects of alcohol consumption on acetaldehyde-DNA adduct formation in oral cells of individuals exposed to increasing doses of alcohol. Levels of N^2-ethyl-dGuo increased in a dose-response manner, reaching 100-fold levels of the baseline within 4 hours after consumption of each alcohol dose. These results provide the first conclusive evidence linking exposure to a lifestyle carcinogen to DNA adduct formation in humans.[116]

Like acetaldehyde, formaldehyde is a toxic and mutagenic aldehyde that is present in cigarette smoke. N^2-hydroxymethyl-dG adducts are produced when formaldehyde reacts with DNA, but can also be generated endogenously. Lu et al. recently reported the use of isotope dilution nano-UPLC-MS/MS to separately quantify endogenous and exogenous N^2-HM-dG adducts in nasal DNA or laboratory rats exposed to 0.7, 2, 5.8, 9.1, or 15.2 ppm [$^{13}CD_2$] formaldehyde for 6 h.[25] At low formaldehyde exposures (≤15.2 ppm), endogenous, background adducts comprised more than 99% of the total N^2-HM-dG, but contributions of exogenous adducts increased in a dose-dependent manner following exposure to formaldehyde. Interestingly, exogenous formaldehyde-DNA adducts were formed in a nonlinear fashion, with 21.7-fold increase in exposure causing a 286-fold increase in N^2-HM-dG adducts.[25]

3.6 Polycyclic aromatic hydrocarbon adducts

Incomplete combustion of organic materials leads to the formation of polycyclic aromatic hydrocarbons (PAH). Hundreds of PAHs have been identified in automobile exhaust, cigarette smoke, and coal tar; many of these compounds are carcinogenic to animals and humans. The most widely studied carcinogenic PAH is benzo[*a*]pyrene. Beland and co-workers employed isotope dilution HPLC-ESI-MS/MS for quantitation of benzo[*a*]pyrene (BP)-DNA adducts *in vivo*.[117] BP is metabolically activated to *trans*-7,8-dihydroxy-*anti*-9,10-epoxy-7,8,9,10- tetrahydro-benzo[*a*]pyrene (BPDE), which can react with DNA to

form adducts (e.g. 10- (deoxyguanosin-N^2-yl)-7,8,9-trihydroxy-7,8,9,10-tetrahydrobenzo[a]pyrene (N^2-BPDE-dG, Chart 6). Previously, N^2-dG-BPDE-dG adducts have been detected via ^{32}P-postlabelling and immunological methods; however, using mass spectrometry, these adducts could be detected with greater accuracy and in as little as 10–100 μg DNA. The HPLC-ESI-MS method developed by Beland et al. was used to analyze BPDE adducts *in vitro* and in mouse and human lung samples.[117] Enzymatically hydrolyzed DNA samples (100 μg) were spiked with 10 pg of the internal standard and loaded onto a capillary HPLC coupled to a quadrupole mass spectrometer. N^2-BPDE-dG adducts were quantified using selected reaction monitoring of *m/z* 570 → 257 for the analyte and the corresponding transition *m/z* 577 →264 for the $^{15}N_5$ labeled internal standard. Using this method, the Beland group was able to detect 7 dG-BPDE adducts/10^8 nucleotides in mice treated with 0.5 mg of [7,8-3H]BP. They also analyzed DNA extracted from tissues of smokers, nonsmokers, and former smokers. BP adducts were only detected in one sample, where they were present at 1.9 adducts/10^8 nucleotides; BP adduct levels in human liver tissue were below the detection limit of this method.[117] Higher adduct amounts (23.7 adducts/10^8 nt) were detected by ^{32}P-postlabelling for the same samples; the authors suggested that N^2-dG-BPDE-dG may represent a small percentage of adducts formed by PAH and only a fraction of the adducts detected by other, less specific methods.

Chen and coworkers studied the BP-induced DNA adducts using isotope dilution HPLC-ESI-MS/MS.[118] This work focused on N7-(benzo[*a*]pyrene-6-yl)guanine adducts (BP-6-N7Gua, Chart 6), which are formed by the one electron oxidation of BP and subsequent radical reaction with guanine. These adducts can be depurinated and excreted in urine as free bases; therefore, Chen's group presented a method for quantifying BP-6-N7Gua (Chart 6) in human urine for use as a biomarker of BP exposure and cancer risk. $^{15}N_5$-labeled BP-6-N7Gua was used as an internal standard for HPLC-ESI-MS/MS. Urine samples (15 mL) were spiked with 1.5 pmol of $^{15}N_5$-labeled internal standard, extracted with acetonitrile, purified by a two-step SPE process, and analyzed by HPLC-ESI-MS/MS. A triple quadrupole mass spectrometer was operated in the SRM mode using the mass transitions of the analyte (*m/z* 402 → 252) and the $^{15}N_5$-internal standard (*m/z* 407 → 252). Validation of the method was performed using blank urine samples spiked with 0.2, 1, and 2 pmol BP-6-N7Gua and 1.5 pmol IS. Method accuracy was between 94–102 % with a 2–4 % error. The method was used for the analysis of a urine sample from a coke oven worker; in this sample 6 fmol BP-6-N7Gua per mg creatinine equivalents were detected. This method allows for urinary BP-guanine adducts to be analyzed as a biomarker of risk in workers exposed to BP.[118]

1-Methylpyrene (1-MP) is an alkylated PAH that requires metabolic activation to its reactive form, 1-sulfooxymethylpyrene (1-SMP). Monien et al. compared the techniques of IDMS and ^{32}P-postlabeling for their ability to quantify 1-methylpyrene adducts of adenine and guanine (MP-dAdo and MP-dG in Chart 6) in tissues of rats treated with 1-SMP.[119] Using nanoflow UPLC and selected reaction monitoring (SRM) on a triple quadrupole MS, the detection limits were 3 and 0.6 molecules of MP-dGuo and MP-dAdo per 10^8 nucleosides, respectively. Interestingly, 3.4 fold greater amounts of adducts were observed by the IDMS methods than by ^{32}P-postlabeling.[119] Furthermore, the limit of detection for ^{32}P-postlabeling experiments were 2–9 fold higher than those for IDMS.

3.7 Epoxide-derived nucleobase adducts

Many environmental and occupational carcinogens are bioactivated by cytochrome P450 to epoxide species capable of reacting with nucleophilic sites on proteins and DNA. For example, 1,3-butadiene (BD) is an industrial chemical and a common environmental toxin present in urban air and cigarette smoke. It is metabolized to epoxybutene (EB), diepoxybutane (DEB), and epoxybutanediol (EBD). DEB is suspected to be the ultimate

carcinogenic species of BD due to its ability to form genotoxic DNA-DNA cross-links and exocyclic adducts.[120] The major BD adduct identified *in vivo* is N7-trihydroxybutyl-guanine (THBG); these adducts are spontaneously released as free bases, leaving behind abasic sites. IDMS methods have been developed for the analysis of THBG adducts in liver and lung DNA of rodents exposed to BD by inhalation.[121] Quantitative analyses were conducted in the SRM mode by monitoring the transitions *m/z* 256 → 152 for THBG and *m/z* 260 → 156 for $^{13}C_4$-THBG (internal standard). Slightly higher levels were observed in mice than rats at same exposure concentrations.[46,122] The differences in levels of adducts between species may be due to increased metabolic activation and lower rates of detoxification of BD in mice as compared to rats.

Our group has developed sensitive analytical methods for DNA-DNA cross-links and exocyclic DNA adducts induced by diepoxybutane (DEB).[123] Multiple DNA-DNA cross-links of DEB have been characterized by our laboratory *in vitro*; these include 1,4-*bis*-(guan-7-yl)-2,3- butanediol (*bis*-N7G-BD), 1-(guan-7-yl)-4-(aden-1-yl)-2,3-butanediol (N7G-N1A-BD), 1-(guan-7-yl)-4-(aden-3-yl)-2,3-butanediol (N7G-N3A-BD), 1-(guan-7-yl)-4-(aden-7-yl)-2,3-butanediol (N7G-N7A-BD), and 1-(guan-7-yl)-4-(aden-6-yl)-2,3-butanediol (N7G-N^6A-BD).[124,125] Quantitative capillary HPLC-ESI^+-MS/MS methods have been developed to analyze these adducts *in vivo*,[45,49] while the exocyclic deoxyadenosine adducts of DEB, *1,*N^6-(1- hydroxymethyl-2-hydroxypropan-1,3-diyl)-2′-deoxyadenosine (*1,* N^6-αHMHP-dA) and *1,*N^6-(2- hydroxy-3-hydroxymethylpropan-1,3-diyl)-2′-deoxyadenosine (*1,* N^6-γHMHP-dA), were analyzed by a capillary column switching method (see Section 4.4).[70] *Bis*-N7G-BD, N7G-N1A-BD, and *1,* N^6-γHMHP-dA were detected in liver DNA of mice exposed to 6.25 – 625 ppm BD. The concentrations of *bis*-N7G-BD were about 10-fold greater than those of N7G-N1A-BD, and *1,* N^6-γHMHP-dA were less abundant.[24,45,49] NanoLC-nanoMS methods were required to detect N7G-N1A-BD in liver DNA of rats and in mice exposed to BD concentrations below 625 ppm.[24] More recently, we reported nanoHPLC-nanoMS analysis of *bis*-N7G-BD in tissues of mice treated with sub-ppm concentrations of BD that approach occupational exposure limits.[63]

Mass spectrometry methodology was employed to evaluate the persistence and repair of bifunctional DEB-DNA adducts in tissues of mice and rats exposed to BD by inhalation.[34] The half-lives of the most abundant cross-links, *bis*-N7G-BD, in mouse liver, kidney, and lungs were 2.3 –2.4 days, 4.6 –5.7 days, and 4.9 days, respectively. In contrast, tissue concentrations of the minor DEB adducts, N7G-N1A-BD and 1,N^6-HMHP-dA, remained essentially unchanged during the course of the experiment, with an estimated $t_{1/2}$ of 36–42 days. As a result, the concentrations of N7G-N1A-BD in tissues 10 days post exposure exceeded those of *bis*-N7G-BD. [34] No differences were observed between DEB-DNA adduct levels in BD-treated wild type mice and the corresponding animals deficient in nucleotide excision repair or methyl purine glycosylase, suggesting that DEB-DNA adducts are not repaired by these pathways.

Acrylamide (AM) is another important industrial and environmental chemical. AM is a component of cigarette smoke and many commonly consumed foods. Animal studies have led some to believe that AM is carcinogenic.[126] AM is metabolized to the reactive epoxide derivative glycidamide (GA). Gamboa da Costa and colleagues administered a single injection of AM or GA (20 mg/kg) to adult and three-day-old mice.[127] Six hours post injection, animals were sacrificed, and their liver, lung, and kidneys were removed for DNA extraction. DNA was spiked with $^{15}N_5$-labeled internal standards, subjected to neutral thermal hydrolysis to release N7-Gua, N7-Ade, and N3-Ade adducts (N7-GA-Gua and N3-GA-Ade in Chart 7), and purified by size exclusion prior to capillary HPLC-ESI-MS/MS analysis using a Quattro Ultima triple stage quadrupole mass spectrometer operated in the ESI^+ SRM mode. Calibration curves with isotopically-labeled internal standards were

constructed for accurate adduct quantitation. In all cases, the authors[127] observed 100-fold greater concentrations of N7-(2-carbamoyl-2-hydroxyethyl)guanine (N7-GA-Gua) adducts than N3-(2-carbamoyl-2-hydroxyethyl)adenine (N3-GA-Ade) adducts. Adult mice contained 1.2 – 1.5 times more GA adducts than AM adducts. Interestingly, three-day-old mice had 5–7 times more adducts when treated with GA due to neonates lacking P450 activity to metabolize AM to GA.[127]

4. New analytical approaches for DNA adduct analysis

Several novel approaches in mass spectrometry have been recently developed to improve the sensitivity and specificity of MS-based methodologies for quantifying DNA adducts *in vivo*. In this section, we will discuss four such approaches: nanospray MS, high resolution mass spectrometry, column switching, and chip-MS. Nanospray mass spectrometry improves the sensitivity of HPLC-MS methods by using lower HPLC flow rates, which improves ionization efficiency and reduces the possibility of significant ion suppression. High resolution mass spectrometry dramatically improves the specificity of DNA adducts detection by targeting compounds by specific accurate mass. Column switching methods directly couple sample clean-up with HPLC separation prior to MS analysis, potentially eliminating offline cleanup steps, reducing time and labor, and preventing sample losses. Chip-MS is the use of a microchip with a electrospray needle or nano column embedded in it. This method increases sample throughput as it eliminates the HPLC component of MS, allowing samples to be directly infused through a nanospray needle into the mass spectrometer.[128]

4.1 Capillary HPLC-nanospray MS

Capillary HPLC-nanospray ionization mass spectrometry (capLC-nanoESI) involves the use of a capillary HPLC column (0.3–0.8 mm I.D.) and flow rates of 5–10 μL/min with a flow splitter and a nanoelectrospray ion source. A capLC-nanoESI-IDMS/MS method has been developed for quantifying estrogen-modified adenine adducts in human breast tissue.[129] Estrone can be metabolized by cytochrome P450 to form 3,4-catechol-estrogen quinone, which in turn can directly react with DNA to form 4-hydroxyestrogen-2-*N*7-guanine (4-OHE_2-N7Gua) and 4- hydroxyestrogen-1-*N*3-adenine (4-OH-E_1-*N*3-Ade) adducts (see Section 3.1 and Chart 1). The developers of this method[129] employed an LCQ Deca ion-trap mass spectrometer (Thermo Scientific) interfaced to a capillary HPLC (Waters Corp.). A custom-packed Luna column (3 μm, 120 mm × 75 μm) with a 15 μm PicoFrit (New Objective, Inc.) nano tip was used for analyses. The initial capillary flow of 8 μL/min was split to achieve a flow rate of 270 nL/min at the tip of the nanospray source. The LOD of the method was 5 fmol 4-OH-E_1-*N*3-Ade/g tissue. DNA was extracted from tissue, and the enzymatic digest was enriched by SPE and offline HPLC prior to capLC-nanoESI-MS/MS analysis. Breast tissues from 6 patients (3 controls, 3 breast cancer patients) were analyzed. 4-OH-E_1-*N*3-Ade was detected in all 6 samples; however, the study size was not large enough to determine whether 4-OH-E_1-*N*3-Ade levels are greater in cancer patients than in controls. [129]

Liu et al. have developed a capLC-nanoESI method for monitoring acrolein-dG adducts (Acro-dG, Chart 4) in DNA from human brain tissue.[130] As discussed above (Section 3.4), Acro-dG adducts are formed from the reaction of a lipid peroxidation product, hydroxyl-2-nonenal, with guanine nucleobases in DNA. Brain tissues of Alzheimer's disease (AD) patients contain increased concentrations of lipid peroxidation products such as hydroxyl-2-nonenal. Liu et al. analyzed Acro-dG in DNA extracted from brain tissue samples of AD patients and matched controls.[131] An UltiMate capillary/nano LC system was interfaced with a Bruker Daltonics ion trap (Bruker nanospray source, 50 μm i.d. tapered stainless steel emitter). Using these methods, the LOD for Acro-dG was 31 amol, which enabled the

authors[131] to observe a significant increase in Acro-dG adduct concentrations in brain tissue samples from AD patients (5150 ± 640 Acro-dG/10^9 nts) versus the corresponding controls (2800 ± 460 Acro-dG/10^9 nts).

A similar capLC-nanoMS methodology was used by the same group to quantify *trans*-4-hydroxy-2-nonenal (HNE) - derived cyclic 1,N^2-propano-deoxyguanosine adducts (HNE-dG, Chart 4).[130] The LOD of the method was 24 amol for pure HNE-dG standard, or 40 adducts/10^9 nts in matrix.[130] It had previously been shown that HNE levels are elevated in the brains of AD patients due to increased lipid peroxidation, so Liu et al.[130] compared HNE-dG levels in control and AD brain samples. However, no statistically significant differences were observed, suggesting that unlike Acro-dG, HNE-dG is not a useful biomarker of oxidative stress in AD.

4.2 Nanoflow HPLC-nanospray ionization mass spectrometry

NanoLC-nanoESI uses nanobore HPLC columns (0.025 – 0.1 mm I.D. eluted at flow rates of 100–500 nL/min) with a nanoelectrospray source. This technique has found broad applications in proteomics.[132] Embrechts et al.[133] have employed nanoLC-nanoESI-MS/MS for trace analysis of estrogen-DNA adducts (17 α-ethynylestradiol-2′-deoxyadenosine, estrone-2′-deoxyguanosine, equilenin-2′-deoxyguanosine, estradiol-2′-deoxyguanosine, Chart 1) in human breast tumor tissue. The reported LOD value was 200 fg; however, they did not use stable isotope internal standards for quantitation.[133]

Chen et al. employed nanoflow HPLC-nanospray ionization tandem mass spectrometry (nanoLC-NSI/MS-MS) for simultaneous quantification of three lipid peroxidation-derived ethane adducts, 1,N^6-etheno-2′-dA (εdAdo), 3,N^4-etheno-2′-dC (εdCyd), and 1,N^2-etheno-2′-dG (1,N^2- εdG) in human DNA.[134] DNA was subjected to enzymatic hydrolysis, and the etheno adducts were enriched by reversed-phase SPE prior to analysis by isotope dilution nanoLC-NSI/MS-MS. Attomole sensitivity was achieved, with detection limits of 0.73, 160, and 34 amol for εdAdo, εdCyd, and 1,N^2-εdG, respectively. Analyses were conducted with 30 mg of DNA isolated from human blood (1–1.5 mL). The concentrations of εdAdo, εdCyd, and 1,N^2-εdG in human leukocyte DNA were 16.2 ± 5.2, 11.1 ± 5.8, and 8.6 ± 9.1 (mean +/− S.D.) adducts per 10^8 normal nucleotides, respectively.[134]

Our laboratory has developed a quantitative nanoLC-nanoESI method for the analysis of 1-(guan-7-yl)-4-(aden-1-yl)-2.3-butanediol cross-links induced by the diepoxide metabolite of 1,3-butadiene (N7G-N1A-BD in Chart 7) (Figure 7). A Waters nanoAcquity pump with a Symmetry C18 (0.18 × 20 mm) trapping column and an Atlantis dC18 (75 × 100 μm) analytical column was coupled to a Thermo Finnigan Ultra TSQ mass spectrometer. The method was employed to quantify N7G-N1A-BD in mouse liver DNA. A 10-fold increase in sensitivity was observed with nanoESI over a similar capLC-ESI-MS/MS method (3 adducts/10^9 nts as compared to 30 adducts/10^9 nts). Using this methodology, we were able to detect N7G-N1A-BD in DNA from mice exposed to 62.5 ppm BD.[24]

A similar nanoLC-nanoESI methodology has been developed for guanine-guanine cross-links of diepoxybutane, 1,4-*bis*-(guan-7-yl)-2,3-butanediol (*bis*-N7G-BD, Chart 7).[63] The LOD value of the method was 0.5 fmol/100 μg DNA, and the LOQ is 1.0 fmol/100 μg DNA, making it possible to quantify *bis*-N7G-BD adducts present at concentrations of 3 per 10^9 nucleotides. Using this methodology, *bis*-N7G-BD was quantified in tissues of laboratory mice treated with low ppm and sub-ppm concentrations of BD. *Bis*-N7G-BD adduct amounts in liver tissues of mice exposed to 0.5, 1.0, 1.5 ppm BD for 2 weeks were 5.7 ± 3.3, 9.2 ± 1.5, and 18.6 ± 6.9 adducts per 10^9 nucleotides, respectively, suggesting that N7G-BD adduct formation is more efficient under low exposure conditions.[63]

4.3 High resolution mass spectrometry

The use of high resolution mass spectrometry can significantly decrease the background noise of mass spectrometry assays, thereby improving both the sensitivity and specificity of detecting DNA adducts in biological samples. High resolution assays cannot be achieved on standard HPLC-ESI-MS/MS systems employing low resolution mass analyzers (quadrupoles and ion traps); high resolution methodologies require the use of FTMS or TOF instruments. Although high resolution mass spectrometry instruments are more expensive than their low resolution counterparts, accurate mass analyses can allow quantitation of DNA adducts in small DNA samples with a high degree of accuracy and precision.

Balbo et al. developed a nanoHPLC – nanoelectrospray high resolution tandem mass spectrometry selected reaction monitoring (LC-NSI-HRMS/MS-SRM) method for the analysis of 7-ethyl-Gua (Chart 5) in human leukocyte DNA. 7-Ethyl-Gua is formed in humans as a result of exposure to unknown ethylating agent(s). [$^{15}N_5$] 7-Ethyl-Gua was used as the internal standard. DNA was subjected to thermal neutral hydrolysis and solid-phase extraction. LC-NSI-HRMS/MS-SRM analyses were conducted using the transitions *m/z* 180 [M + H] → 152.05669 [Gua + H]$^+$ for 7-ethyl-Gua and *m/z* 185→ 157.04187 for the internal standard. The detection limit of the new method was approximately 10 amol on column, while the limit of quantitation was about 8 fmol/μmol Gua starting with 180 μg DNA (corresponding to 36 μg DNA oncolumn). 7-ethyl-Gua was present in leukocyte DNA from smokers and non-smokers, at concentrations of 14.6 – 181 fmol/μmol Gua.[60]

Our laboratory recently developed a method to quantify 1,3-butadiene induced N7-(2,3,4-trihydroxybut-1-yl) guanine (THBG) in human leukocyte DNA by capillary HPLC - high resolution tandem mass spectrometry (capLC -HRMS/MS-SRM). Authentic [$^{15}N_5$] THBG was used as an internal standard. Cap HPLC-HRMS/MS-SRM analyses were conducted using the transitions *m/z* 256.1 [M + H] → 152.05669 [Gua + H]$^+$ for THBG and *m/z* 261.1→ 157.04187 for the internal standard. The method was used to quantify THBG in DNA isolated from blood samples of smokers and non-smokers (Figure 10). This high resolution approach had a greatly improved sensitivity and reliability as compared to standard capillary HPLC-MS/MS methodologies.

4.4 Online sample purification via column switching

As discussed above, HPLC-ESI-MS/MS quantification of DNA adducts in biological samples can be difficult due to ESI signal suppression resulting from the presence of the sample matrix (salts, proteins, unmodified nucleosides). Extensive sample processing is required to remove potentially suppressing agents prior to injecting the sample extract onto an analytical column for LC-MS analysis; the process is time-consuming and can lead to significant analyte loss. Column switching methods can avoid sample loss and increase analytical throughput.

Column switching essentially involves two HPLC systems operating in series (Figure 8). The sample is first loaded onto a trapping column which retains the analytes and allows salts and other polar contaminants to be washed away to waste (Figure 8, valve position A). The HPLC valves controlling the flow of the two LC systems are then switched, and the second HPLC pumping system back-flushes the analyte from the trapping column onto the analytical column for separation and subsequent MS analysis (Figure 8, valve position B). Column switching has been successfully used by several groups to quantify DNA adducts in biological samples.[71–74,135–138] Several examples are discussed below.

Doerge et al. developed an HPLC-ESI-MS/MS method using column switching to quantify εdA and εdC adducts (Chart 4) in liver and lung DNA of mice exposed to urethane.[138] The method employed a reverse phase trapping column (Luna C18, 2 mm × 30 mm, 3 μm) and a

Luna C18, 2 mm × 150 mm, 3 μm analytical column coupled to a Quattro LC-triple quadrupole operated in the positive ion ESI mode. SRM transitions corresponding to a loss of deoxyribose from protonated nucleosides εdA and εdC were monitored. The LODs were 0.3 – 0.9 εdA adducts per 10^8 normal nucleotides and 0.7 – 1.8 εdC adducts per 10^8 normal nucleotides. Liver DNA from untreated and exposed mice contained 1.0 and 2.2 εdA adducts per 10^8 normal nucleotides and 1.0 and 2.7 εdC adducts per 10^8 normal nucleotides, respectively. The method for εdC had lower sensitivity than that for εdA, and the authors suggested that immunoaffinity online cleanup could be used to increase sensitivity in the future.

Poulson et al. have developed a column switching method for analyzing *1,N*^{6}-etheno-2′-deoxyadenosine adducts (εdA, Chart 4) in human urine.[72] The 2D separation was performed with a Luna trapping column (75 × 4.6 mm, 5 μm) and a Synergi Polar-RP (150 × 4.6 mm, 4 μm) analytical column. An API3000 triple quadrupole was used for the analysis. Urine (3 mL) was purified by Oasis HLB solid phase extraction prior to loading the sample onto HPLC for online column switching APCI-MS/MS analysis. The LOQ value for etheno-dA was 600 amol for pure standard on column, or 0.7 pmol/L urine; however, no increase in etheno-dA levels were observed in smoker's urine compared to healthy non-smoker's urine.[72] The same group has modified the above method to measure etheno-dC adducts in human urine with an LOQ of 100 pM for εdC.[73]

Brink et al.[71] have developed a column switching and APCI-MS/MS method for the simultaneous determination of *O*^{6}-methyl-dG (Chart 3), 8-oxo-7,8-dihydro-2′deoxyguanosine (Chart 8), and 1,*N*^{6}- εdA (Chart 4) in rat liver DNA. All three adducts can be formed endogenously or can be produced as a result of exposure to exogenous chemicals. The LOQs for these three adducts ranged from 24 to 48 fmol. Isotopically labeled *O*^{6}-Me-dG, was used as an internal standard. All three adducts were observed in rats dosed with dimethylnitrosamine. A major advantage of this method was that much lower levels of artifact 8-oxo-dG were observed as compared to other LC-MS/MS methods utilizing off-line sample cleanup methods.[71] As discussed in Section 1.3, 8-oxo-dG is readily formed from dG under aerobic conditions.[50–52]

A similar column switching approach was employed by Chao and co-workers for quantitative analysis of 8-oxo-dG in mouse and rat liver DNA.[137] The presence of dG can lead to artifactual formation of 8-oxo-dG in the ESI ion source, potentially interfering with quantitation.[62] Chao et al.[137] reported the removal of greater than 99% of dG from DNA hydrolysates using an ODS-3 trapping column (Intersil). PolyaminII endcapped HPLC column (150 × 4.6 mm, YMC) was used as an analytical column. The LOD value of the method was 0.13 adducts/10^6 dG (1.8 fmol on column) when using 20 μg mouse liver DNA per analysis, which is lower than background levels of 8-oxo-dG in human lymphocytes (0.3 adducts/10^6 dG). The low LOD coupled with short analysis time makes this method ideal for high throughput analysis of 8- oxo-dG.[137]

Most recent column switching method for 8-oxo-dG quantitation simultaneously analyzes 8-oxo-dG and 8-oxo-dA (Chart 8).[74] The reported LOD value for both adducts using this method was 5 fmol. While 8-oxo-dA was roughly 30 fold less abundant than 8-oxo-dG in rat liver DNA, there was less artifactual formation of 8-oxo-dA. It was concluded that the combination of 8- oxo-dG and 8-oxo-dA provides accurate quantitation of DNA oxidation.

Column switching has also been used for quantifying alkylguanine DNA adducts.[136] For example, Chao et al. have developed a column switching method for the simultaneous analysis of N7-methyl guanine (N7MeG, Chart 3) and N7-ethyl guanine (N7EtG, Chart 5).[136] The method employs a Nucleosil NH2 trapping column (35 mm × 4.6 mm, 10 μm)

and a Polyamine-II endcapped analytical column (150 mm × 4.6 mm, 5 μm, YMC). The resulting HPLC method was only 15 min long and possessed LODs of 0.42 fmol N7MeG and 0.17 fmol N7EtG on column. This method was reported to have a greater sensitivity than previously developed methodologies and was used to develop dose response curves in liver DNA of mosquito fish exposed to N-nitrosodiethylamine (NDEA) and N-nitrosodimethylamine (NDMA).[136]

Our laboratory has developed a column switching method for exocyclic DNA adducts of 1,3,-butadiene (BD): *1,N*^{6}-(1-hydroxymethyl-2-hydroxypropan-1,3-diyl)-2′-deoxyadenosine (*1*, *N*^{6}-αHMHP-dA) and *1,N*^{6}-(2-hydroxy-3-hydroxymethylpropan-1,3-diyl)-2′-deoxyadenosine (*1*, *N*^{6}-γHMHP-dA) (Chart 7).[70] These low abundance adducts are formed as a result of sequential alkylation of the N-1 and the N^6 positions of adenine by the genotoxic metabolite of BD, 1,2,3,4- diepoxybutane (DEB) (see Section 3.7). DNA was enzymatically digested to 2′-deoxynuclosides and fractionated by SPE on Extract Clean Carbo cartridges. Positively charged HMHP-dA adducts were selectively trapped on strong cation exchange (SCX) trapping column, followed by separation on Synergi Hydro-RP C18 column, resulting in low noise levels and excellent sensitivity (Figure 9). The limit of detection of this method was 1.1 *1,N*^{6}-HMHP-dA adducts/10^9 nts, sensitive enough to obtain dose response curves for these novel adducts in liver of mice exposed to 62.5 – 625 ppm BD. Based on their structure and their persistence in tissues,[34] *1,N*^{6}- HMHP-dA adducts may contribute to A → T mutations observed following treatment with BD.

4.5 Chip-MS

Chip-MS utilizes a silicon chip containing an array of ESI nozzles. Sample is directly loaded onto the chip, eliminating the need for time consuming HPLC separations.[30] Another advantage of this method is that it uses small sample volumes, thereby decreasing the amounts of biological matrix entering the mass spectrometer. A major disadvantage is the absence of chromatography, which means that the analyte enters the MS system at the same time as all matrix components; thus matrix effects such as ion suppression and interference may occur. In some cases, performing a simple liquid/liquid extraction of samples prior to chip-MS/MS can greatly reduce matrix effects.[128]

The majority of applications of chip-MS have been for the analysis of peptides or drugs/drug metabolites.[128,139] Recently, the Vouros group at Northeastern University has developed novel chip-MS methodologies for rapid and sensitive quantitation of ABP-DNA adducts (C8-dG-4ABP in Chart 2). Their methods employed an Agilent LC/MSD XCT Ultra Ion Trap and Agilent small molecule Chip Zorbax 80SB-C18, 5 μm particle size. The Agilent Chip contains an enrichment column (40 nL) and an analytical column (75 μm i.d., 43 μm in length). Analyte and internal standard molecular ions are isolated and fragmented using the transitions corresponding to C8-dG-4ABP and C8-dG-4ABP-d_9 (*m/z* 435.4 → 319 and *m/z* 444 → 328, respectively).[140] C8-dG-4ABP adducts were analyzed in DNA extracted from bladder tissue of rats exposed to 4-ABP.[140] The limit of detection for this method was 2 C8-dG- 4ABP/10^8 nts, requiring only 1.25 μg DNA. The method was used to quantify C8-dG-4ABP in bladder DNA from rats dosed with ABP by IP injection; in these samples, C8-dG-4ABP was detected at levels starting at 80 adducts/10^8 nts.[140] Glick et al. also reported a chip-based nano- LC/MS ion trap method for the quantitation of 2-amino-1-methyl-6-phenylimidazo[4,5- b]pyridine (PhIP) induced DNA adducts (Chart 2).[141] Human bronchial epithelial cells (BEAS- 2A) were treated with 10^{-6} – 10^{-9} M N-OH-PhIP for 24 hours. DNA was extracted and digested to deoxynucleosides, followed by analysis by chip-based nano-LC/MS. They found that cells treated with 10^{-7} M N-OH-PhIP contained 23 adducts per 10^8 normal nucleotides.[141]

4.6 Adductomics methodologies

Human exposure to carcinogens is not confined to a single compound: we are routinely exposed to complex mixtures of different chemicals. Reactive species can interact with DNA at various sites generating multiple adducts with various biological effects. Because chemicals can influence the extent of metabolic activation of other mixture components to DNA-reactive intermediates, their interactions may lead to additive, synergistic or antagonistic effects in terms of DNA adduct formation.[142] Furthermore, the presence of specific DNA adducts can influence the repair rates of structurally distinct types of DNA damage. It is therefore desirable to use a systematic approach to evaluate the formation of DNA adducts following exposures to mixtures of compounds. This approach has been termed “adductomics”, by analogy with other “omics” fields. For example, Singh et al. have developed a targeted DNA adductomic approach for assessing exposure to mixtures of PAHs using liquid chromatography/tandem mass spectrometry (LC/MS/MS).[75] Sensitive and specific detection of a range of of PAH-adducted 2′-deoxynucleosides was achieved using online column-switching HPLC-ESI-MS/MS (Section 4.4) in conjunction with constant neutral loss and selected reaction monitoring (SRM, Section 2.4). While a number of PAH-DNA adducts were detected by employing constant neutral loss scanning monitoring the neutral loss of deoxyribose (M – 116, Scheme 5D), the best sensitivity of detection was achieved with targeted SRM methodology.[75]

Inagaki et al.[143] employed an adductomics approach to discover novel DNA adducts of acrylamide (AM). Calf thymus DNA was treated with the ultimate reactive metabolite of AM, glycidamide, and the alkylated DNA was acid hydrolyzed with HCl to release purine bases. The hydrolysates were injected onto an Agilent HPLC interfaced with a Waters CT Premier XE ESI time-of-flight (TOF) mass spectrometer. The instrument was operated in the precursor ion scan mode (Scheme 5B) using the product ions at *m/z* 152 (protonated guanine) or *m/z* 135 (protonated adenine). These analyses have detected known adducts, N1-(2-carboxy-2- hydroxyethyl)-N7-(2-carbamoyl-2-hydroxyethyl)-guanine (Chart 7), as well as several previously unknown AM-DNA lesions.[143] Spillberg et al. employed a similar tandem mass spectrometry-based approach to identify 90 damaged nucleosides derived from dietary DNA.[144]

An important limitation of the adductomics approach is that constant neutral loss and precursor scanning techniques that are used to discover new adducts are less sensitive if a targeted mass list is not used. Furthermore, validated methods for a clear identification of unknown adducts are still needed to ensure reproducible detection of novel lesions. Despite these limitations, the adductomic approach have a great potential for human biomonitoring due to its ability to provide a global and unbiased view of all types of DNA damage in a given sample.

5. Conclusions

Isotope dilution based HPLC-ESI-MS/MS is a powerful analytical methodology that allows for sensitive, accurate, and specific detection of DNA adducts in complex biological samples. This technique is superior to other methods of DNA adduct detection such as ^{32}P-post-labelling, immunoassay, and fluorescence because it ensures accurate quantitation and provides structural information about each modified nucleoside. Although this methodology requires the synthesis of stable isotope labeled internal standards, the use of such standards accounts for any sample losses and takes into account matrix effects, leading to unprecendented accuracy, sensitivity, and reproducibility. Recent improvements in biological mass spectrometry, such as the application of nanoscale HPLC separations, nanospray MS, accurate mass instrumentation, and chip-cube methodology, have increased the sensitivity of MS methods to levels surpassing the sensitivity of ^{32}P post-labeling.

Advancements in column switching methodologies have led to cleaner samples, resulting in reduced signal suppression, lower quantitation limits, and a higher analytical throughput. The use of accurate mass MS in combination with nanoHPLC adducts shows great promise for measuring low abundance adducts in human samples. Other state of the art methodologies for DNA adduct detection include inductive plasma mass spectrometry[96] and accelerator mass spectrometry,[145] which are beyond the scope of the present review. While many of the earlier applications of mass spectrometry in DNA adduct analysis have been limited to studies in laboratory animals where high exposure concentrations induce significant degree of DNA damage, recent advancements in HPLC and MS instrumentation have led to unparalleled sensitivity, enabling their increased use in human biomonitoring, analysis of endogenous DNA damage, and risk assessment. These new capabilities will enable researchers to use DNA adducts as indicators of human susceptibility, biomarkers of disease, and specific measures of individual response to anticancer therapy.

Acknowledgments

6. Funding Support

This work is supported by grants from the National Cancer Institute (C.A. 100670), the National Institute of Environmental Health Sciences (ES 12689), the Health Effects Institute (Agreement 05-12), and the American Chemistry Council (OLF-163.0).

We are thankful to Bob Carlson and Dewakar Sangaraju (University of Minnesota Masonic Cancer Center) for preparing figures and tables for this manuscript and Drs. Silvia Balbo and Peter Villalta (University of Minnesota Masonic Cancer Center) for their valuable comments and suggestions on the manuscript.

Abbreviations

***1,N*^{6}-γHMHP-dA**	*1,N*^{6}-(2-hydroxy-3-hydroxymethylpropan-1,3-diyl)-2′-deoxyadenosine
***bis*-N7G-BD**	1,4-*bis*-(guan-7-yl)-2,3-butanediol
1,*N*^{2}-εdG	1,*N*^{2}-etheno-2′-dG
1,*N*^{2}-εdGuo	1,*N*^{2}- etheno-2′-deoxyguanosine
1-SMP	1-sulfooxymethylpyrene
4-ABP	4-aminobiphenyl
4-OHE^1- *N*3-Ade	4-hydroxyestrogen-1-*N*3-adenine
7-POB-Gua	7-[4-(3-pyridyl)-4-oxobut-1- yl]guanine
8-oxo-dG	8-oxoguanine
AM	acrylamide
AA	aristolochic acid
Aag	alkyladenine DNA glycosylase
Acro-dGuo	(8R/S)-3-(2′-deoxyribos-1′-yl)-5,6,7,8-tetrahydro-8-hydroxypyrimido[1,2-a]purine-10(3H)one
AD	Alzheimer’s disease
Arco	acrolein
BD	1,3- butadiene
***bis*-N7G-BD**	1,2,3,4-diepoxybutane

***bis*-N7G-BD**	1,4-*bis*-(guan-7-yl)-2,3- butanediol
BP	benzo[a]pyrene
BP-6-N7Gua	N7-(benzo[a]pyrene-6-yl)guanine
BPDE	*trans*- 7,8-dihydroxy-*anti*-9,10-epoxy-7,8,9,10-tetrahydrobenzo[a]-pyrene
C8(1-HE)g	C8-(1- hydroxyethyl)guanine
C8-dG-4-ABP	N-(deoxyguanosine-8-yl)-4-ABP adducts
C8-dG-MeIQx	N-(deoxyguanosine-8-yl) MeIQx
capLC-HRMS/MS-SRM	capillary HPLC - high resolution tandem mass spectrometry
capLC-nanoESI	capillary HPLC-nanoelectrospray ionization-tandem mass spectrometry
CEdG	N^2-(1-carboxyethyl)-2′-deoxyguanosine
CID	collision induced dissociation
CNL	constant neutral loss
CPA	cyclophosphamide
CP-d(GpG)	cisplatin 1,2-guanine-guanine intrastrand cross-link
dA-AAI	7-(deoxyadenosin-N^6-yl)aristolactam I
dc	direct current
DEB	1,2,3,4-diepoxybutane
dG-BPDE	10-(deoxyguanosin-N^2-yl)-7,8,9- trihydroxy-7,8,9,10-tetrahydrobenzo[a]-pyrene
dG-C8-4-ABP	N-(deoxyguanosin-8-yl)-4- ABP
dG-C8-IQ	*N*-(deoxyguanosine-8-yl)-2-amino-3-methylimidazo [4,5-*f*] quinoline
dG-desMeTam	(*E*)-α-(deoxyguanosin-N^2-yl)-N-desmethyl tamoxifen
dG-Tam	(*E*)-α-(deoxyguanosin-N^2-yl) tamoxifen
dI	2′-deoxyinosine
dU	2′-deoxyuridine
EB	epoxybutene
EBD	epoxybutanediol
EPI	enhanced product ion
ESI	electrospray ionization
FT	Fourier transformation
GA	glycidamide
gdG	glyoxal deoxyguanosine
G-NOR-G	*N,N-bis*[2-(*N7*-guaninyl) ethyl] amine DNA-DNA cross-links

HILIC	hydrophilic interaction chromatography
HNE	*trans*-4-hydroxy-2-nonenal
HNE-dG	1,N^2-propano-deoxyguanosine adducts
HPLC-ESIMS/MS	high performance liquid chromatography-electrospray ionization-tandem mass spectrometry
IDMS	isotope dilution mass spectrometry
IQ	2-amino-3-methylimidazo [4,5-*f*] quinoline
IS	internal standard
LC-NSI-HRMS/MS-SRM	nanoHPLC – nanoelectrospray high resolution tandem mass spectrometry selected reaction monitoring
LIT	linear quadrupole ion trap
LOD	limit of detection
LOQ	limit of quantitation
MeIQx	2-amino-3,8-dimethylimidazo- [4,5f]quinoxaline
mel-dGuo	melphalan-deoxyguanosine
MP-dAdo	methylpyrene deoxyadenosine
MP-dGuo	methylpyrene deoxyguanosine
MRM	multiple reaction monitoring
N^2-BPDE-dG	10-(deoxyguanosin-N^2-yl)-7,8,9-trihydroxy-7,8,9,10-tetrahydrobenzo[a]pyrene
***N^2*-dG-MeIQx**	5-(deoxyguanosin-*N^2*-yl) MeIQx
N3-GA-Ade	N3-(2-carbamoyl-2-hydroxyethyl)adenine
N7EtG	N7-ethyl guanine
N7-GA-Gua	N7-(2-carbamoyl-2- hydroxyethyl)guanine
N7G-N1A-BD	1-(guan-7-yl)-4-(aden-1-yl)-2,3-butanediol
N7G-N3ABD	1-(guan-7-yl)-4-(aden-3-yl)-2,3-butanediol
N7G-N^6A-BD	1-(guan-7-yl)-4-(aden-6-yl)-2,3-butanediol
N7G-N7A-BD	1-(guan-7-yl)-4-(aden-7-yl)-2,3-butanediol
N7MeG	N7-methyl guanine
nanoLC	nano flow HPLC
nanoLC-NSI/MS-MS	nanoflow HPLC-nanospray ionization tandem mass spectrometry
NDELA	N-nitrosodiethanolamine
NNK	4-(methylnitrosamino)-1-(3-pyridyl)-1-butanone
***O^2*-POB-Cyt**	*O^2*-[4-(3-pyridyl)-4-oxobut-1-yl]cytosine
***O^2*-POB-dThd**	*O^2*-[4-(3-pyridyl)-4-oxobut-1-yl]thymidine
***O^6*-POB-dGuo**	*O^6*-[4- (3-pyridyl)-4-oxobut-1-yl]-2′-deoxyguanosine

OHEdG	O^6-2-hydroxyethyl-2′-deoxyguanosine
OHEG	O^6-2-hydroxyethyl-2′-doexyguanosine
oxazolone	2,2-diamino-4-(2-deoxy-β-D-*erythro*-pentofuranosyl) amino]5(2H)-oxazolone
PAH	polycyclic aromatic hydrocarbons
PHB	pyridylhydroxybutyl
PhIP	2-amino-1-methyl-6-phenylimidazo[4,5-b]pyridine
POB	pyridyloxobutyl
Q	quadrupole mass analyzer
QqQ	triple quadrupoles
QqQtrap	triple quadrupole-linear ion trap
Q-TOF	quadrupole-time-of-flight
rf	radiofrequency
ROS	reactive oxygen species
SCX	strong cation exchange
SPE	Solid phase extraction
SRM	selected reaction monitoring
THBG	N7-(2,3,4-trihydroxybut-1-yl) guanine
TOF	time of flight
UPLC-MS/MS	ultra-performance liquid chromatography-tandem mass spectrometry
εdA	exocyclic 1,N^6-etheno-dA adducts
εdAdo	1,N^6-etheno-2′-dA
εdCyd	3,N^4-etheno-2′-dC

References

1. Weinberg, RA. The Biology of Cancer. Garland Science; New York, NY: 2006.
2. Singer, B.; Grunberger, D. Molecular Biology of Mutagens and Carcinogens. Plenum Press; New York and London: 1983.
3. Williams, DA. Foye's principals of medicinal chemisty. Lippincott Wolliams & Wilkins; Wolters Kluver: 2008. Drug metabolism; p. 253-326.
4. Harris CC. Chemical and physical carcinogenesis: advances and perspectives for the 1990s. Cancer Res. 1991; 51:5023s–5044s. [PubMed: 1884379]
5. Hecht SS. Tobacco smoke carcinogens and lung cancer. J Natl Cancer Inst. 1999; 91:1194–1210. [PubMed: 10413421]
6. Rajski SR, Williams RM. DNA cross-linking agents as antitumor drugs. Chem Rev. 1998; 98:2723–2796. [PubMed: 11848977]
7. Essigmann JM, Loechler EL, Green CL. Mutagenesis and repair of O^6-substituted guanines. IARC Sci Publ. 1986:393–399. [PubMed: 3539791]
8. Ellison KS, Dogliotti E, Connors TD, Basu AK, Essigmann JM. Site-specific mutagenesis by O^6-alkylguanines located in the chromosomes of mammalian cells: influence of the mammalian O^6-

alkylguanine-DNA alkyltransferase. Proc Natl Acad Sci U S A. 1989; 86:8620–8624. [PubMed: 2813414]

9. Lindahl T, Wood RD. Quality control by DNA repair. Science. 1999; 286:1897–1905. [PubMed: 10583946]
10. Jones GW, Hooley P, Farrington SM, Shawcross SG, Iwanejko LA, Strike P. Cloning and characterisation of the sagA gene of Aspergillus nidulans: a gene which affects sensitivity to DNA-damaging agents. Mol Gen Genet. 1999; 261:251–258. [PubMed: 10102359]
11. Hang B, Chenna A, Guliaev AB, Singer B. Miscoding properties of *1,N*^{6}-ethanoadenine, a DNA adduct derived from reaction with the antitumor agent 1,3-bis(2-chloroethyl)-1-nitrosourea. Mutat Res. 2003; 531:191–203. [PubMed: 14637255]
12. Evans JW, Chernikova SB, Kachnic LA, Banath JP, Sordet O, Delahoussaye YM, Treszezamsky A, Chon BH, Feng Z, Gu Y, Wilson WR, Pommier Y, Olive PL, Powell SN, Brown JM. Homologous recombination is the principal pathway for the repair of DNA damage induced by tirapazamine in mammalian cells. Cancer Res. 2008; 68:257–265. [PubMed: 18172318]
13. Delaney JC, Smeester L, Wong C, Frick LE, Taghizadeh K, Wishnok JS, Drennan CL, Samson LD, Essigmann JM. AlkB reverses etheno DNA lesions caused by lipid oxidation in vitro and in vivo. Nat Struct Mol Biol. 2005; 12:855–860. [PubMed: 16200073]
14. Hang B. Repair of exocyclic DNA adducts: rings of complexity. Bioessays. 2004; 26:1195–1208. [PubMed: 15499577]
15. Levine RL, Yang IY, Hossain M, Pandya GA, Grollman AP, Moriya M. Mutagenesis induced by a single *1,N*^{6}-ethenodeoxyadenosine adduct in human cells. Cancer Res. 2000; 60:4098–4104. [PubMed: 10945616]
16. Niedernhofer LJ, Lalai AS, Hoeijmakers JH. Fanconi anemia (cross)linked to DNA repair. Cell. 2005; 123:1191–1198. [PubMed: 16377561]
17. Broyde S, Wang L, Rechkoblit O, Geacintov NE, Patel DJ. Lesion processing: high-fidelity versus lesion-bypass DNA polymerases. Trends Biochem Sci. 2008; 33:209–219. [PubMed: 18407502]
18. Plosky BS, Woodgate R. Switching from high-fidelity replicases to low-fidelity lesion-bypass polymerases. Curr Opin Genet Dev. 2004; 14:113–119. [PubMed: 15196456]
19. Nair DT, Johnson RE, Prakash L, Prakash S, Aggarwal AK. Hoogsteen base pair formation promotes synthesis opposite the 1,*N*^{6}-ethenodeoxyadenosine lesion by human DNA polymerase iota. Nat Struct Mol Biol. 2006; 13:619–625. [PubMed: 16819516]
20. Prakash S, Johnson RE, Prakash L. Eukaryotic translesion synthesis DNA polymerases: specificity of structure and function. Annu Rev Biochem. 2005; 74:317–353. [PubMed: 15952890]
21. Swenberg JA, Fryar-Tita E, Jeong YC, Boysen G, Starr T, Walker VE, Albertini RJ. Biomarkers in toxicology and risk assessment: informing critical dose-response relationships. Chem Res Toxicol. 2008; 21:253–265. [PubMed: 18161944]
22. Koc H, Swenberg JA. Applications of mass spectrometry for quantitation of DNA adducts. J Chromatogr B Analyt Technol Biomed Life Sci. 2002; 778:323–343.
23. Walker VE, Wu KY, Upton PB, Ranasinghe A, Scheller N, Cho MH, Vergnes JS, Skopek TR, Swenberg JA. Biomarkers of exposure and effect as indicators of potential carcinogenic risk arising from in vivo metabolism of ethylene to ethylene oxide. Carcinogenesis. 2000; 21:1661–1669. [PubMed: 10964097]
24. Goggin M, Swenberg JA, Walker VE, Tretyakova N. Molecular dosimetry of 1,2,3,4-diepoxybutane-induced DNA-DNA cross-links in B6C3F1 mice and F344 rats exposed to 1,3-butadiene by inhalation. Cancer Res. 2009; 69:2479–2486. [PubMed: 19276346]
25. Lu K, Moeller B, Doyle-Eisele M, McDonald J, Swenberg JA. Molecular dosimetry of *N*^{2}-hydroxymethyl-dG DNA adducts in rats exposed to formaldehyde. Chem Res Toxicol. 2011; 24:159–161. [PubMed: 21155545]
26. Nestmann ER, Bryant DW, Carr CJ. Toxicological significance of DNA adducts: summary of discussions with an expert panel. Regul Toxicol Pharmacol. 1996; 24:9–18. [PubMed: 8921541]
27. Farmer PB, Brown K, Tompkins E, Emms VL, Jones DJ, Singh R, Phillips DH. DNA adducts: mass spectrometry methods and future prospects. Toxicol Appl Pharmacol. 2005; 207:293–301. [PubMed: 15990134]

28. Farmer PB, Singh R. Use of DNA adducts to identify human health risk from exposure to hazardous environmental pollutants: the increasing role of mass spectrometry in assessing biologically effective doses of genotoxic carcinogens. Mutat Res. 2008; 659:68–76. [PubMed: 18468947]
29. Otteneder M, Lutz WK. Correlation of DNA adduct levels with tumor incidence: carcinogenic potency of DNA adducts. Mutat Res. 1999; 424:237–247. [PubMed: 10064864]
30. Singh R, Farmer PB. Liquid chromatography-electrospray ionization-mass spectrometry: the future of DNA adduct detection. Carcinogenesis. 2006; 27:178–196. [PubMed: 16272169]
31. Banoub, JH.; Miller-Banoub, J.; Jahouh, F.; Joly, N.; Martin, P. Overview of recent developments in the mass spectrometry of nucleic acid and constituents. In: Banoub, JH.; Limbach, PA., editors. Mass spectrometry of nucleosides and nucleic acids. CRC Press; Boca Raton: 2010. p. 1-90.
32. Ciccimaro E, Blair IA. Stable-isotope dilution LC-MS for quantitative biomarker analysis. Bioanalysis. 2010; 2:311–341. [PubMed: 20352077]
33. Koivisto P, Peltonen K. Analytical methods in DNA and protein adduct analysis. Anal Bioanal Chem. 2010; 398:2563–2572. [PubMed: 20922519]
34. Goggin M, Sangaraju D, Walker VE, Wickliffe J, Swenberg JA, Tretyakova N. Persistence and repair of bifunctional DNA adducts in tissues of laboratory animals exposed to 1,3-butadiene by inhalation. Chem Res Toxicol. 2011; 24:809–817. [PubMed: 21452897]
35. Ishii Y, Suzuki Y, Hibi D, Jin M, Fukuhara K, Umemura T, Nishikawa A. Detection and quantification of specific DNA adducts by liquid chromatography-tandem mass spectrometry in the livers of rats given estragole at the carcinogenic dose. Chem Res Toxicol. 2011; 24:532–541. [PubMed: 21384859]
36. Bessette EE, Spivack SD, Goodenough AK, Wang T, Pinto S, Kadlubar FF, Turesky RJ. Identification of carcinogen DNA adducts in human saliva by linear quadrupole ion trap/multistage tandem mass spectrometry. Chem Res Toxicol. 2010; 23:1234–1244. [PubMed: 20443584]
37. Chen HJ, Lin WP. Quantitative analysis of multiple exocyclic DNA adducts in human salivary DNA by stable isotope dilution nanoflow liquid chromatography-nanospray ionization tandem mass spectrometry. Anal Chem. 2011; 83:8543–8551. [PubMed: 21958347]
38. Bransfield LA, Rennie A, Visvanathan K, Odwin SA, Kensler TW, Yager JD, Friesen MD, Groopman JD. Formation of two novel estrogen guanine adducts and HPLC/MS detection of 4-hydroxyestradiol-N7-guanine in human urine. Chem Res Toxicol. 2008; 21:1622–1630. [PubMed: 18582124]
39. Egner PA, Groopman JD, Wang JS, Kensler TW, Friesen MD. Quantification of aflatoxin-B1-*N7*-guanine in human urine by high-performance liquid chromatography and isotope dilution tandem mass spectrometry. Chem Res Toxicol. 2006; 19:1191–1195. [PubMed: 16978023]
40. Dudley E, Lemiere F, Van Dongen W, Esmans E, El Sharkawi AM, Games DE, Brenton AG, Newton RP. Urinary modified nucleosides as tumor markers. Nucleosides Nucleotides Nucleic Acids. 2003; 22:987–989. [PubMed: 14565327]
41. Tuytten R, Lemiere F, Van Dongen W, Witters E, Esmans EL, Newton RP, Dudley E. Development of an on-line SPE-LC-ESI-MS method for urinary nucleosides: Hyphenation of aprotic boronic acid chromatography with hydrophilic interaction LC-ESI-MS. Analytical Chemistry. 2008; 80:1263–1271. [PubMed: 18198895]
42. Chao MR, Wang CJ, Chang LW, Hu CW. Quantitative determination of urinary *N7*-ethylguanine in smokers and non-smokers using an isotope dilution liquid chromatography/tandem mass spectrometry with on-line analyte enrichment. Carcinogenesis. 2006; 27:146–151. [PubMed: 16000398]
43. Chen HJ, Chiu WL. Association between cigarette smoking and urinary excretion of *1,N*^{2}-ethenoguanine measured by isotope dilution liquid chromatography-electrospray ionization/tandem mass spectrometry. Chem Res Toxicol. 2005; 18:1593–1599. [PubMed: 16533024]
44. Chen HJ, Chang CM. Quantification of urinary excretion of 1,*N*^{6}-ethenoadenine, a potential biomarker of lipid peroxidation, in humans by stable isotope dilution liquid chromatography-electrospray ionization-tandem mass spectrometry: comparison with gas chromatography-mass spectrometry. Chem Res Toxicol. 2004; 17:963–971. [PubMed: 15257622]

45. Goggin M, Loeber R, Park S, Walker V, Wickliffe J, Tretyakova N. HPLC-ESI^{+}-MS/MS analysis of *N7*-guanine-*N7*-guanine DNA cross-links in tissues of mice exposed to 1,3-butadiene. Chem Res Toxicol. 2007; 20:839–847. [PubMed: 17455958]

46. Koc H, Tretyakova NY, Walker VE, Henderson RF, Swenberg JA. Molecular dosimetry of N-7 guanine adduct formation in mice and rats exposed to 1,3-butadiene. Chem Res Toxicol. 1999; 12:566–574. [PubMed: 10409395]

47. Wu KY, Ranasinghe A, Upton PB, Walker VE, Swenberg JA. Molecular dosimetry of endogenous and ethylene oxide-induced N7-(2-hydroxyethyl) guanine formation in tissues of rodents. Carcinogenesis. 1999; 20:1787–1792. [PubMed: 10469625]

48. Park S, Seetharaman M, Ogdie A, Ferguson D, Tretyakova N. 3′-Exonuclease resistance of DNA oligodeoxynucleotides containing O^6-[4-oxo-4-(3-pyridyl)butyl]guanine. Nucleic Acids Res. 2003; 31:1984–1994. [PubMed: 12655016]

49. Goggin M, Anderson C, Park S, Swenberg J, Walker V, Tretyakova N. Quantitative high-performance liquid chromatography-electrospray ionization-tandem mass spectrometry analysis of the adenine-guanine cross-links of 1,2,3,4-diepoxybutane in tissues of butadiene-exposed B6C3F1 mice. Chem Res Toxicol. 2008; 21:1163–1170. [PubMed: 18442269]

50. Cadet J, Douki T, Frelon S, Sauvaigo S, Pouget JP, Ravanat JL. Assessment of oxidative base damage to isolated and cellular DNA by HPLC-MS/MS measurement. Free Radic Biol Med. 2002; 33:441–449. [PubMed: 12160926]

51. Ravanat JL, Cadet J, Douki T. Oxidatively generated DNA lesions as potential biomarkers of *in vivo* oxidative stress. Curr Mol Med. 2012 2012 Jan 27. [Epub ahead of print].

52. Ravanat JL, Douki T, Duez P, Gremaud E, Herbert K, Hofer T, Lasserre L, Saint-Pierre C, Favier A, Cadet J. Cellular background level of 8-oxo-7,8-dihydro-2′-deoxyguanosine: an isotope based method to evaluate artefactual oxidation of DNA during its extraction and subsequent work-up. Carcinogenesis. 2002; 23:1911–1918. [PubMed: 12419840]

53. Boysen G, Collins LB, Liao S, Luke AM, Pachkowski BF, Watters JL, Swenberg JA. Analysis of 8-oxo-7,8-dihydro-2′-deoxyguanosine by ultra high pressure liquid chromatography-heat assisted electrospray ionization-tandem mass spectrometry. J Chromatogr B Analyt Technol Biomed Life Sci. 2010; 878:375–380.

54. Dong M, Dedon PC. Relatively small increases in the steady-state levels of nucleobase deamination products in DNA from human TK6 cells exposed to toxic levels of nitric oxide. Chem Res Toxicol. 2006; 19:50–57. [PubMed: 16411656]

55. Dong M, Vongchampa V, Gingipalli L, Cloutier JF, Kow YW, O'Connor T, Dedon PC. Development of enzymatic probes of oxidative and nitrosative DNA damage caused by reactive nitrogen species. Mutat Res. 2006; 594:120–134. [PubMed: 16274707]

56. Pang B, Zhou X, Yu H, Dong M, Taghizadeh K, Wishnok JS, Tannenbaum SR, Dedon PC. Lipid peroxidation dominates the chemistry of DNA adduct formation in a mouse model of inflammation. Carcinogenesis. 2007; 28:1807–1813. [PubMed: 17347141]

57. Ramesh A, Archibong AE, Niaz MS. Ovarian susceptibility to benzo[a]pyrene: tissue burden of metabolites and DNA adducts in F-344 rats. Journal of Toxicology and Environmental Health-Part A-Current Issues. 2010; 73:1611–1625.

58. Chen L, Wang M, Villalta PW, Hecht SS. Liquid chromatography-electrospray ionization tandem mass spectrometry analysis of 7-ethylguanine in human liver DNA. Chem Res Toxicol. 2007; 20:1498–1502. [PubMed: 17887725]

59. Kotandeniya D, Murphy D, Seneviratne U, Guza R, Pegg A, Kanugula S, Tretyakova N. Mass spectrometry based approach to study the kinetics of O^6-alkylguanine DNA alkyltransferase-mediated repair of O^6-pyridyloxobutyl-2′-deoxyguanosine adducts in DNA. Chem Res Toxicol. 2011; 24:1966–1975. [PubMed: 21913712]

60. Balbo S, Villalta PW, Hecht SS. Quantitation of 7-ethylguanine in leukocyte DNA from smokers and nonsmokers by liquid chromatography-nanoelectrospray- high resolution tandem mass spectrometry. Chem Res Toxicol. 2011; 24:1729–1734. [PubMed: 21859140]

61. Ham AJ, Engelward BP, Koc H, Sangaiah R, Meira LB, Samson LD, Swenberg JA. New immunoaffinity-LC-MS/MS methodology reveals that Aag null mice are deficient in their ability

to clear *1,N*^{6}-etheno-deoxyadenosine DNA lesions from lung and liver *in vivo*. DNA Repair (Amst). 2004; 3:257–265. [PubMed: 15177041]

62. Matter B, Malejka-Giganti D, Csallany AS, Tretyakova N. Quantitative analysis of the oxidative DNA lesion, 2,2-diamino-4-(2-deoxy-β-D-*erythro*-pentofuranosyl) amino]-5(2H)-oxazolone (oxazolone), *in vitro* and *in vivo* by isotope dilution-capillary HPLC-ESI-MS/MS. Nucleic Acids Res. 2006; 34:5449–5460. [PubMed: 17020926]
63. Sangaraju D, Goggin M, Walker V, Swenberg J, Tretyakova N. NanoHPLC-nanoESI$^+$-MS/MS quantitation of *bis-N7*-guanine DNA-DNA cross-links in tissues of B6C3F1 mice exposed to subppm levels of 1,3-butadiene. Anal Chem. 2012; 84:1732–1739. [PubMed: 22220765]
64. Gong LZ, McCullagh JSO. Analysis of oligonucleotides by hydrophilic interaction liquid chromatography coupled to negative ion electrospray ionization mass spectrometry. Journal of Chromatography A. 2011; 1218:5480–5486. [PubMed: 21741051]
65. Pucci V, Giuliano C, Zhang RA, Koeplinger KA, Leone JF, Monteagudo E, Bonelli F. HILIC LC-MS for the determination of 2′-C-methyl-cytidine-triphosphate in rat liver. Journal of Separation Science. 2009; 32:1275–1283. [PubMed: 19347863]
66. Zhao HQ, Chen JH, Shi Q, Li X, Cao W, Li JX, Wang XR. New fingerprinting method based on the distribution of nucleoside compounds for marine animal drugs by HILIC-ESI-TOF/MS. Chemical Journal of Chinese Universities-Chinese. 2012; 33:44–48.
67. Fenn JB, Mann M, Meng CK, Wong SF, Whitehouse CM. Electrospray ionization-principles and practice. Mass Spectrometry Reviews. 1990; 9:37–70.
68. Cappiello A, Famiglini G, Mangani F, Palma P. New trends in the application of electron ionization to liquid chromatography-mass spectrometry interfacing. Mass Spectrometry Reviews. 2001; 20:88–104. [PubMed: 11455563]
69. Throck Watson, J.; David Sparkman, O. Introduction to mass spectrometry. John Wiley and Sons; West Sussex, England: 2007.
70. Goggin M, Seneviratne U, Swenberg JA, Walker VE, Tretyakova N. Column switching HPLC-ESI$^+$-MS/MS methods for quantitative analysis of exocyclic dA adducts in the DNA of laboratory animals exposed to 1,3-butadiene. Chem Res Toxicol. 2010; 23:808–812. [PubMed: 20229982]
71. Brink A, Lutz U, Volkel W, Lutz WK. Simultaneous determination of *O*^{6}-methyl-2′-deoxyguanosine, 8-oxo-7,8-dihydro-2′-deoxyguanosine, and 1,*N*^{6}-etheno-2′-deoxyadenosine in DNA using on-line sample preparation by HPLC column switching coupled to ESI-MS/MS. J Chromatogr B Analyt Technol Biomed Life Sci. 2006; 830:255–261.
72. Hillestrom PR, Hoberg AM, Weimann A, Poulsen HE. Quantification of 1,*N*^{6}-etheno-2′-deoxyadenosine in human urine by column-switching LC/APCI-MS/MS. Free Radic Biol Med. 2004; 36:1383–1392. [PubMed: 15135174]
73. Hillestrom PR, Weimann A, Poulsen HE. Quantification of urinary etheno-DNA adducts by column-switching LC/APCI-MS/MS. J Am Soc Mass Spectrom. 2006; 17:605–610. [PubMed: 16504536]
74. Singh R, Teichert F, Verschoyle RD, Kaur B, Vives M, Sharma RA, Steward WP, Gescher AJ, Farmer PB. Simultaneous determination of 8-oxo-2′-deoxyguanosine and 8-oxo-2′-deoxyadenosine in DNA using online column-switching liquid chromatography/tandem mass spectrometry. Rapid Commun Mass Spectrom. 2009; 23:151–160. [PubMed: 19065576]
75. Singh R, Teichert F, Seidel A, Roach J, Cordell R, Cheng MK, Frank H, Steward WP, Manson MM, Farmer PB. Development of a targeted adductomic method for the determination of polycyclic aromatic hydrocarbon DNA adducts using online column-switching liquid chromatography/tandem mass spectrometry. Rapid Commun Mass Spectrom. 2010; 24:2329–2340. [PubMed: 20658679]
76. Tretyakova NY, Burney S, Pamir B, Wishnok JS, Dedon PC, Wogan GN, Tannenbaum SR. Peroxynitrite-induced DNA damage in the *supF* gene: correlation with the mutational spectrum. Mutat Res. 2000; 447:287–303. [PubMed: 10751613]
77. Kim J, Park S, Tretyakova NY, Wagner CR. A method for quantitating the intracellular metabolism of AZT amino acid phosphoramidate pronucleotides by capillary high-performance liquid chromatography-electrospray ionization mass spectrometry. Mol Pharm. 2005; 2:233–241. [PubMed: 15934784]

78. Garaguso I, Halter R, Krzeminski J, Amin S, Borlak J. Method for the rapid detection and molecular characterization of DNA alkylating agents by MALDI-TOF mass spectrometry. Anal Chem. 2010; 82:8573–8582. [PubMed: 20866025]
79. Boyd, RK.; Basic, C.; Bethem, RA. Trace Quantitative Analysis by Mass Spectrometry. John Wiley & Sons; West Sussex, England: 2008. Tools of the trade V. Mass analyzers for quantitation: separation of ions by *m/z* values; p. 266-301.
80. Dass, C. Mass Analysis and Ion Detection. In: Desiderio, DM.; Nibbering, NMM., editors. Principles and Practice of Biological Mass Spectrometry. Wiley-Interscience; New York: 2001. p. 59-93.
81. Seneviratne U, Antsypovich S, Goggin M, Quirk Dorr D, Guza R, Moser A, Thompson C, York DM, Tretyakova N. Exocyclic deoxyadenosine adducts of 1,2,3,4-diepoxybutane: synthesis, structural elucidation, and mechanistic studies. Chem Res Toxicol. 2010; 23:118–133. [PubMed: 19883087]
82. Bessette EE, Goodenough AK, Langouet S, Yasa I, Kozekov ID, Spivack SD, Turesky RJ. Screening for DNA adducts by data-dependent constant neutral loss-triple stage mass spectrometry with a linear quadrupole ion trap mass spectrometer. Anal Chem. 2009; 81:809–819. [PubMed: 19086795]
83. Goodenough AK, Schut HA, Turesky RJ. Novel LC-ESI/MS/MS(n) method for the characterization and quantification of 2′-deoxyguanosine adducts of the dietary carcinogen 2-amino-1-methyl-6-phenylimidazo[4,5-b]pyridine by 2-D linear quadrupole ion trap mass spectrometry. Chem Res Toxicol. 2007; 20:263–276. [PubMed: 17305409]
84. Gu D, Turesky RJ, Tao Y, Langouet SA, Nauwelaers GC, Yuan JM, Yee D, Yu MC. DNA adducts of 2-amino-1-methyl-6-phenylimidazo[4,5-b]pyridine and 4-aminobiphenyl are infrequently detected in human mammary tissue by liquid chromatography/tandem mass spectrometry. Carcinogenesis. 2012; 33:124–130. [PubMed: 22072616]
85. Lacorte S, Fernandez-Alba AR. Time of flight mass spectrometry applied to the liquid chromatographic analysis of pesticides in water and food. Mass Spectrom Rev. 2006; 25:866–880. [PubMed: 16752429]
86. Kristensen DB, Imamura K, Miyamoto Y, Yoshizato K. Mass spectrometric approaches for the characterization of proteins on a hybrid quadrupole time-of-flight (Q-TOF) mass spectrometer. Electrophoresis. 2000; 21:430–439. [PubMed: 10675024]
87. Makarov A. Electrostatic axially harmonic orbital trapping: a high-performance technique of mass analysis. Anal Chem. 2000; 72:1156–1162. [PubMed: 10740853]
88. Zhang NR, Yu S, Tiller P, Yeh S, Mahan E, Emary WB. Quantitation of small molecules using high-resolution accurate mass spectrometers - a different approach for analysis of biological samples. Rapid Commun Mass Spectrom. 2009; 23:1085–1094. [PubMed: 19263405]
89. Perry RH, Cooks RG, Noll RJ. Orbitrap mass spectrometry: instrumentation, ion motion and applications. Mass Spectrom Rev. 2008; 27:661–699. [PubMed: 18683895]
90. Bryant MS, Lay JO Jr. Development of fast atom bombardment mass spectral methods for the identification of carcinogen-nucleoside adducts. J Am Soc Mass Spectrom. 1992; 3:360–371.
91. Van den Driessche B, Esmans EL, Van der Linden A, Van Dongen W, Schaerlaken E, Lemiere F, Witters E, Berneman Z. First results of a quantitative study of DNA adducts of melphalan in the rat by isotope dilution mass spectrometry using capillary liquid chromatography coupled to electrospray tandem mass spectrometry. Rapid Commun Mass Spectrom. 2005; 19:1999–2004. [PubMed: 15954175]
92. Malayappan B, Johnson L, Nie B, Panchal D, Matter B, Jacobson P, Tretyakova N. Quantitative high-performance liquid chromatography-electrospray ionization tandem mass spectrometry analysis of *bis-N7*-guanine DNA-DNA cross-links in white blood cells of cancer patients receiving cyclophosphamide therapy. Anal Chem. 2010; 82:3650–3658. [PubMed: 20361772]
93. Reece DE, Connors JM, Spinelli JJ, Barnett MJ, Fairey RN, Klingemann HG, Nantel SH, O'Reilly S, Shepherd JD, Sutherland HJ. Intensive therapy with cyclophosphamide, carmustine, etoposide ± cisplatin, and autologous bone marrow transplantation for Hodgkin's disease in first relapse after combination chemotherapy. Blood. 1994; 83:1193–1199. [PubMed: 8118023]

94. Demirer T, Buckner CD, Appelbaum FR, Bensinger WI, Sanders J, Lambert K, Clift R, Fefer A, Storb R, Slattery JT. Busulfan, cyclophosphamide and fractionated total body irradiation for autologous or syngeneic marrow transplantation for acute and chronic myelogenous leukemia: phase I dose escalation of busulfan based on targeted plasma levels. Bone Marrow Transplant. 1996; 17:491–495. [PubMed: 8722344]

95. Johnson LA, Malayappan B, Tretyakova N, Campbell C, Macmillan ML, Wagner JE, Jacobson PA. Formation of cyclophosphamide specific DNA adducts in hematological diseases. Pediatr Blood Cancer. 2012; 58:708–714. [PubMed: 21793181]

96. Harrington CF, Le Pla RC, Jones GD, Thomas AL, Farmer PB. Determination of cisplatin 1,2-intrastrand guanine-guanine DNA adducts in human leukocytes by high-performance liquid chromatography coupled to inductively coupled plasma mass spectrometry. Chem Res Toxicol. 2010; 23:1313–1321. [PubMed: 20666396]

97. Sar DG, Montes-Bayon M, Blanco-Gonzalez E, Sanz-Mendel A. Quantitative methods for studying DNA interactions with chemotherapeutic cisplatin. Trends in Analytical Chemistry. 2010; 29:1390–1398.

98. Baskerville-Abraham IM, Boysen G, Troutman JM, Mutlu E, Collins L, Dekrafft KE, Lin W, King C, Chaney SG, Swenberg JA. Development of an ultraperformance liquid chromatography/mass spectrometry method to quantify cisplatin 1,2 intrastrand guanine-guanine adducts. Chem Res Toxicol. 2009; 22:905–912. [PubMed: 19323581]

99. Bolton JL, Thatcher GR. Potential mechanisms of estrogen quinone carcinogenesis. Chem Res Toxicol. 2008; 21:93–101. [PubMed: 18052105]

100. Guo L, Wu H, Yue H, Lin S, Lai Y, Cai Z. A novel and specific method for the determination of aristolochic acid-derived DNA adducts in exfoliated urothelial cells by using ultra performance liquid chromatography-triple quadrupole mass spectrometry. J Chromatogr B Analyt Technol Biomed Life Sci. 2011; 879:153–158.

101. Ricicki EM, Soglia JR, Teitel C, Kane R, Kadlubar F, Vouros P. Detection and quantification of N-(deoxyguanosin-8-yl)-4-aminobiphenyl adducts in human pancreas tissue using capillary liquid chromatography-microelectrospray mass spectrometry. Chem Res Toxicol. 2005; 18:692–699. [PubMed: 15833029]

102. Soglia JR, Turesky RJ, Paehler A, Vouros P. Quantification of the heterocyclic aromatic amine DNA adduct N-(deoxyguanosin-8-yl)-2-amino-3-methylimidazo[4,5-f]quinoline in livers of rats using capillary liquid chromatography/microelectrospray mass spectrometry: a dose-response study. Anal Chem. 2001; 73:2819–2827. [PubMed: 11467522]

103. Turesky RJ, Box RM, Markovic J, Gremaud E, Snyderwine EG. Formation and persistence of DNA adducts of 2-amino-3-methylimidazo[4,5-f]quinoline in the rat and nonhuman primates. Mutat Res. 1997; 376:235–241. [PubMed: 9202760]

104. Paehler A, Richoz J, Soglia J, Vouros P, Turesky RJ. Analysis and quantification of DNA adducts of 2-amino-3,8-dimethylimidazo[4,5-f]quinoxaline in liver of rats by liquid chromatography/electrospray tandem mass spectrometry. Chem Res Toxicol. 2002; 15:551–561. [PubMed: 11952342]

105. Dennehy MK, Loeppky RN. Mass spectrometric methodology for the determination of glyoxaldeoxyguanosine and O^6-hydroxyethyldeoxyguanosine DNA adducts produced by nitrosamine bident carcinogens. Chem Res Toxicol. 2005; 18:556–565. [PubMed: 15777095]

106. Loeppky RN, Ye Q, Goelzer P, Chen Y. DNA adducts from N-nitrosodiethanolamine and related beta-oxidized nitrosamines *in vivo*: ^{32}P-postlabeling methods for glyoxal- and O^6-hydroxyethyldeoxyguanosine adducts. Chem Res Toxicol. 2002; 15:470–482. [PubMed: 11952332]

107. Lao Y, Villalta PW, Sturla SJ, Wang M, Hecht SS. Quantitation of pyridyloxobutyl DNA adducts of tobacco-specific nitrosamines in rat tissue DNA by high-performance liquid chromatography-electrospray ionization-tandem mass spectrometry. Chem Res Toxicol. 2006; 19:674–682. [PubMed: 16696570]

108. Lao Y, Yu N, Kassie F, Villalta PW, Hecht SS. Formation and accumulation of pyridyloxobutyl DNA adducts in F344 rats chronically treated with 4-(methylnitrosamino)-1-(3-pyridyl)-1-butanone and enantiomers of its metabolite, 4-(methylnitrosamino)-1-(3-pyridyl)-1-butanol. Chem Res Toxicol. 2007; 20:235–245. [PubMed: 17305407]

109. Upadhyaya P, Kalscheuer S, Hochalter JB, Villalta PW, Hecht SS. Quantitation of pyridylhydroxybutyl-DNA adducts in liver and lung of F-344 rats treated with 4-(methylnitrosamino)-1-(3-pyridyl)-1-butanone and enantiomers of its metabolite 4-(methylnitrosamino)-1-(3-pyridyl)-1-butanol. Chem Res Toxicol. 2008; 21:1468–1476. [PubMed: 18570389]

110. Stepanov I, Hecht SS. Mitochondrial DNA adducts in the lung and liver of F344 rats chronically treated with 4-(methylnitrosamino)-1-(3-pyridyl)-1-butanone and (S)-4-(methylnitrosamino)-1-(3-pyridyl)-1-butanol. Chem Res Toxicol. 2009; 22:406–414. [PubMed: 19166332]

111. Mutlu E, Collins LB, Stout MD, Upton PB, Daye LR, Winsett D, Hatch G, Evansky P, Swenberg JA. Development and application of an LC-MS/MS method for the detection of the vinyl chloride-induced DNA adduct N^2,3-ethenoguanine in tissues of adult and weanling rats following exposure to $^{13}C_2$-VC. Chem Res Toxicol. 2010; 23:1485–1491. [PubMed: 20799743]

112. Loureiro AP, Marques SA, Garcia CC, Di MP, Medeiros MH. Development of an on-line liquid chromatography-electrospray tandem mass spectrometry assay to quantitatively determine 1,N^2-etheno-2′-deoxyguanosine in DNA. Chem Res Toxicol. 2002; 15:1302–1308. [PubMed: 12387629]

113. Zhang S, Balbo S, Wang M, Hecht SS. Analysis of acrolein-derived 1,N^2-propanodeoxyguanosine adducts in human leukocyte DNA from smokers and nonsmokers. Chem Res Toxicol. 2011; 24:119–124. [PubMed: 21090699]

114. Nakao LS, Fonseca E, Augusto O. Detection of C8-(1-hydroxyethyl)guanine in liver RNA and DNA from control and ethanol-treated rats. Chem Res Toxicol. 2002; 15:1248–1253. [PubMed: 12387621]

115. Wang M, Yu N, Chen L, Villalta PW, Hochalter JB, Hecht SS. Identification of an acetaldehyde adduct in human liver DNA and quantitation as N2-ethyldeoxyguanosine. Chem Res Toxicol. 2006; 19:319–324. [PubMed: 16485909]

116. Balbo S, Meng L, Bliss RL, Jensen JA, Hatsukami DK, Hecht SS. Time course of DNA adduct formation in peripheral blood granulocytes and lymphocytes after drinking alcohol. Mutagenesis. 2012 Mar 9.2012 [Epub ahead of print].

117. Beland FA, Churchwell MI, Von Tungeln LS, Chen S, Fu PP, Culp SJ, Schoket B, Gyorffy E, Minarovits J, Poirier MC, Bowman ED, Weston A, Doerge DR. High-performance liquid chromatography electrospray ionization tandem mass spectrometry for the detection and quantitation of benzo[a]pyrene-DNA adducts. Chem Res Toxicol. 2005; 18:1306–1315. [PubMed: 16097804]

118. Chen YL, Wang CJ, Wu KY. Analysis of *N7*-(benzo[*a*]pyrene-6-yl)guanine in urine using two-step solid-phase extraction and isotope dilution with liquid chromatography/tandem mass spectrometry. Rapid Commun Mass Spectrom. 2005; 19:893–898. [PubMed: 15739243]

119. Monien BH, Muller C, Engst W, Frank H, Seidel A, Glatt H. Time course of hepatic 1-methylpyrene DNA adducts in rats determined by isotope dilution LC-MS/MS and 32P-postlabeling. Chem Res Toxicol. 2008; 21:2017–2025. [PubMed: 18788758]

120. Swenberg JA, Bordeerat NK, Boysen G, Carro S, Georgieva NI, Nakamura J, Troutman JM, Upton PB, Albertini RJ, Vacek PM, Walker VE, Sram RJ, Goggin M, Tretyakova N. 1,3-Butadiene: Biomarkers and application to risk assessment. Chem Biol Interact. 2011; 192:150–154. [PubMed: 20974116]

121. Powley MW, Li Y, Upton PB, Walker VE, Swenberg JA. Quantification of DNA and hemoglobin adducts of 3,4-epoxy-1,2-butanediol in rodents exposed to 3-butene-1,2-diol. Carcinogenesis. 2005; 26:1573–1580. [PubMed: 15888494]

122. Tretyakova NY, Chiang SY, Walker VE, Swenberg JA. Quantitative analysis of 1,3-butadiene-induced DNA adducts in vivo and in vitro using liquid chromatography electrospray ionization tandem mass spectrometry. J Mass Spectrom. 1998; 33:363–376. [PubMed: 9597770]

123. Cochrane JE, Skopek TR. Mutagenicity of butadiene and its epoxide metabolites: I. Mutagenic potential of 1,2-epoxybutene, 1,2,3,4-diepoxybutane and 3,4-epoxy-1,2-butanediol in cultured human lymphoblasts. Carcinogenesis. 1994; 15:713–717. [PubMed: 8149485]

124. Park S, Hodge J, Anderson C, Tretyakova NY. Guanine-adenine cross-linking by 1,2,3,4-diepoxybutane: potential basis for biological activity. Chem Res Toxicol. 2004; 17:1638–1651. [PubMed: 15606140]

125. Park S, Anderson C, Loeber R, Seetharaman M, Jones R, Tretyakova N. Interstrand and intrastrand DNA-DNA cross-linking by 1,2,3,4-diepoxybutane: role of stereochemistry. J Am Chem Soc. 2005; 127:14355–14365. [PubMed: 16218630]

126. Von Tungeln LS, Churchwell MI, Doerge DR, Shaddock JG, McGarrity LJ, Heflich RH, Gamboa da CG, Marques MM, Beland FA. DNA adduct formation and induction of micronuclei and mutations in B6C3F(1)/Tk mice treated neonatally with acrylamide or glycidamide. Int J Cancer. 2008; 124:2006–2015. [PubMed: 19123476]

127. Gamboa da Costa G, Churchwell MI, Hamilton LP, Von Tungeln LS, Beland FA, Marques MM, Doerge DR. DNA adduct formation from acrylamide via conversion to glycidamide in adult and neonatal mice. Chem Res Toxicol. 2003; 16:1328–1337. [PubMed: 14565774]

128. Wickremsinhe ER, Ackermann BL, Chaudhary AK. Validating regulatory-compliant wide dynamic range bioanalytical assays using chip-based nanoelectrospray tandem mass spectrometry. Rapid Commun Mass Spectrom. 2005; 19:47–56. [PubMed: 15570573]

129. Zhang Q, Aft RL, Gross ML. Estrogen carcinogenesis: specific identification of estrogen-modified nucleobase in breast tissue from women. Chem Res Toxicol. 2008; 21:1509–1513. [PubMed: 18672910]

130. Liu X, Lovell MA, Lynn BC. Detection and quantification of endogenous cyclic DNA adducts derived from trans-4-hydroxy-2-nonenal in human brain tissue by isotope dilution capillary liquid chromatography nanoelectrospray tandem mass spectrometry. Chem Res Toxicol. 2006; 19:710–718. [PubMed: 16696574]

131. Liu X, Lovell MA, Lynn BC. Development of a method for quantification of acrolein-deoxyguanosine adducts in DNA using isotope dilution-capillary LC/MS/MS and its application to human brain tissue. Anal Chem. 2005; 77:5982–5989. [PubMed: 16159131]

132. Lee JR, Lee SJ, Kim TW, Kim JK, Park HS, Kim DE, Kim KP, Yeo WS. Chemical approach for specific enrichment and mass analysis of nitrated peptides. Anal Chem. 2009; 81:6620–6626. [PubMed: 19610626]

133. Embrechts J, Lemiere F, Van DW, Esmans EL, Buytaert P, Van ME, Kockx M, Makar A. Detection of estrogen DNA-adducts in human breast tumor tissue and healthy tissue by combined nano LC-nano ES tandem mass spectrometry. J Am Soc Mass Spectrom. 2003; 14:482–491. [PubMed: 12745217]

134. Chen HJ, Lin GJ, Lin WP. Simultaneous quantification of three lipid peroxidation-derived etheno adducts in human DNA by stable isotope dilution nanoflow liquid chromatography nanospray ionization tandem mass spectrometry. Anal Chem. 2010; 82:4486–4493. [PubMed: 20429514]

135. Beland FA, Churchwell MI, Hewer A, Phillips DH, da Costa GG, Marques MM. Analysis of tamoxifen-DNA adducts in endometrial explants by MS and ^{32}P-postlabeling. Biochem Biophys Res Commun. 2004; 320:297–302. [PubMed: 15219826]

136. Chao MR, Wang CJ, Yen CC, Yang HH, Lu YC, Chang LW, Hu CW. Simultaneous determination of *N7*-alkylguanines in DNA by isotope-dilution LC-tandem MS coupled with automated solid-phase extraction and its application to a small fish model. Biochem J. 2007; 402:483–490. [PubMed: 17134374]

137. Chao MR, Yen CC, Hu CW. Prevention of artifactual oxidation in determination of cellular 8-oxo-7,8-dihydro-2′-deoxyguanosine by isotope-dilution LC-MS/MS with automated solid-phase extraction. Free Radic Biol Med. 2008; 44:464–473. [PubMed: 17983606]

138. Doerge DR, Churchwell MI, Fang JL, Beland FA. Quantification of etheno-DNA adducts using liquid chromatography, on-line sample processing, and electrospray tandem mass spectrometry. Chem Res Toxicol. 2000; 13:1259–1264. [PubMed: 11123967]

139. Liu J, Chen CF, Tsao CW, Chang CC, Chu CC, DeVoe DL. Polymer microchips integrating solid-phase extraction and high-performance liquid chromatography using reversed-phase polymethacrylate monoliths. Anal Chem. 2009; 81:2545–2554. [PubMed: 19267447]

140. Randall K, Argoti D, Paonessa J, Ding Y, Oaks Z, Zhang Y, Vouros P. An improved liquid chromatography-tandem mass spectrometry method for the quantification of 4-aminobiphenyl DNA adducts in urinary bladder cells and tissues. J Chromatogr A. 2010; 1217:4135–4143. [PubMed: 19932483]

141. Glick, J.; Zarbl, H.; Vouros, P. DNA adducts and you: When bad things happen to good cells. Abstract presented at the 234th ACS National Meeting; Boston, MA. August 19–23, 2007; 2007.
142. Tarantini A, Maitre A, Lefebvre E, Marques M, Rajhi A, Douki T. Polycyclic aromatic hydrocarbons in binary mixtures modulate the efficiency of benzo[a]pyrene to form DNA adducts in human cells. Toxicology. 2011; 279:36–44. [PubMed: 20849910]
143. Inagaki S, Hirashima H, Esaka Y, Higashi T, Min JZ, Touo-Oka T. Screening DNA adducts by LC-ESI-MS-MS: Application to screening new adducts formed from acrylamide. Chromatographia. 2010; 72:1043–1048.
144. Spilsberg B, Rundberget T, Johannessen LE, Kristoffersen AB, Holst-Jensen A, Berdal KG. Detection of food-derived damaged nucleosides with possible adverse effects on human health using a global adductomics approach. J Agric Food Chem. 2010; 58:6370–6375. [PubMed: 20429587]
145. Hah SS, Henderson PT, Turteltaub KW. Towards biomarker-dependent individualized chemotherapy: exploring cell-specific differences in oxaliplatin-DNA adduct distribution using accelerator mass spectrometry. Bioorg Med Chem Lett. 2010; 20:2448–2451. [PubMed: 20335033]
146. Gamboa da Costa G, Marques MM, Beland FA, Freeman JP, Churchwell MI, Doerge DR. Quantification of tamoxifen DNA adducts using on-line sample preparation and HPLC-electrospray ionization tandem mass spectrometry. Chem Res Toxicol. 2003; 16:357–366. [PubMed: 12641436]
147. Doerge DR, Churchwell MI, Marques MM, Beland FA. Quantitative analysis of 4-aminobiphenyl-C8-deoxyguanosyl DNA adducts produced in vitro and in vivo using HPLC-ES-MS. Carcinogenesis. 1999; 20:1055–1061. [PubMed: 10357788]
148. Means JC, Olsen PD, Schoffers E. Development of an isotope dilution liquid chromatography/tandem mass spectrometry detection method for DNA adducts of selected aromatic amines. J Am Soc Mass Spectrom. 2003; 14:1057–1066. [PubMed: 12954174]
149. Fu PP, Chou MW, Churchwell M, Wang Y, Zhao Y, Xia Q, Gamboa dC, Marques MM, Beland FA, Doerge DR. High-performance liquid chromatography electrospray ionization tandem mass spectrometry for the detection and quantitation of pyrrolizidine alkaloid-derived DNA adducts in vitro and in vivo. Chem Res Toxicol. 2010; 23:637–652. [PubMed: 20078085]
150. Thomson NM, Mijal RS, Ziegel R, Fleischer NL, Pegg AE, Tretyakova NY, Peterson LA. Development of a quantitative liquid chromatography/electrospray mass spectrometric assay for a mutagenic tobacco specific nitrosamine-derived DNA adduct, O^6-[4-oxo-4-(3-pyridyl)butyl]-2′-deoxyguanosine. Chem Res Toxicol. 2004; 17:1600–1606. [PubMed: 15606135]
151. Churchwell MI, Beland FA, Doerge DR. Quantification of O^6-methyl and O^6-ethyl deoxyguanosine adducts in C57BL/6N/Tk+/− mice using LC/MS/MS. J Chromatogr B Analyt Technol Biomed Life Sci. 2006; 844:60–66.
152. Williams MV, Lee SH, Pollack M, Blair IA. Endogenous lipid hydroperoxide-mediated DNA-adduct formation in min mice. J Biol Chem. 2006; 281:10127–10133. [PubMed: 16449227]
153. Stout MD, Jeong YC, Boysen G, Li Y, Sangaiah R, Ball LM, Gold A, Swenberg JA. LC/MS/MS method for the quantitation of trans-2-hexenal-derived exocyclic 1,N^2-propanodeoxyguanosine in DNA. Chem Res Toxicol. 2006; 19:563–570. [PubMed: 16608168]
154. Zhang S, Villalta PW, Wang M, Hecht SS. Detection and quantitation of acrolein-derived 1,N^2-propanodeoxyguanosine adducts in human lung by liquid chromatography-electrospray ionization-tandem mass spectrometry. Chem Res Toxicol. 2007; 20:565–571. [PubMed: 17385896]
155. Zhang S, Villalta PW, Wang M, Hecht SS. Analysis of crotonaldehyde- and acetaldehyde-derived 1,N^2-propanodeoxyguanosine adducts in DNA from human tissues using liquid chromatography electrospray ionization tandem mass spectrometry. Chem Res Toxicol. 2006; 19:1386–1392. [PubMed: 17040109]
156. Matsuda T, Yabushita H, Kanaly RA, Shibutani S, Yokoyama A. Increased DNA damage in ALDH2-deficient alcoholics. Chem Res Toxicol. 2006; 19:1374–1378. [PubMed: 17040107]

157. Balbo S, Meng L, Bliss RL, Jensen JA, Hatsukami DK, Hecht SS. Kinetics of DNA adduct formation in the oral cavity after drinking alcohol. Cancer Epidemiol Biomarkers Prev. 2012; 21:601–608. [PubMed: 22301829]

158. Chen L, Wang M, Villalta PW, Luo X, Feuer R, Jensen J, Hatsukami DK, Hecht SS. Quantitation of an acetaldehyde adduct in human leukocyte DNA and the effect of smoking cessation. Chem Res Toxicol. 2007; 20:108–113. [PubMed: 17226933]

159. Arlt VM, Stiborova M, Henderson CJ, Thiemann M, Frei E, Aimova D, Singh R, Gamboa da CG, Schmitz OJ, Farmer PB, Wolf CR, Phillips DH. Metabolic activation of benzo[*a*]pyrene *in vitro* by hepatic cytochrome P450 contrasts with detoxification *in vivo*: experiments with hepatic cytochrome P450 reductase null mice. Carcinogenesis. 2008; 29:656–665. [PubMed: 18204078]

160. Singh R, Gaskell M, Le Pla RC, Kaur B, zim-Araghi A, Roach J, Koukouves G, Souliotis VL, Kyrtopoulos SA, Farmer PB. Detection and quantitation of benzo[*a*]pyrene-derived DNA adducts in mouse liver by liquid chromatography-tandem mass spectrometry: comparison with ^{32}P-postlabeling. Chem Res Toxicol. 2006; 19:868–878. [PubMed: 16780367]

161. Zhang SM, Chen KM, Aliaga C, Sun YW, Lin JM, Sharma AK, Amin S, El Bayoumy K. Identification and quantification of DNA adducts in the oral tissues of mice treated with the environmental carcinogen dibenzo[a,l]pyrene by HPLC-MS/MS. Chem Res Toxicol. 2011; 24:1297–1303. [PubMed: 21736370]

162. Powley MW, Walker VE, Li Y, Upton PB, Swenberg JA. The importance of 3,4-epoxy-1,2-butanediol and hydroxymethylvinyl ketone in 3-butene-1,2-diol associated mutagenicity. Chem Biol Interact. 2007; 166:182–190. [PubMed: 17349618]

163. Huang CC, Shih WC, Wu CF, Chen MF, Chen YL, Lin YH, Wu KY. Rapid and sensitive on-line liquid chromatographic/tandem mass spectrometric determination of an ethylene oxide-DNA adduct, *N7*-(2-hydroxyethyl)guanine, in urine of nonsmokers. Rapid Commun Mass Spectrom. 2008; 22:706–710. [PubMed: 18257114]

164. Marsden DA, Jones DJ, Lamb JH, Tompkins EM, Farmer PB, Brown K. Determination of endogenous and exogenously derived *N7*-(2-hydroxyethyl)guanine adducts in ethylene oxide-treated rats. Chem Res Toxicol. 2007; 20:290–299. [PubMed: 17263564]

165. Tompkins EM, Jones DJ, Lamb JH, Marsden DA, Farmer PB, Brown K. Simultaneous detection of five different 2-hydroxyethyl-DNA adducts formed by ethylene oxide exposure, using a high-performance liquid chromatography/electrospray ionisation tandem mass spectrometry assay. Rapid Commun Mass Spectrom. 2008; 22:19–28. [PubMed: 18041793]

166. Pathak S, Singh R, Verschoyle RD, Greaves P, Farmer PB, Steward WP, Mellon JK, Gescher AJ, Sharma RA. Androgen manipulation alters oxidative DNA adduct levels in androgen-sensitive prostate cancer cells grown in vitro and in vivo. Cancer Lett. 2008; 261:74–83. [PubMed: 18096312]

167. Evans MD, Singh R, Mistry V, Sandhu K, Farmer PB, Cooke MS. Analysis of urinary 8-oxo-7,8-dihydro-purine-2′-deoxyribonucleosides by LC-MS/MS and improved ELISA. Free Radic Res. 2008; 42:831–840. [PubMed: 18985483]

168. Li CS, Wu KY, Chang-Chien GP, Chou CC. Analysis of oxidative DNA damage 8-hydroxy-2′-deoxyguanosine as a biomarker of exposures to persistent pollutants for marine mammals. Environ Sci Technol. 2005; 39:2455–2460. [PubMed: 15884335]

169. Synold T, Xi B, Wuenschell GE, Tamae D, Figarola JL, Rahbar S, Termini J. Advanced glycation end products of DNA: quantification of N^2-(1-carboxyethyl)-2′-deoxyguanosine in biological samples by liquid chromatography electrospray ionization tandem mass spectrometry. Chem Res Toxicol. 2008; 21:2148–2155. [PubMed: 18808156]

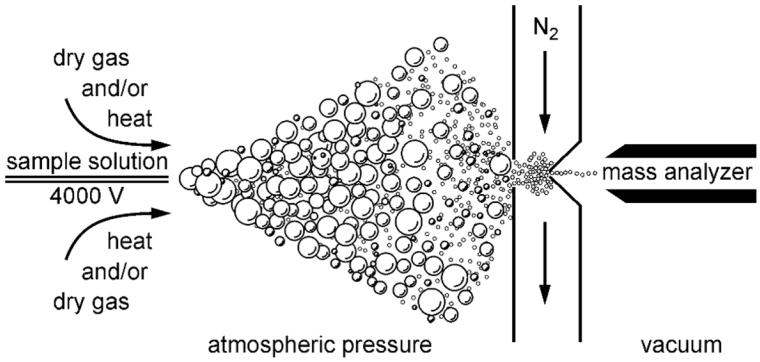

Figure 1.

Ion formation in electrospray ionization mass spectrometry. Sample dissolved in an aqueous solvent is continuously sprayed through a stainless narrow bore capillary maintained under a high voltage relative to the ion sampling orifice (3–4 kV), leading to the formation of a mist of fine, highly charged droplets. The solvent is removed using heat and/or drying gas, generating either protonated or deprotonated analyte ions in the gas phase.

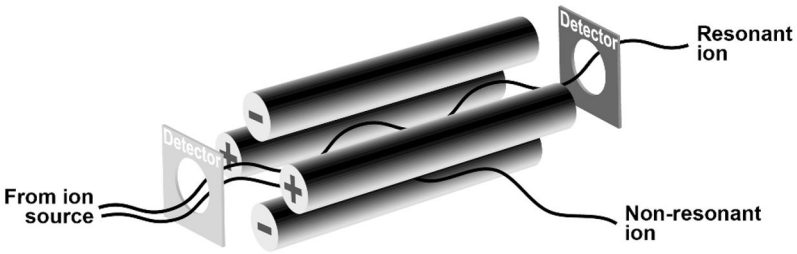

Figure 2.

Schematic of a quandrupole mass analyzer. Four precisely engineered, parallel rods are arranged symmetrically in a square array, with opposite pairs of electrodes electrically connected. A quadrupole field is created by applying a positive direct current (dc) at a potential U with a superimposing radiofrequency (rf) potential V cosωt to the first electrode pair. The alternating pair of electrodes receives the dc potential of – U and an rf potential of V cosωt, which is out of phase by 180°. At a given value of U and V, only ions of specified mass to charge ratio (*m/z*) have stable trajectories and are able to move through the quadrupole mass filter and reach the detector, while all the other ions are lost.

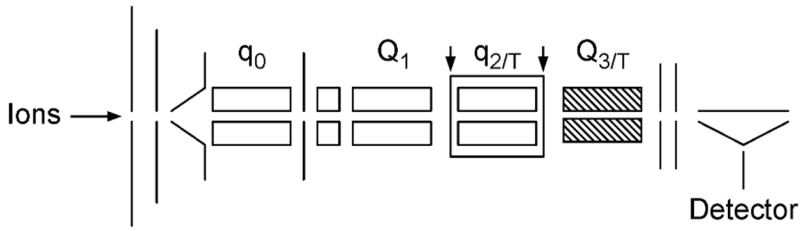

Figure 3.
Schematic of a triple quadrupole mass analyzer ($Q_1q_2Q_3$). Triple quadrupole instruments contain two quadrupole mass filters (Q_1 and Q_3) separated by a quadrupole collision cell/ion guide (q_2). IN a typical experiment, analyte ions (precursor ions) are selected in the first mass analyzer (Q_1) and then are accelerated into the second quadrupole (q_2) utilized as a collision cell. Analyte ions selected in Q_1 are fragmented in q_2 to produce mass fragments, which are analyzed in Q_3.

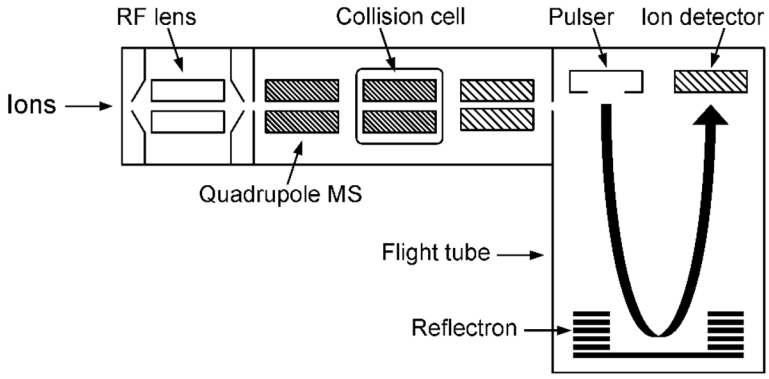

Figure 4.

QqTOF hybrid mass analyzers couple a mass selective quadrupole and a collision cell to a TOF analyzer. The QqTOF design is similar to a triple quadrupole (Figure 3), with the exception that the third quadrupole is replaced by a TOF mass analyzer. The QqTOF can be operated in SIM/SRM scanning mode similar to that of a triple quadripole, but afford an improved mass resolution for the fragment ions, allowing to increased selectivity and improved signal to noise ratios.

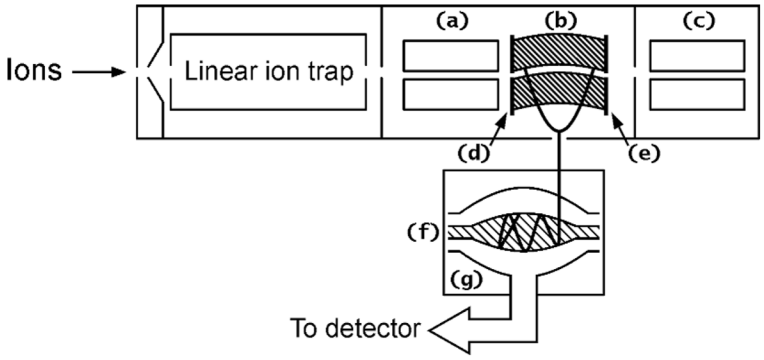

Figure 5.

Drawing of an Orbitrap mass analyzer: (a) transfer octapole; (b) curved RF-only quadrupole (C-trap); (c) octapole collision cell; (d) gate electrode; (e) trap electrode; (f) inner orbitrap electrode (central electrode); (g) outer orbitrap electrode.

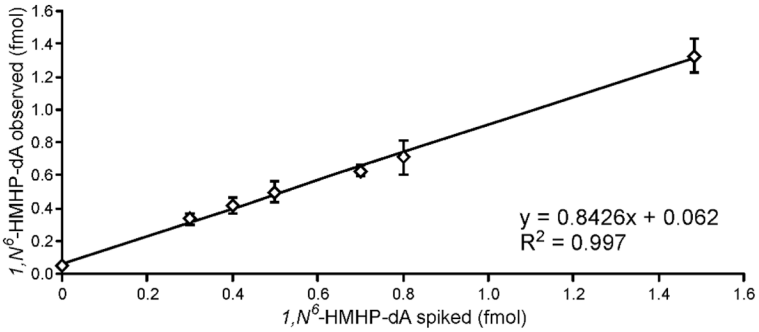

Figure 6.

Validation results for column switching HPLC-ESI$^+$-MS/MS analysis of *1,N^6*-(2-hydroxy-3-hydroxymethylpropan-1,3-diyl)-dA in rodent DNA. Reprinted with permission from Goggin, M., Seneviratne, U., Swenberg, J. A., Walker, V. E., and Tretyakova, N. (2010) Column switching HPLC-ESI$^+$-MS/MS methods for quantitative analysis of exocyclic dA adducts in the DNA of laboratory animals exposed to 1,3-butadiene. *Chem. Res. Toxicol. 23*, 808–812. Copyright 2010 American Chemical Society.[70]

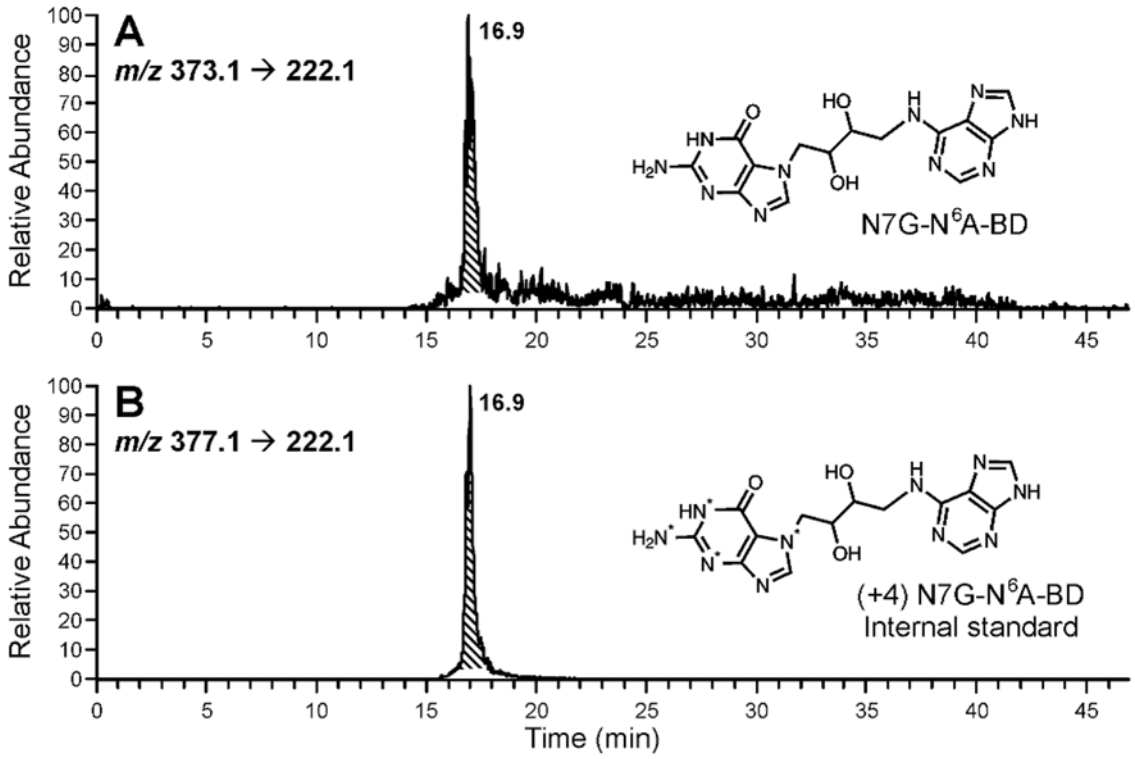

Figure 7.

NanoLC-nanoESI$^+$-MS/MS analysis of N7G-N^{6}A-BD in liver DNA from a mouse exposed to 625 ppm BD for 2 weeks. Reprinted with permission from Goggin, M., Sangaraju, D., Walker, V. E., Wickliffe, J., Swenberg, J. A., and Tretyakova, N. (2011) Persistence and repair of bifunctional DNA adducts in tissues of laboratory animals exposed to 1,3-butadiene by inhalation. *Chem. Res. Toxicol. 24*, 809–817. Copyright 2011 American Chemical Society.[34]

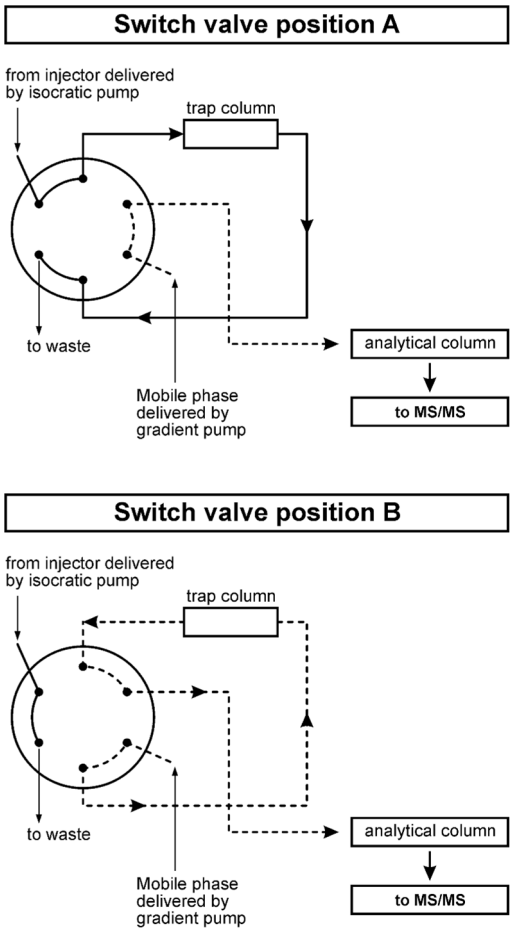

Figure 8.

Diagram of valve positions employed in column switching HPLC-ESI-MS/MS. Sample is loaded onto trapping column in position A and washed to remove contaminants. In position B, the second pump backflushes the analyte from the trapping column onto the analytical column and into the mass spectrometer.

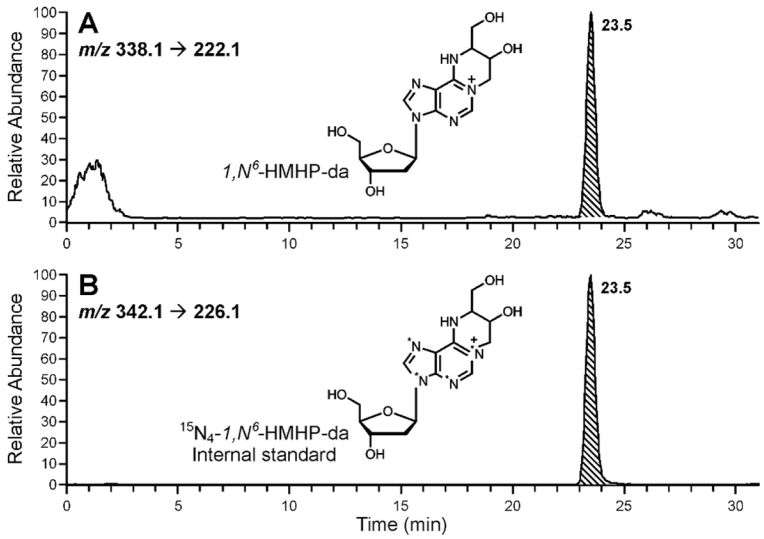

Figure 9.

Column switching capLC-ESI$^+$-MS/MS analysis of 1,N^6-HMHP-dA in liver DNA from a mouse exposed to 200 ppm BD for 2 weeks. Reprinted with permission from Goggin, M., Seneviratne, U., Swenberg, J. A., Walker, V. E., and Tretyakova, N. (2010) Column switching HPLC-ESI$^+$-MS/MS methods for quantitative analysis of exocyclic dA adducts in the DNA of laboratory animals exposed to 1,3-butadiene. *Chem. Res. Toxicol. 23*, 808–812. Copyright 2010 American Chemical Society.[70]

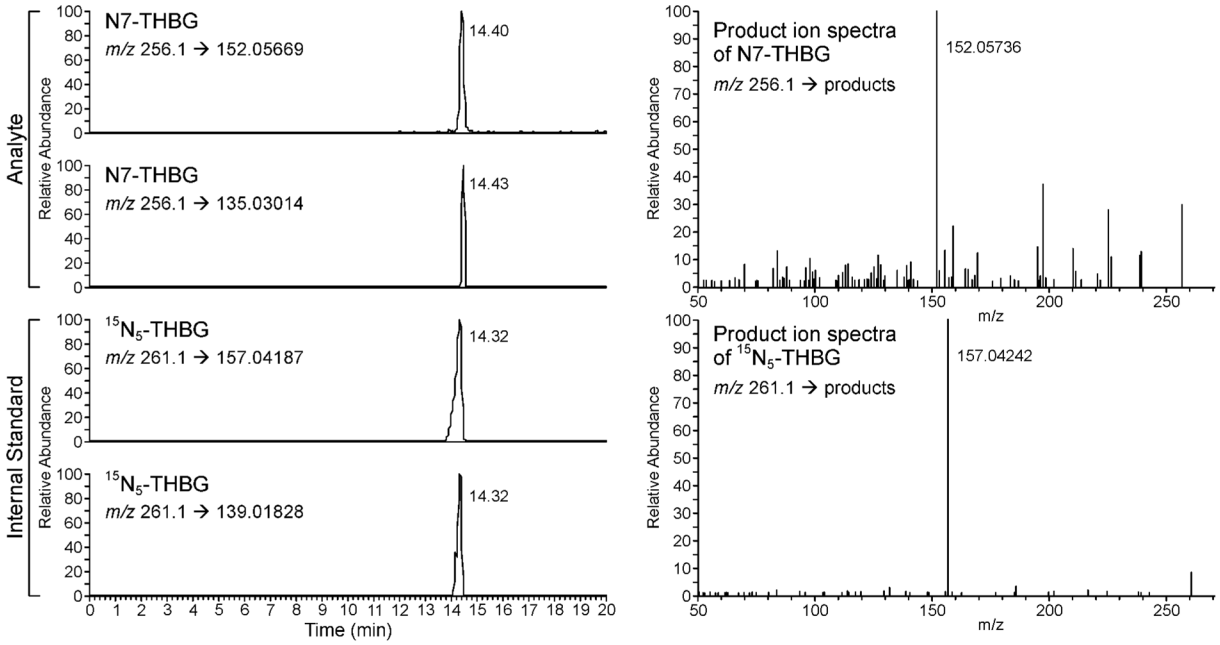

Figure 10.

Capillary HPLC- accurate mass nanospray MS/MS analysis of N7-trihydroxybutylguanine adducts of 1,3-butadiene in DNA extracted from blood of a confirmed smoker. Two separate mass transitions are used to monitor the analyte and the internal standard ($^{15}N_5$- THBG).

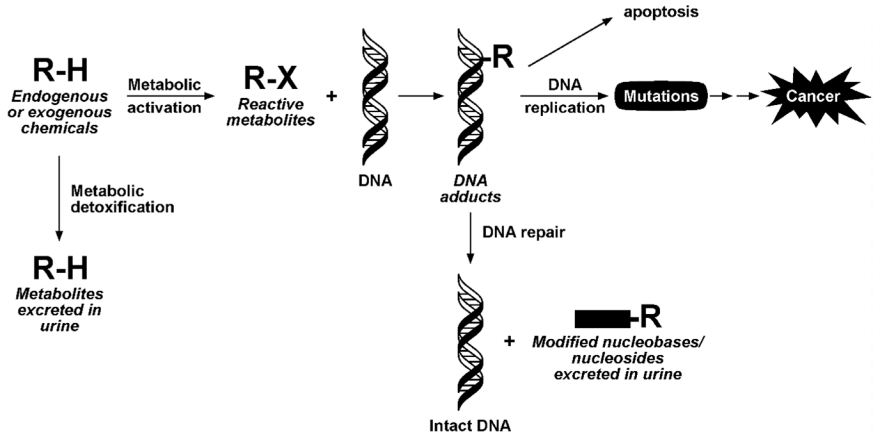

Scheme 1.
Role of DNA adducts in chemical carcinogenesis.

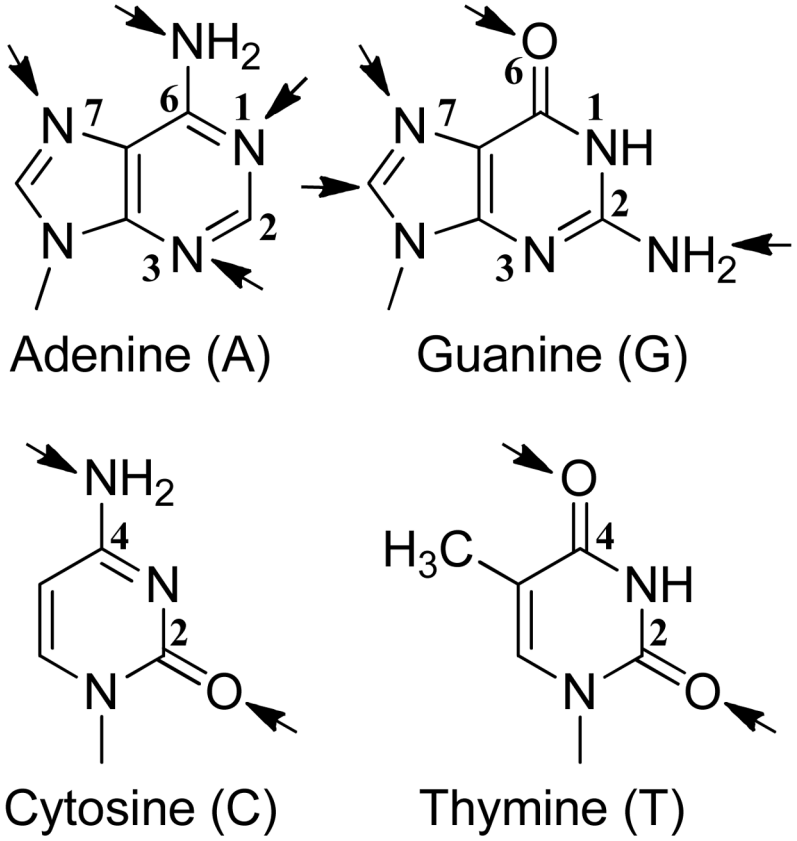

Scheme 2.
Nucleobase positions in DNA frequently modified by electrophiles.

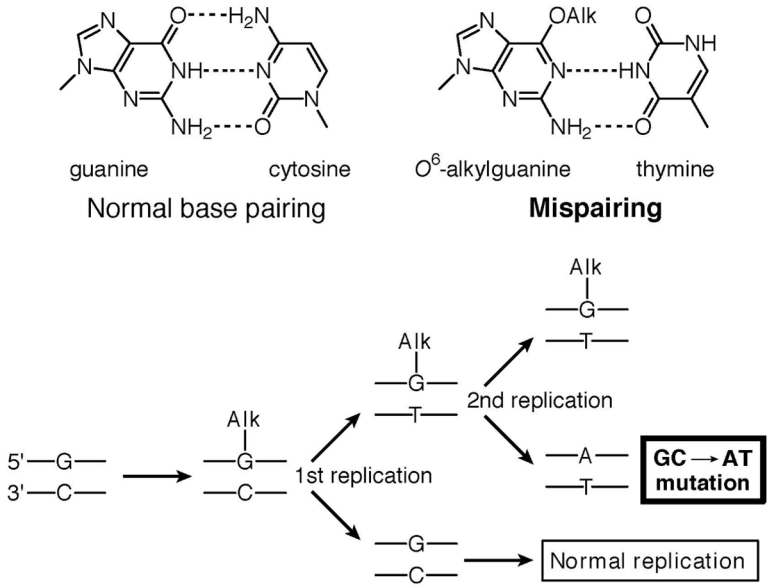

Scheme 3.
The mechanism of G to A transition mutations induced by O^6-alkylguanines.

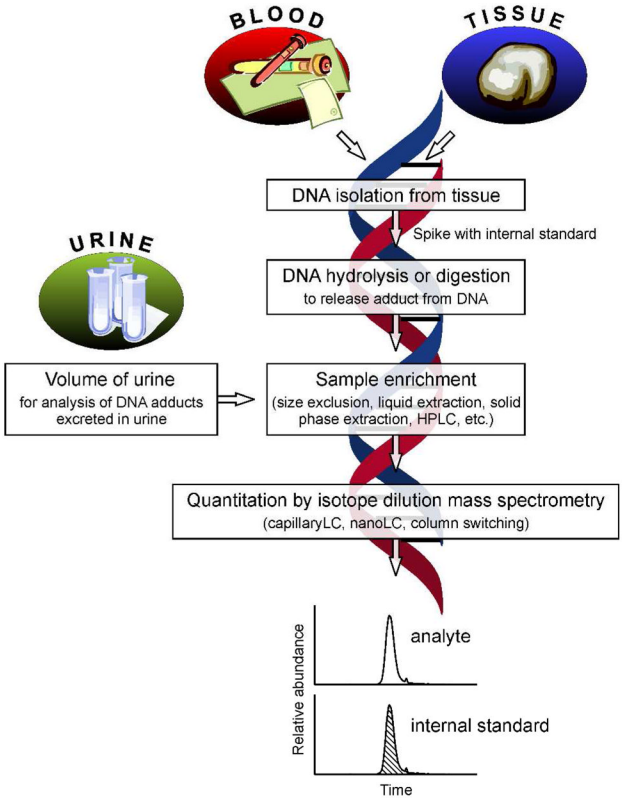

Scheme 4.

Sample processing scheme for isotope dilution HPLC-ESI-MS/MS analysis of DNA adducts.

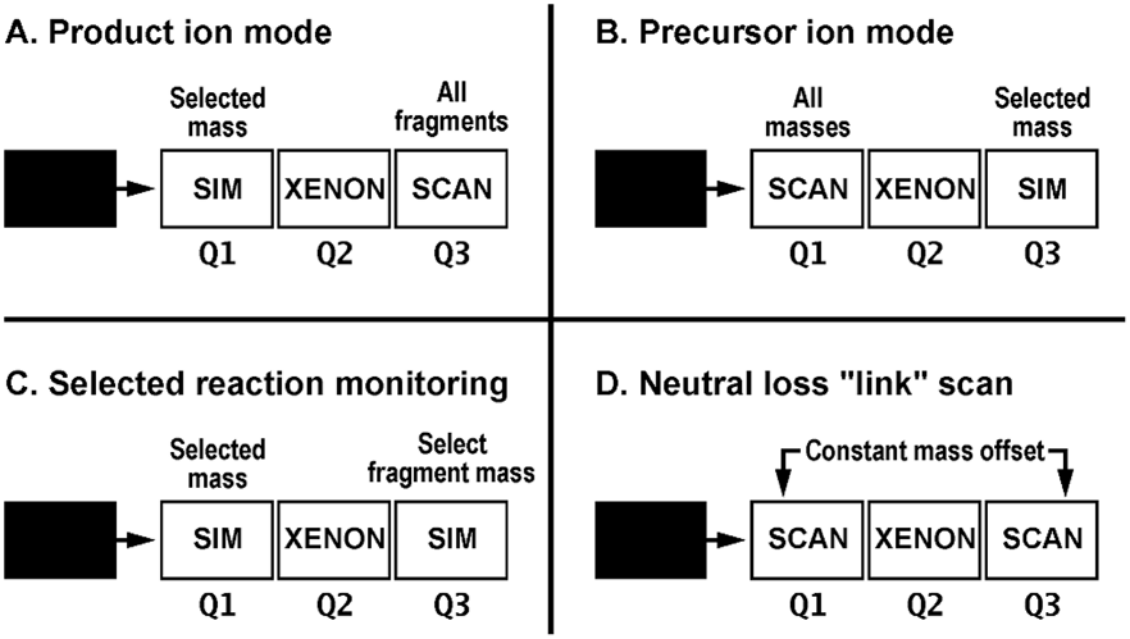

Scheme 5.
Mass spectrometry scanning modes.

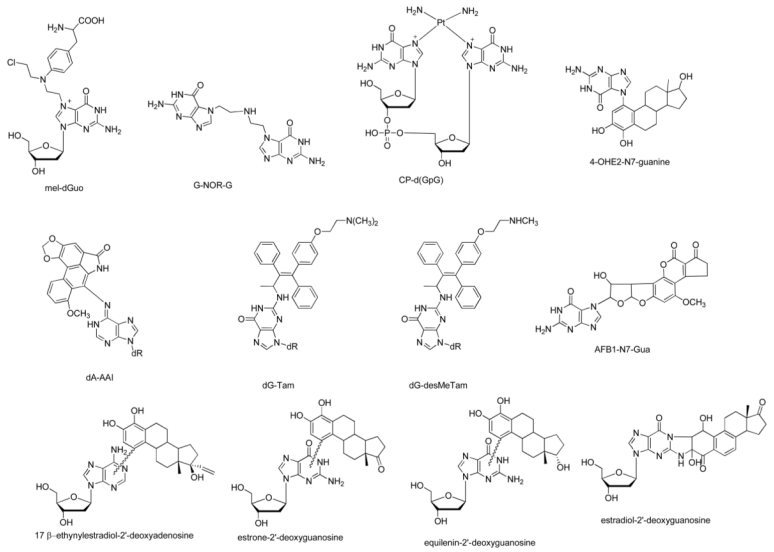

Chart 1.

Structures of representative DNA adducts formed from natural products and drugs: N7-melphalan-deoxyguanosine (mel-dGuo); *N,N-bis*[2-(*N7*-guaninyl) ethyl] amine DNA-DNA cross-links (G-NOR-G); cisplatin 1,2-guanine-guanine intrastrand cross-link (CP-d(GpG); 4- hydroxyestradiol-*N7*-guanine (4-OHE_2-N_7G); 7-(deoxyadenosin-N^6-yl)aristolactam I (dA-AAI); (*E*)-α-(deoxyguanosin-N^2-yl) tamoxifen (dG-Tam); (*E*)-α-(deoxyguanosin-N^2-yl)-N-desmethyl tamoxifen (dG-desMeTam); aflatoxinB^1- *N7*-guanine (AFB_1- *N7*-Gua), 17α-ethynylestradiol-2′-deoxyadenosine; estrone-2′-deoxyguanosine, equilenin-2′-deoxyguanosine; estradiol-2′-deoxyguanosine.

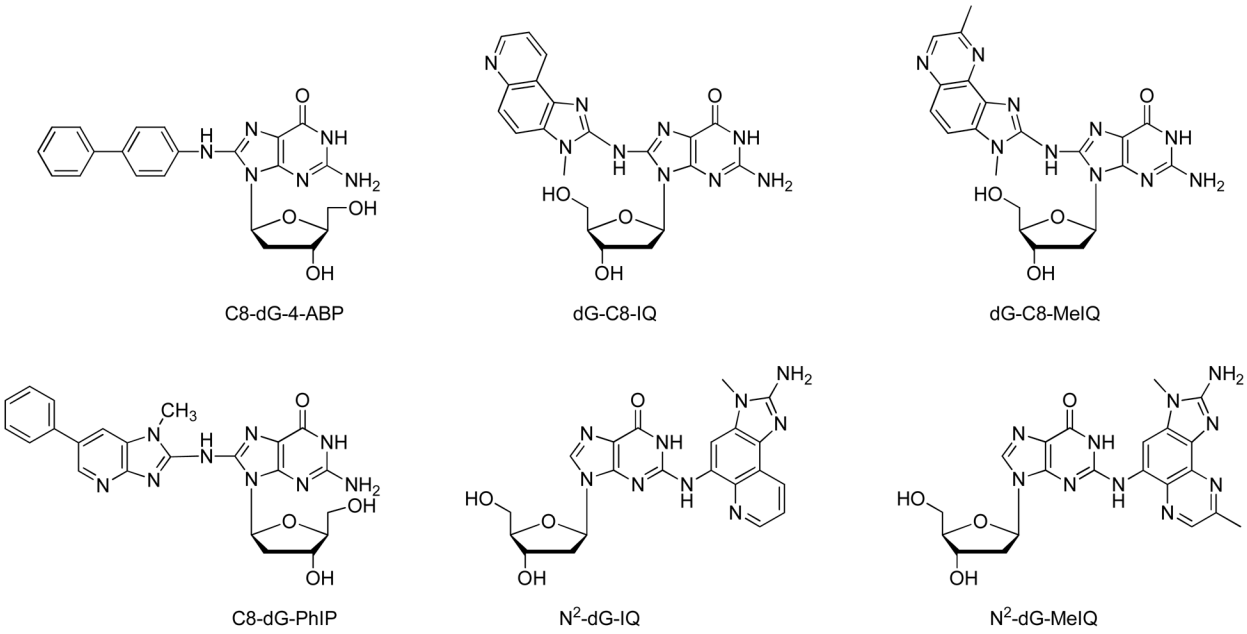

Chart 2.

Structures of DNA adducts formed by aromatic amines, N-(deoxyguanosin-8-yl)-4- ABP (C8- dG-4-ABP); *N*-(deoxyguanosine-8-yl)-2-amino-3-methylimidazo [4,5-*f*] quinoline (C8-dG-IQ); *N*-(deoxyguanosine-8-yl)-MeIQx (C8- dG-MeIQ); 5-(deoxyguanosin-N^2-yl)-MeIQx (N^2-dG- MeIQ); and 5-(deoxyguanosine-N^2-yl)-2-amino-3-methylimidazo [4,5-*f*] quinoline (N^2- dG-IQ).

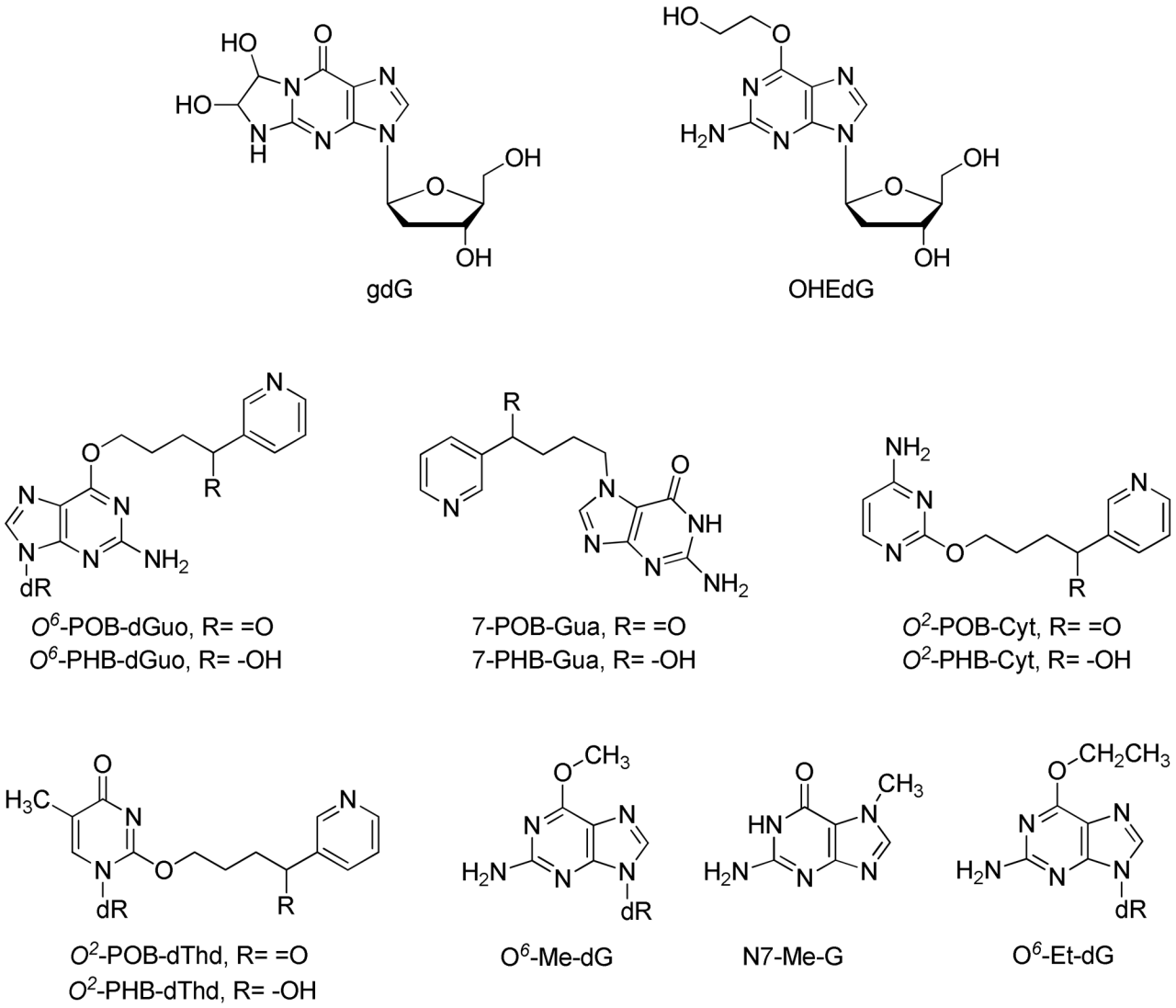

Chart 3.

Nitrosamine-derived DNA adducts: glyoxal-deoxyguanosine (gdG); *O*^{6}-2- hydroxyethyl-2′-doexyguanosine (OHEdG); *O*^{6}-[4-(3-pyridyl)-4-oxobut-1-yl]-2′-deoxyguanosine (*O*^{6}-POB-dG); *O*^{6}-[4-(3-pyridyl)-4-hydroxybut-1-yl]-2′-deoxyguanosine (*O*^{6}-PHB-dG); 7-[4-(3-pyridyl)-4-oxobut-1-yl]guanine (7-POB-Gua); 7-[4-(3-pyridyl)-4-hydroxybut-1-yl]guanine (7- PHB-Gua); *O*^{2}-[4-(3-pyridyl)-4-oxobut-1-yl]cytosine (*O*^{2}-POB-Cyt); *O*^{2}-[4-(3-pyridyl)-4- ohydroxybut-1-yl]cytosine (*O*^{2}-PHB-Cyt); *O*^{2}-[4-(3-pyridyl)-4-oxobut-1-yl]thymidine (*O*^{2}-POBdThd); *O*^{2}-[4-(3-pyridyl)-4-hydroxybut-1-yl]thymidine (*O*^{2}-POB-dThd); *O*^{6}-methyl-2′-deoxyguanosine (*O*^{6}-Me-dG); *N7*-methylguanine (N7-Me-G); *O*^{6}-ethyl-2′-deoxyguanosine (*O*^{6}- Et-dG).

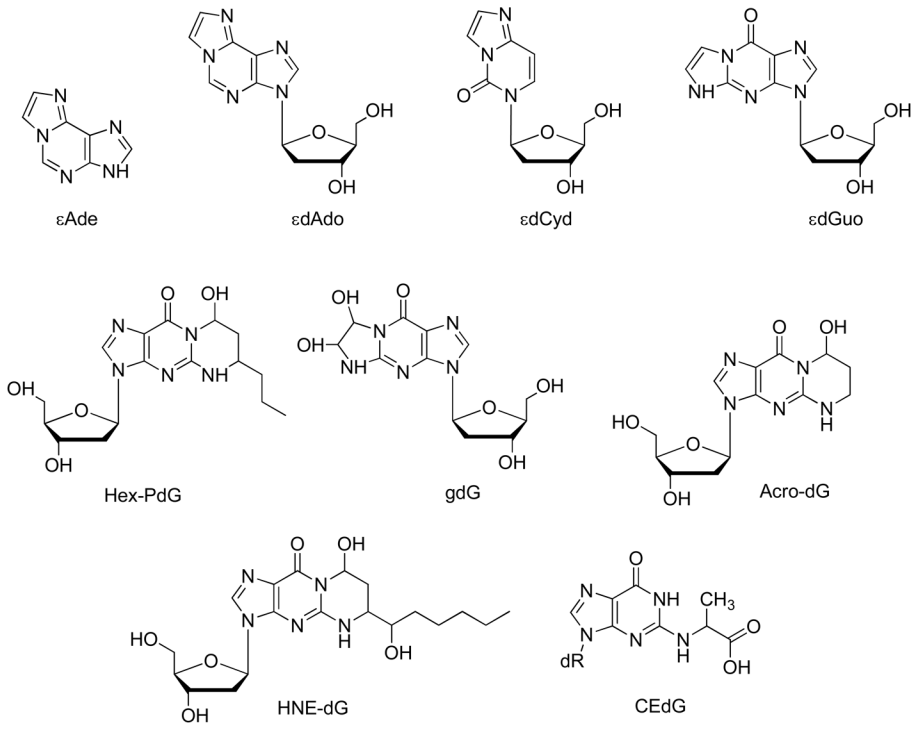

Chart 4.

Exocyclic DNA adduct structures, *1,N*^{6}-etheno-adenine (εA); *1,N*^{6}-etheno-2′-deoxyadenosine (εdA); *3,N*^{4}-etheno-2′-deoxycytosine (εdC); *1,N*^{2}-etheno-2′-deoxyguanosine (εdG); hexenal-derived exocyclic 1, *N*^{2}-propanodeoxyguanosine (Hex-PdG); glyoxal-2′-deoxyguanosine (gdG); 1, *N*^{2}-propanodeoxyguanosine; acrolein-dG (Acro-dG); 1,*N*^{2}- hydroxynonenal-dG (HNE-dG); and *N*^{2}-(1-carboxyethyl)-2′-deoxyguanosine (CEdG).

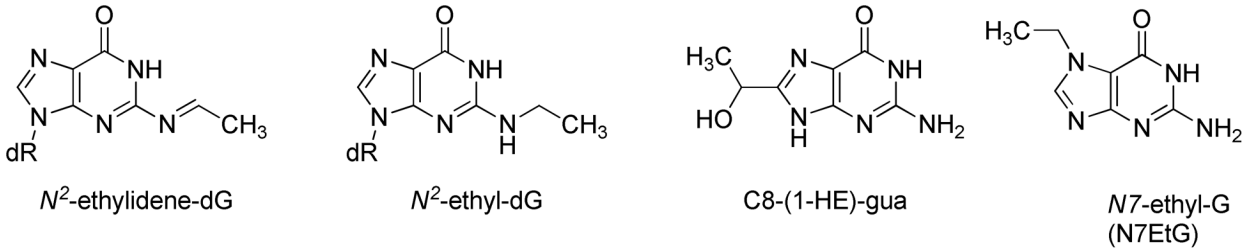

Chart 5.

Structures of ethanol and acetaldehyde induced DNA adducts: N^2-ethylidene-2′-deoxyguanosine (N^2-ethylidene-dG); N^2-ethyl-2′-deoxyguanosine (N^2-ethyl-dG); C8-(1-hydroxyethyl)guanine (C8-(1-HE)-Gua; and $N7$-ethylguanine ($N7$-ethyl-G).

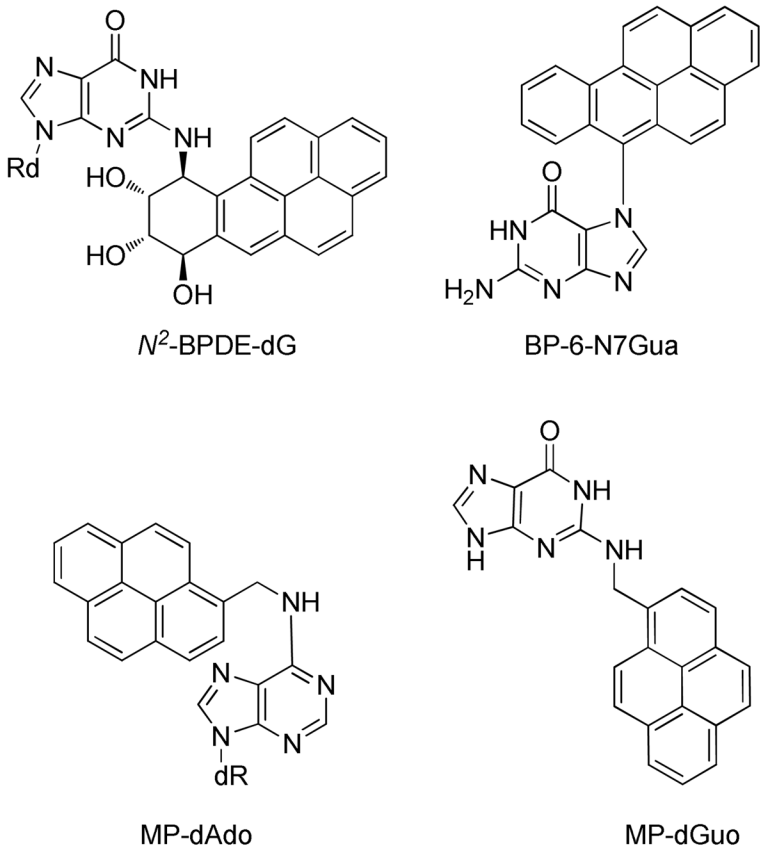

Chart 6.
Polycyclic aromatic hydrocarbon-derived DNA adducts: 7,8,9-trihydroxy-10-(N^2-deoxyguanosyl)-7,8,9,10-tretrahydrobenzo[*a*]pyrene (N^2-BPDE-dG); *N7*-(benzo[*a*]pyrene-6- yl)guanine (BP-6-N7Gua); methypyrene-2′-deoxyadenosine (MP-dAdo); and methylpyrene-2′-deoxyguanosine (MP-dGuo).

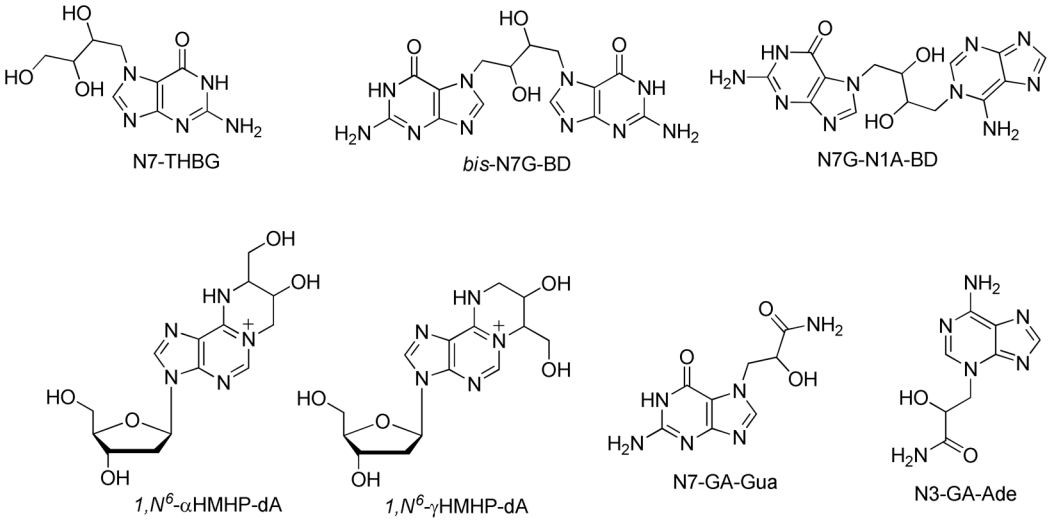

Chart 7.

Structures of epoxide induced DNA adducts, N7-(2,3,4-trihydroxybutyl)guanine (N7-THBG); 1,4-*bis*-(guan-7-yl)-2,3-butanediol (*bis*-N7G-BD); 1-(guan-7-yl)-4-(aden-1-yl)-2,3-butanediol (N7G-N1A-BD); *1,N*^{6}-(1-hydroxymethyl-2-hydroxypropan-1,3-diyl)-2′-deoxyadenosine (*1,N*^{6}-αHMHP-dA); *1,N*^{6}-(2-hydroxy-3-hydroxymethyl-propan-1,3-diyl)-2′-deoxyadenosine (*1,N*^{6}-γHMHP-dA); N7-(2-carbamoyl-2-hydroxyethyl)guanine (N7-GA-Gua); and N3-(2-carbamoyl-2-hydroxyethyl)adenine (N3-GA-Ade).

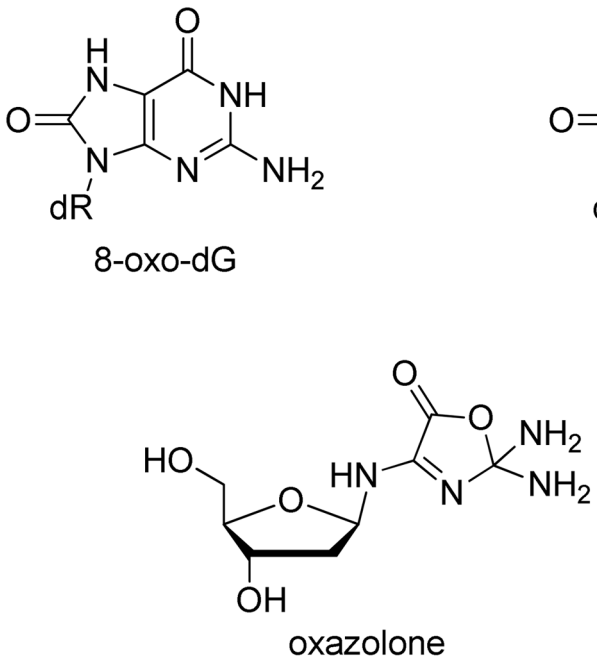

Chart 8.

Structures of oxidative DNA adducts, 8-oxo-7,8-dihydro-2′deoxyguanosine (8-oxo-dG); 8-oxo-7,8-dihydro-2′deoxyadenosine (8-oxo-dA); 2,2-diamino-4-[(2-deoxy-β-D-*erythro*-pentofuranosyl) amino]-5(2*H*)-oxazolone (oxazolone).

Table 1

Characteristics and performances of mass spectrometers commonly used for DNA adduct analysis. Check marks indicate available, check marks in parentheses indicate optional.

	Quadrupole	Triple quadrupole	Ion Trap	QQ-TOF	Orbitrap	QQ-LIT
Mass accuracy	Low	Low	Good	Excellent	Excellent	Medium
Resolving power	Low	Low	High	Very high	Excellent	Low
Sensitivity (LOD)	Low	High	High	Medium	High	High
Dynamic range	High	High	Medium	Medium	High	High
MS/MS capabilities	x	✓	✓	✓	✓	✓
Additional capabilities		Precursor, Neutral loss, SRM	Seq. MS/MS (MS^n)		Seq. MS/MS (MS^n)	MS^n, Precursor, Neutral loss
Identification	*+*	*++*	*+++*	*+++*	*++++*	*+++*
Quantification	*+*	*+++*	*++*	*++*	*++*	*++*
Throughput	*+++*	*+++*	*+++*	*++*	*++*	*++*

+, ++, +++, and ++++ respectively indicate *possible or moderate*, *good or high*, and *excellent, and very high*. Seq., sequential.

Chem Res Toxicol. Author manuscript; available in PMC 2013 October 15.

Table 2

Adduct	Method	LOD	Sample Prep.	Species	Source	Ref.
Adducts induced by DNA alkylating drugs and natural products (Chart 1)						
Urinary 4-OHE$_2$-N7G	IDMS	70 pg	MCX SPE, BondElut SPE	human	urine	38
Mel-dGuo (melphalan)	IDMS w/column switching	900 fg		rat	liver, mammary	91
dG-Tam (tamoxifen)	IDMS w/column switching	1 adduct/10^8 nts		rat	liver, uteri	146
AFB1-N7Gua (aflatoxin)	IDMS	0.02 pg	OasisMCX SPE, immunoaffinity column, BondElut LRC SPE	human	urine	39
4-OH-E$_1$-*N*3Ade	capLC-nanoESI	5 fmol/g tissue	SPE, offline HPLC	human	breast	129
ES-3′-N^6-dA, ES-3′-N^2-dG, ES-3′-C8-dG (Estragole)	IDMS-SIM mode	0.2–0.5 fmol	SPE	rats	liver	35
G-NOR-G cross-links (Cyclophosphamide)	Cap LC-IDMS	5 fmol	Thermal hydrolysis, SPE (Oasis Max)	human	blood	92
DHP-dA, DHP-dG (pyrrolizidine alkaloids)	ID HPLC-ESI-MS/MS					
Aromatic amine adducts (Chart 2)						
IQ-dG	IDMS	6 fmol	C18 SPE	rat	liver	102
dG-C8-ABP	IDMS	5fmol/300 μg DNA	C18 isolute SPE	human	pancreas	101
dG-C8-ABP	IDMS, column switching	0.72/10^7 nts	DNA digest w/on-line column switching	mouse	liver	147
dG-C8-MeIQx	IDMS	500 fg	SepPak C18 SPE	rat	liver	104
dG-N2-MeIQx	IDMS	750 fg	SepPak C18 SPE	rat	liver	104
N8-Ade-benzidine	IDMS	22 pg	SepPak C18 SPE			148
N8-Ade-2-aminofluorene	IDMS	51 pg	SepPak C18 SPE			148
dG-C8-MeIQx, dG-C8- PhIP, dG-C8-4-ABP	capLC-IDMS linear ion trap-MS^3	5–10 adducts per 10^9 nts	Enzymatic digest, SPE (HyperSep)	human	saliva	36
			Enzymatic digest	rat	liver	149
Nitrosamine adducts (Chart 3)						
Hydroxyethyl-dG	CapLC-ESI-MS/MS	100–150 fmol	4mm syringe filter	rat	liver	105
O^6-POBdG	IDMS	50 fmol	Strata-X C18 SPE	mouse	liver	150
POB adducts	IDMS	3fmol G, 1 fmol dGuo, 100 amol Thd, 2 fmol Cyt	StrataX SPE	rat	liver/lung	107

Chem Res Toxicol. Author manuscript; available in PMC 2013 October 15.

Adduct	Method	LOD	Sample Prep.	Species	Source	Ref.
Adducts induced by DNA alkylating drugs and natural products (Chart 1)						
7-POB-Gua	IDMS		Strata-X SPE	rat	liver/lung	110
O^6-mdGuo	IDMS w/column switching	24 fmol O^6-mdGuo		rat	liver	71
O^6-methyl/O^6-ethyl-dG	IDMS w/column switching	0.03 O^6-Me-dG/10^8 nts 0.05 O^6-Et-dG/10^8 nts	Centrifugation	mouse	liver	151
Exocyclic adducts						
C-ɛdC, C-ɛdG, H-ɛdA, H- ɛdC, H-ɛdG	Cap. HPLC-ESI- MS/MS, MRM mode	Not specified	0.2 um filter, Supelclean LC-C18 SPE	mouse	intestine	152
gdG	IDMS Capillary LC- MS/MS, SRM	gdG: 1.5–2pmol	4 mm syringe filter	rat	liver	105
Etheno guanine	IDMS LC-ESI^+- MS/MS	1 pg	SCX, C18-OH SPE	human	urine	43
ɛA	IDMS HPLC-ESI-MS/MS MRM	2–3 pg	C18-OH SPE	human	urine	44
ɛdA	IDMS, column switching, APCI MS	8 pM	Oasis HLB SPE	human	urine	72
1,N^2-propano-dG	IDMS LC-MS/MS	0.015 fmol/μg DNA	Centrifugation (YM-10), Oasis HLB SPE	rat	liver	153
Propane-dG	IDMS	4 adducts/10^9 nts	Strata-X SPE	human	lung	154
Cro-dGuo	IDMS	0.2 fmol	Strata-X SPE	human	liver/lung	155
PdG, Et-dG	IDMS	250 fg?	DNA digest w/Liquid extraction	human	blood	156
1,N^2-ɛdGuo	IDMS w/column switching	20 fmol	Chloroform extraction	rat	liver	112
ɛdC ɛdA ɛAde	Column switching, IDMS(APCI)	70 pM dAde, 100 pM dC, 17 pM dA	OasisHLB	human	urine	73
ɛdC, ɛdA, ɛdG	nanoLC-NSI-MS/MS	0.18 fmol (ɛdC), 4.0 fmol (ɛdA), 3.4 fmol (ɛdG)	Enzymatic digest, reverse phase SPE	human	blood, placenta	134
Ethanol/acetaldehyde induced DNA adducts						
N7-Ethyl-dG	IDMS	0.25 fmol	Ym-30, Strata-X SPE	human	liver	58
N7-Ethyl-dG	column switching IDMS	0.59 pg/mL urine	SepPak C18 SPE	human	urine	42
N^2-ethyl-dGuo	IDMS	0.4 fmol	StrataX, OasisMAX	human	liver, lung, leukocytes, oral cells	115,116,157
N^2-ethyl-Gua	IDMS	0.05 fmol on column, 3 adducts/10^9 nts	Strata-X, OasisMAX SPE	human	leukocytes	158
N^2-ethyl-Gua	nanoHPLC-nanospray HRMS (Orbitrap)	10 amol standard, 2 adducts per 10^9 nts	Thermal hydrolysis, ultrafiltration, Strata-X SPE	human	leukocytes	60

Adduct	Method	LOD	Sample Prep.	Species	Source	Ref.
Adducts induced by DNA alkylating drugs and natural products (Chart 1)						
C8-HEG	IDMS	50 fmol	HPLC	rat	liver	114
Polyaromatic hydrocarbon DNA adducts (Chart 6)						
MP-dGuo, MP-dAdo	IDMS	10 fmol/2 fmol in 100 μg DNA	OasisHLB SPE	rat	liver	119
dG-N^2-BPDE	IDMS	NA	NA	mouse	liver, lung, kidney	159
dG-N^2-BPDE	IDMS		Oasis HLB	mouse	liver	160
dG-BPDE	IDMS column switching	$1/10^8$ nts	DNA digest	mouse	liver	117
BP-6-N7Gua	IDMS w/column switching	2.5 fmol/1 mL urine	SepPak C8 and Strata-SCX SPE	human	urine	118
DB[*a,l*]P-N^6-dA (dibenzo- [*a,l*]pyrene	ID HPLC-ESI-MS.MS	8 fmol/100 μg DNA	Enzymatic digestion ADD	mice	oral tissue	161
Epoxide derived DNA adducts (Chart 7)						
THBG	IDMS	3.5 fmol	YM-10 filtration	mouse/rat	liver/lung	121
HMVK-dGuo	IDMS	5fmol/200 μg DNA	Centricon-10, HPLC	rat	liver	162
N7-GA-Gua, N3-GA-Ade	IDMS	1.5–2 adducts/10^8 nts	Centrifugal filtration	mouse	liver/lung/kidney	127
Bis-N7G-BD	IDMS	6 adducts/10^9 nts	YM-10 filtration, offline HPLC	mouse/rat	liver, lung, kidney, brain, thymus	24
N7G-N^6A-BD	nanoLC-nanoESI- MS/MS	3 adducts/10^9 nts	YM-10 filtration, SepPak C18 SPE	mouse/rat	liver	24
N7-HEG	IDMS column switching	0.25 ng/mL urine	Centrifugation	human	urine	163
N7-HEG	IDMS	0.1 fmol	YM-10 filtration	rat	liver, heart, spleen, kidney, colon, stomach, lung	164
N7-HEG, N1-HedA	IDMS	0.5 fmol ea.	YM-3 filtration, HPLC	rat	liver	165
Bis-N7G-BD	nanoHPLC-nanoESI- MS/MS	0.5 fmol/100 μg DNA	Thermal hydrolysis, untrafiltration, off-line HPLC	mouse	liver; lung, kidney	34,63
1,N^6-HMHP-dA	IDMS column switching	1.5 adducts/10^9 nts	Enxymatic hydrolysis, Clean Carbo SPE	mouse	liver	70
Oxidative DNA adducts (Chart 8)						
8-oxo-dG	IDMS	2 fmol	Immunoaffinity column purification	mouse	prostate	166
8-oxo-dG/A	IDMS	10 fmol 8-oxodA	Oasis HLB SPE	human	urine	167
8-OH-dG	IDMS	0.024 ng/mL	SepPak C18 SPE			168
CEdG	IDMS	0.2 pg	Strata-X-C	rat	urine	169

Chem Res Toxicol. Author manuscript; available in PMC 2013 October 15.

Adducts induced by DNA alkylating drugs and natural products (Chart 1)						
Adduct	**Method**	**LOD**	**Sample Prep.**	**Species**	**Source**	**Ref.**
Others						
N^2-hydroxymethyl-dG	Nano-UPLC-MS/MS	20 amol	Offline HPLC	rat	nasal tissue	[25]

Chem Res Toxicol. Author manuscript; available in PMC 2013 October 15.